INVESTIGATION OF DIESEL AND BIO-DIESEL FUEL DEPOSITS ON A HOT WALL SURFACE BY USING SIMPLIFIED METHOD TEST

MOHAMAD HAZIM BIN MOHD TAJULADNAN

UNIVERSITI TEKNIKAL MALAYSIA MELAKA

INVESTIGATION OF DIESEL AND BIO-DIESEL FUEL DEPOSITS ON A HOT WALL SURFACE BY USING SIMPLIFIED METHOD TEST

MOHAMAD HAZIM BIN MOHD TAJULADNAN

A report submitted
in fulfillment of the requirements for the degree of
Bachelor of Mechanical Engineering with Honours

Faculty of Mechanical Engineering

UNIVERSITI TEKNIKAL MALAYSIA MELAKA

2021

SUPERVISOR’S DECLARATION

I have checked this report and the report can now be submitted to JK-PSM to be delivered back to supervisor and to the second examiner.

Signature :...................................

Name of Supervisor :...................................

Date :...................................

APPROVAL

I hereby declare that I have read this project report and in my opinion this report is sufficient in terms of scope and quality for the award of the degree of Bachelor of Mechanical Engineering with Honours.

Signature :..................................

Name of Supervisor :..................................

Date :..................................

DEDICATION

To my beloved mother and father

ABSTRACT

Deposit formation is a complex phenomenon which causes various problems in the combustion chamber of an engine such as reduce the engine performance, increase the engine emissions, and cause engine damage to the diesel engine. Therefore, the aim of this study is to investigate and analyze the deposit formation of diesel and bio-diesel fuels using a simplified method known as Hot Surface Deposition Test (HSDT). In this investigation, it was carried out by dripping different types of fuel droplets which are diesel and bio-diesel (B20) fuels continuously for 3000 repetitions onto an aluminum alloy sheets with a curved surface as the hot surface plate. The hot surface plate temperature will be set at various temperature which are 250 °C, 357 °C, 450 °C and 600 °C with an impingement interval of 1 and 5 seconds. These intervals are appropriate to simulate between wet and dry condition, respectively which the impingement interval of 1 second is used for wet condition and 5 seconds is used for dry conditions. The dry condition means all volatile components of the first fuel droplet are vaporized or all non-volatile components of the first fuel droplet formed into deposits before the next impingement of the second fuel droplet occur. As for the wet condition, the second impingement of the fuel droplet occurs when the volatile components of the first fuel droplet are not completely vaporized, creating an overlapped state. Based on the results, the amount of mass fuel deposit, M_D of diesel fuel deposit is higher compared to B20 fuel deposit and the highest M_D is produced at surface temperature of 250 °C, followed by 357 °C, 450 °C and 600 °C. This is because as the temperature increases to the point where the Leidenfrost effect is more prominent, the higher oxygen content in B20 fuel molecule aids in better fuel combustion thus, lesser deposit is formed compared to diesel fuel deposit. Therefore, bio-diesel has a potential to replace diesel in the consumer market.

ABSTRAK

Pembentukan deposit adalah fenomena kompleks yang menyebabkan pelbagai masalah di ruang pembakaran mesin seperti mengurangkan prestasi mesin, meningkatkan pelepasan mesin, dan menyebabkan kerosakan mesin pada mesin diesel. Oleh itu, tujuan kajian ini adalah untuk menyelidiki dan menganalisis pembentukan deposit bahan bakar diesel dan bio-diesel menggunakan kaedah yang dipermudah yang dikenali sebagai Uji Pemendapan Permukaan Panas (HSDT). Dalam penyelidikan ini, ia dilakukan dengan meneteskan berbagai jenis tetesan bahan bakar yang merupakan bahan bakar diesel dan bio-diesel (B20) secara berterusan selama 3000 pengulangan ke kepingan aloi aluminium dengan permukaan melengkung sebagai plat permukaan panas. Suhu plat permukaan panas akan ditetapkan pada pelbagai suhu iaitu 250 °C, 357 °C, 450 °C dan 600 °C dengan selang pengurangan 1 dan 5 saat. Selang ini sesuai untuk mensimulasikan antara keadaan basah dan kering, masing-masing yang selang pengurangan 1 saat digunakan untuk keadaan basah dan 5 saat digunakan untuk keadaan kering. Keadaan kering bermaksud semua komponen yang tidak stabil dari titisan bahan bakar pertama diuap atau semua komponen yang tidak mudah menguap dari titisan bahan bakar pertama dibentuk menjadi deposit sebelum terjadinya gangguan tetesan bahan bakar kedua. Bagi keadaan basah, hambatan kedua dari tetesan bahan bakar terjadi apabila komponen yang tidak stabil dari titisan bahan bakar pertama tidak sepenuhnya menguap, mewujudkan keadaan tumpang tindih. Berdasarkan hasilnya, jumlah deposit bahan bakar massa, M_D deposit bahan bakar diesel lebih tinggi dibandingkan dengan deposit bahan bakar B20 dan M_D tertinggi dihasilkan pada suhu permukaan 250 ℃, diikuti oleh 357 ℃, 450 ℃ dan 600 ℃. Ini kerana ketika suhu meningkat ke titik di mana kesan Leidenfrost lebih menonjol, kandungan oksigen yang lebih tinggi dalam molekul bahan bakar B20 membantu pembakaran bahan bakar yang lebih baik sehingga, deposit yang lebih rendah terbentuk dibandingkan dengan simpanan bahan bakar diesel. Oleh itu, bio-diesel berpotensi untuk menggantikan diesel di pasaran pengguna.

ACKNOWLEDGEMENT

First and foremost, I would like to take this opportunity to express my indebtedness appreciation to my supervisor Ir. Ts. Dr. Mohd Zaid Bin Akop from Faculty of Mechanical Engineering of Universiti Teknikal Malaysia Melaka (UTeM) for his essential supervision, advice, reproach, and encouragement that helps me to complete this project report. The special thanks go to my beloved parents for giving me their moral support and patience. Finally, I would also like to thank my classmates for sharing their knowledge throughout this evaluation and all those who have aided me to complete my project report, both directly and indirectly.

TABLE OF CONTENTS

CHAPTER

LIST OF FIGURES

LIST OF TABLES

LIST OF ABBREVIATIONS

HSDT - Hot Surface Deposition Test

EDT - Engine Deposition Test

NOx - Oxides of nitrogen

POME - Palm oil methyl ester

TGA - Thermogravimetric analysis

CCD - Combustion chamber deposit

HCCI - Homogeneous charge compression ignition

HC - Hydrocarbon

A/F - Air/Fuel

DI - Direct injection

DF - Diesel fuel

JO - Jatropha oil

MEP - Maximum Evaporation Rate Point

LIST OF SYMBOLS

$T_{Deposit}$	-	Surface temperature of deposit
T_{Wall}	-	Surface temperature of clean wall
T_i	-	Indicated temperature
T_S	-	Surface temperature
T_d	-	Surface temperature of deposits
°C	-	Degree Celsius
mm	-	Millimeter
mg	-	Milligram
h	-	Hour
m_T	-	Total mass of petri dish with fuel droplet
m_p	-	Mass of the empty petri dish
m_d	-	Mass of a fuel droplet
V_d	-	Volume of a fuel droplet

d - Diameter of a fuel droplet

ρ - Density of a fuel droplet

$\frac{M_D}{m_D}$ - Diameter of A Fuel Droplet, d (mm)

N_D - Number of droplets

CHAPTER 1

INTRODUCTION

1.1 Background

For couple of years, diesel engines have advantages over petrol engines such as high thermal efficiency, high power/weight ratio, rigid structure, simple mechanisms, high fuel economy and low breakdown rate. Due to these reasons, diesel engine has been widely used in transport. The diesel’s higher efficiency makes it possible to use less fuel at the same distance compared to petrol. The big explanation for the success of diesel engines is the usage of low fuel consumption. Unfortunately, emissions released from diesel engines during combustion have been known as the world's main source of air pollution. The rising price of oil is another issue concerning diesel fuels instead of environmental pollution. Moreover, the global economic growth has been affected by this phenomenon.

One of the factors behind the production of new technology is that the oil prices and air pollution. Numerous analysts have looked for to form unused sorts of fuel in arrange to overcome issues related with diesel fuel. A few of them stretch the capacity of palm oil ester, which is alluded to as bio-diesel fuel as a substitution for customary diesel fuel. Palm-oil methyl ester was used by Kalam and Masjuki (2004). From the studies, it found that the engine production was comparable to diesel fuel by the mixing of Palm-oil methyl ester with standard diesel fuel in the automotive diesel engine. The blends from the bio-diesel fuel are moreover able of bringing down emanations. In expansion, the grade of cetane, which is an indicator of ignition efficiency, is higher than that of commercial diesel fuel when it is mixing with the oil methyl ester.

Bio-diesel fills have preferences in lessening outflows and their mixing with diesel fuel has appeared comparable engine effectiveness. The properties of bio-diesel fuel cause the diverse behaviors and impacts of bio-diesel and bio-blended diesel fuel within the engine compared to diesel fuel. Among the properties are such as viscosity, density, chemical properties, and distillation properties. By alluding to the properties, these forms of fuel would have a higher propensity towards the creation of deposits. The aspects of the creation of deposits when utilizing bio-diesel fuel are not well archived or caught on. The usage of bio-diesel fuel in engines often causes numerous problems, as stated by (Senda et al., 1988).

Investigations on gasoline and diesel engine deposits were carried out probably about more than 50 years ago. Several studies have been performed to understand the effects of engine deposits including about how these deposits are carried out in engines. Deposits were found to form in combustion chambers by three different forms of forming process which are: (1) condensation from unburned gases on cooler walls in combustion chambers; (2) impingement droplets on walls of unburned fuel; and (3) fuel flow on walls such as intake valves and injector tips.

Usually, three main repository inquiries still exist due to the numerous engine types and the latest innovations in engine technology. The surveys cover: (1) the influence of engine deposits; (2) the factors leading to deposit formation; and (3) inquiries into deposit properties. (Güralp et al., 2006). Emissions, loss of heat, engine outputs and engine damage include deposit effects on engines. However, for different engine types, factors which influence deposits formation, such as wall temperatures, operating conditions, fuel and oil, and ratios of air/fuel are still being considered. To learn more about the thermal properties and their structures, deposit properties were also studied.

The purpose of this project is to analyze the deposition of diesel and bio-diesel fuels formation on the piston wall which, a simpler method known as the Hot Surface Deposition Test (HSDT), is used instead of using the Engine Deposition Test (EDT). This method is more important when used with biodiesel fuel, where these forms of fuel are more likely than traditional diesel to produce more fuel deposits in engines. In addition, engine damage due to uncertainty in the accumulation of deposits where various forms of bio-diesel fuel are used can also be avoided and the costs of engine service due to long operation can be avoided (Agarwal and Agarwal, 2021).

1.2 Problem Statement

Detailed research on deposit formation is still lacking in information. Deposits formation in the combustion chamber were not well understood and further study is needed. This is a major prerequisite, as stated above, for dealing with deposit-related issues. The formation of deposit in the internal combustion of an engine have cause the deterioration of engine performance and diminished the drivability of the car. Example of the effect that cause by the deposits are engine stalling, increased fuel consumption, engine power restriction and reduce the engine power. Clarifying understanding of deposit formation can help to minimize the formation of engine deposits. It is also possible to solve any problems relating to the formation of deposits.

1.3 Objective

The objectives of this project are as follows:

1. To investigate deposit formation for diesel and bio-diesel fuels.
2. To analyze deposit formation between diesel and bio-diesel fuels.

1.4 Scope of Project

The scopes of this project are:

1. Record total mass deposit of diesel and bio-diesel fuels at different surface temperature with different time interval.
2. Analyze the growth percentage of diesel and bio-diesel fuels at different surface temperature.
3. Diesel and bio-diesel blends fuel namely B20 is used in this investigation.

CHAPTER 2

LITERATURE REVIEW

2.1 Introduction

In this chapter, it describes further understanding about the phenomena of deposit that will be studied. The literature review is mainly about the understanding of deposit formation that formed due to the fuel droplets in the combustion engine, bio-diesel properties, deposit mechanism, factors of deposit formation, engine problem that cause by the deposits and the preventive measure of deposit formation.

2.2 Bio-diesel Fuel

A study of characterization of the properties of palm oil bio-diesel blended fuel compared to the ASTM D7467 blended fuel standard, was made by (Ali et al., 2015). Bio-diesel fuel is a blend of mono alkyl esters of long-chain fatty acids that are saturated and unsaturated and with high density and low cold flow characteristics, compared to diesel minerals. The combination of bio-diesel fuel and mineral diesel is the most common approach to overcome low temperature flow problems in bio-diesel fuel and improve its properties because of similar features. Fuel energy levels are one of the most significant technical issues indicating the use of mixing bio-diesel fuel at a high mixing ratio since the engine power output is directly affected by the energy content of the fuel (Karmakar et al., 2010).

The density, acidity, and viscosity of the mixed fuel increase with the increase in the mixture of bio-diesel fuel and meet ASTM D7464 mixed fuel standard for up to 30% bio-diesel fuel. The poor point of the mixed fuel is raised as the methyl ester concentration of the mixture increases with a lower cloud gap. The increasing bio-diesel ratio in the blend, with a lower heating value for palm oil bio-diesel fuel, is seen to have a substantial linear reduction in blended fuel heating value, which is about 14% less than mineral diesel. The results of the fuel property showed a pour point of about 0 °C of the combined fuel B30. In the case of the mixed fuel norm, the density is 857.3 kg/m^3 and kinematic viscosity of 3.952 mm^2/s.

In contrast to mineral diesel fuels, the decrease in heating value was approximately 4.6%. Engine testing showed that an improvement in the bio-diesel fuel ratios of up to 30% decreases the strength of engine brake power by around 2.6% and raises the fuel consumption in brake specific applications by 3%. However, the thermal efficiency of the engine brake with the mixed fuels compared to mineral diesel did not vary statistically significantly. The indicated average effective pressure time series showed both the variation coefficient and wavelet analyzes with lower cyclical variations on the engine at increased blending. In addition, relative to other fuel samples, the lowest motor cyclic variance was obtained with B30. As a result, a mixed ratio of up to 30% palm bio-diesel palm oil (B30) compared to mineral diesel, is recommended with a smoother engine operation (Ali et al., 2015).

2.3 Engine Deposit

The model used by Slavchov et al. (2018) indicates that high temperature combinations with the presence of the combustion of NOx lead to a reaction between the leaked fuel and the oxygen dissolved in it. The oxidation products are then added as a polar proto-deposit step to the injector surface. Two limiting mechanisms: (1) adsorption; and (2) precipitation is expected for deposit formation rate. A viscous liquid that contains products of low-temperature fuel oxidative degradation (such as alkyl hydroperoxide, aldehydes, ketones, alcohols, ethers, and acids, contained in deposits) may be the first nascent deposit (proto-deposit).

The deposit also includes a variety of aromatic species native to the fuel. As the deposit grows, the organic oxygen is lost over time – for example, the fresh deposit of 20% oxygen in the injector tip, while the aged carbonaceous material is reduced by approximately 10% that is located far away from the nozzle. The evolution of deposits also contributes to increased fragrance, porosity, and advanced polymerization. The lubricant and corrosion material bind to the deposit and gradually together with the organic compound, which can be so difficult to extract, forms a familiar enhanced composite material.

2.4 Deposit Origin

Generally, petrol, lubricant oil, or a mixture of both can be used as the main contributor of chamber deposits. The fuel and lubricant oil dominance in the supply deposits. However, it depends on different factors such as the type of engine and the position of engine parts inside the combustion chamber. As stated by Lepperhoff and Houben (1993), at high temperature, the deposition locations in an engine are largely due to nonmetallic waste that is caused from evaporating or burning fuel and/or lubricants. There has been a role of lubricating oil in the deposit formation in the presence of lubricating oil components and elements. For example, residue of ash residues, inorganic materials, hydrocarbons at the high-boiling point. When initial deposits accumulate, deposit growth will last to a degree before processes for removal and formation are balanced. Thus, only by avoiding the induction process can make the deposits be stopped completely. Either washing the deposit components or preventing the formation of a liquid surface layer can achieve this. Thus, fuel additives that avoid mainly the deposit formation induction process help to significantly reduce deposit problems.

2.5 Deposit Characteristics

2.5.1 Deposit Structure

A study conducted by Husnawan et al. (2009), is about to evaluate the diesel engine carbon deposit of the cylinder head fuel by four samples of 0%, 5%, 10% and 15%, respectively. A thermogravimetric analysis (TGA/DSC) was conducted on air medium in water and 20% Palm Oil Methyl Ester (POME). It was found that, with water rising in fuel, deposits would form less aromatic and less reactive. Besides that, the combustion chamber wall, head, and piston top were found to contain deposits in diesel engines that accumulate over a minimum period of 100 hours in equilibrium density. The development of combustion chamber deposits would seem to have a major effect on engine output and driving capabilities. They include lower volume efficiency, improved thermal efficiency due to cylinder insulation, physical interference in valve closure, or with piston movement. Moreover, the configuration of the engine deposits is subject to many parameters, including the composition of base fuel and engine operating temperatures (Zerda et al., 2001).

2.5.1.1 Wall Temperature Effect

Suryantoro et al. (2019) stated that the time of evaporation affects the produced deposit area and the deposit amount created. The faster the time of evaporation, the smaller the volume of deposit area. In the study, the evaporation time of diesel (B0) is higher than biodiesel (B100). At temperatures 300 °C and 350 °C, the B0 deposit mass is less than B100. The results of the deposition process are shown in Figure 2.1. Besides that, the shaped deposits are very thin, soft, and dry at high temperature (>550 °C) in the combustion chamber and can be easily transported by the gas flow. The deposit is made from carbon. However, the deposit is made from fuel, adhesive, and carbon at low temperatures (<200 °C). According to Sadashiva Prabhu et al. (2017), as the temperature increases, evaporation and decomposition of the urea increase and then decrease the deposit formation. Thus, temperature and flow rate are having important effects on Urea Water Solution (UWS) decomposition and the formation of deposits.

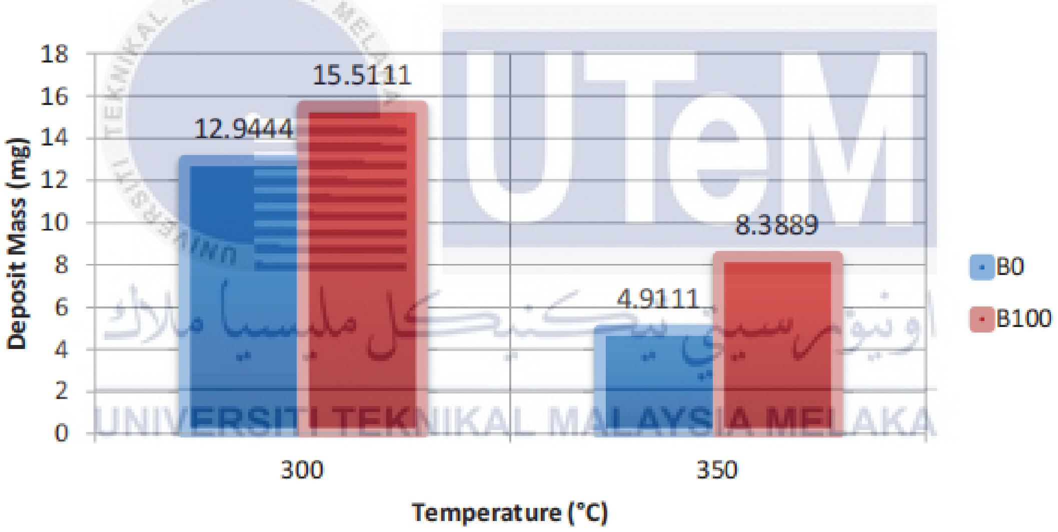

Figure 2. 1: B0 and B100 Mass Growth Deposit at 300°C and 350°C (Suryantoro et al., 2019)

2.5.1.2 Location of Deposit

As stated by Zerda et al. (2001), the studied shown that the morphological of deposit is different in the combustion chamber. The surface area and the total pores volume is depending on where the deposit is extracted. For example, from the cylinder head, piston top or the intake valve as shown in Figure 2.2. The deposit structure separated from cylinder heads of the combustion chamber is more porous compared to at the top deposits. Deposit found at the intake valve were found to be less porous than the deposit in combustion chamber. Pore size for the cylinder head is the highest distribution, followed by piston top and valve intake deposits.

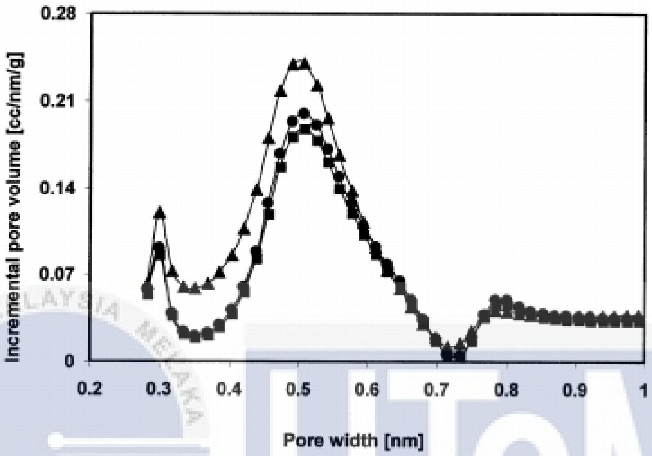

Figure 2. 2: Distributions of pore size deposits formed by the fuel on different engine parts without any additional additives (Zerda et al., 2001)

2.5.1.3 Fuel Component Effect on Deposit Structure

The implications of additives on the deposit structure has been studied by Zerda et al. (2001) and has found that the additives modify pores distribution in deposits as shown in Figure 2.3. In the figure, PEA-1 (polyether amine-based) and PBA-1 (polybutene amine) additive concentrations are close. The study also revealed that increased additive levels lead to decreased surface areas. This impact is combined with a slight rise in deposit mass. It is possibly by filling out and blocking entry to those cavities, that additives or their fragments are incorporated into the deposits. With increased additive concentration, the surface area of the deposits decreases.

Besides that, the carbon deposit characteristics of an engine after 200 hours, have been studied by Razak et al. (2017). Based on this study, the results from Thermogravimetric Analysis (TGA) noted that the characteristics of the surfactant in the ratio of 10:89:1 v/v% (E10) carbon deposit and its higher volatile content differed from the surfactant in the ratio of 20:79:1 v/v% (E20) and low-grade diesel (D2) engines in terms of their darker color, while the Metal Element Analysis (MEA) results noted a decrease in the elemental metal deposit concentration with a higher water content. In comparison with carbon deposition D2 and E20, due to the complete combustion, the intensity of the C-H range was higher for the carbon deposit engine E10.

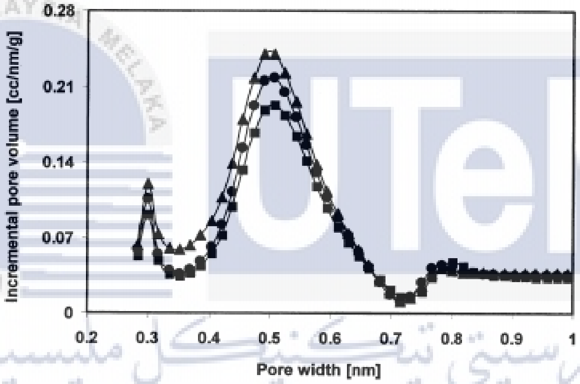

Figure 2. 3: Comparison of the distribution of pore sizes of deposits of fuel at the same concentration with various additives (Zerda et al., 2001)

2.5.1.4 Deposit Structure at Different Layers

In the preceding analysis, two distinct CCD morphologies were identified in higher temperature deposits as shown in Figure 2.4 (Daly et al., 1994). The first layer is the lower layer closest to the metal surface, where extremely volatile fuel and oil compounds are condensed. This deposit has a "lacquer-type" structure in this layer, which is very difficult to extract. This layer also reveals an aliphatic portion of a coal-like structure that are higher than the higher layers subsequently. The deposits in this layer are more uniform and cohesive. The second layer that corresponds to the top layer is made up of molecules that have fewer binding tendencies and can be removed more easily. This layer is characterized with carbonates and its chemical composition is a soot-like. Deposits with an aromatic content like soot have been found in this layer. More loose particles with various shapes and dull edges were present in this deposit layer. It was more structurally scattered and coated with very viscous liquid or polymer.

Moreover, a studied made by Stanuch et al. (2020), is to analyze the dispersion of chemical elements in cross-sections of landfill biogas-driven engine deposits. Scanning Electron Microscopy used in combination with Energy Dispersion Spectroscopy (SEM-EDS) examined the chemical composition of extreme mineral layers extracted from the engine piston and its four piston cross sections and one head. Differences in surface morphology between the bottom layer of the piston adhesion and the top surface in contact with the combustion chamber were found, based on studies of elemental composition of the sample of 9T1-1/17 in extreme layer. The lower layer showed significantly lower surface topography heterogeneity than the top, creating various spatial forms.

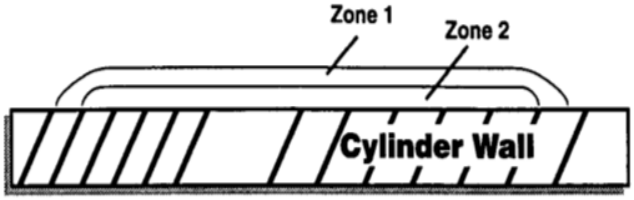

Figure 2. 4: Deposit layers (Daly et al., 1994)

2.5.2 Deposit Properties

The ratio between the local maximum temperature phase and the thickness of the combustion chamber deposits along with the thermal diffusivity formula is studied by (Güralp et al., 2006) and the results were determined in Figure 2.5. The result showed a strong association between deposit thickness and the diffusivity of the deposit layer of the combustion chamber at two separate cylindrical head surfaces for the HCCI engine. Larger material layers have lower thermal diffusiveness efficiency. This is because the morphology changes continuously as the deposit forms. There is a constantly changing degree of porosity, consistency and the HC molecules which form various layers of the total material.

In addition, deposit formation and carbon blackness typically occur at temperatures above 350°C. Deposits are associated with varnish and sludge formation (Hoang and Pham, 2019). Incomplete combustion is considered the typical trait during a spreading period of ignition, while most fuel is burnt. The combustion chamber deposits can be classified as following: (1) deposits produced by the gas phase; and (2) unburnt materials are being used to produce deposits that make up the cenosphere and the cokes.

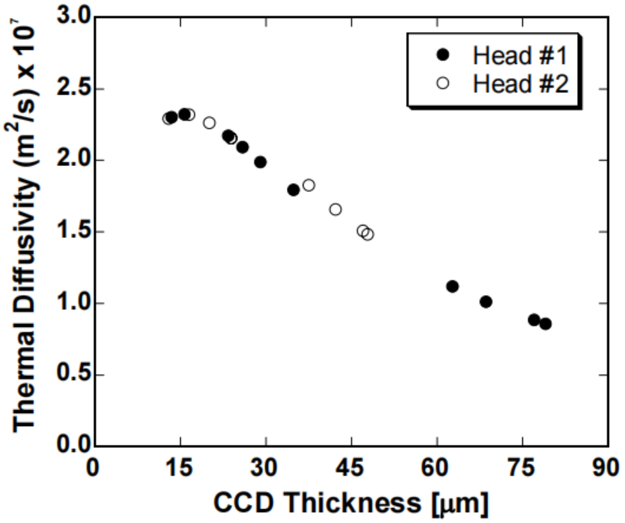

Figure 2. 5: Plot of measured efficient thermal diffusiveness as a CCD thickness feature at the location of each head flux probe (Güralp et al., 2006)

2.6 Deposit Mechanism

Understanding how deposits are produced in engine combustion chambers and what controlling parameters, can be used to identify any deposition formation at different locations. In addition, if the fundamental mechanisms of deposit formation are well understood in engine combustion chambers, engine deposits can be expected to increase the engine durability. As illustrated in Figures 2.6 and Figure 2.7, Lepperhoff and Houben (1993) recommended the physical deposit mechanisms which included formation and removal mechanisms.

A deposit forming system is considered to be a time function and physical conditions, divided into two groups, high molecular fluid substances and particles, related to temperature, fuel properties, flow concentrations and concentration gradients (Anjaneyulu et al., 2017). In the meantime, the operation and combustion chamber of the engine also have a major impact on the deposit removal mechanism. The carbon deposits and deposits are shown to be the heterogeneous mixture originating from carbon residue and carbonaceous mixtures mixed in complex oxidizing reactions with the organic material to form the resinous material (F. Jorand et al., 2000).

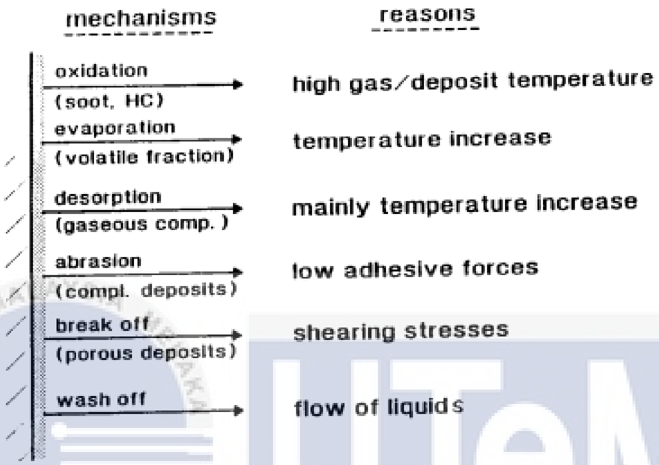

Figure 2. 6: Deposit formation mechanism (Lepperhoff and Houben, 1993)

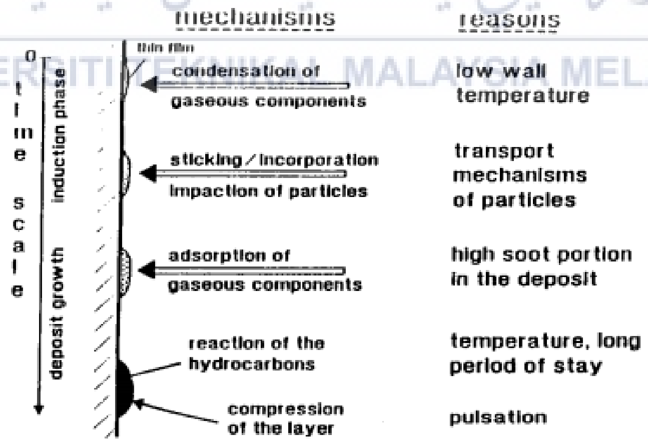

Figure 2. 7: Deposit removal mechanism (Lepperhoff and Houben, 1993)

2.6.1 Formation Mechanism

The mechanisms of the deposit formation are defined as time. This mechanism is depending on the location of the deposit formation. For example, the flow concentrations, temperature gradients, temperature, and gradients of the deposited components. The deposit part may be divided into various groups: (1) gaseous and high-molecular liquid matter that following the gas flow; and (2) particulate matter that does not following the path of the gas flow.

2.6.1.1 Liquid Film Formation

Lepperhoff and Houben (1993) studied the effects of surface temperature, gas temperature, turbulent gas flow, and gas composition on deposit formation in internal combustion engines. The condensation of heavy gas components and the impingement of fuel on the surface of the wall will cause fluid film formation. The liquid components on the wall surface result in deposits due to reactivity and evaporation behavior. This mechanism is primarily affected by the wall in the case of condensation. The cooled wall's temperature gradient caused heavy gas components to thermally disperse. It contributed to a rise in heavy gaseous component concentrations that are close to the wall. These gas components are high boiling, which are hydrocarbons. Due to low wall temperatures, the gas components condense and adsorb at the wall. This condensation of high-boiling hydrocarbons on the wall allows the deposit to form. The forming of fuel film by the fuel impingement also helps to create a deposit formation on the wall where the film also serves as a barrier to the chamber particles. The regions that are directly exposed to spray pollution is very likely to achieve a significant number of attached deposits.

2.6.1.2 Impaction of Particles

The cooled wall temperature gradient contributes to a strong thermophoretic forces that transport the particles to the wall. Increased temperature gradients result in increased thermophoresis. This results in an increased concentration of particles close to a cold wall. Incorporation, sticking, and impaction are used to deposit the particles. The adhesive force between the wall and the particles produces the adhesive effect. The binding of the particles to a liquid surface layer shall be integrated. The effect of the thermophoresis phenomenon produces the impaction (Arifin et al., 2008).

2.6.1.3 Adsorption of Gaseous Component

The addition and impaction of particles probably forms the structure of high soot deposits. In the adsorption of gaseous components, the porosity of the deposit plays a significant role. Gas components disperse through a porous deposit layer and are adsorbed or concentrated in a lower-temperature layers. This will cause the density of the layer assisted by gas flow pulsation is increased (Arifin et al., 2008).

2.6.1.4 Reaction of Hydrocarbon

If combustion chamber fuel is sprayed, it burns when oxygen is in contact with. The combustion chamber undergoes high temperature and pressure during the spraying phase, along with available flames in a way to prevent delayed ignition, but the preliminary oxidation is still present. The fuel is continuously pumped under the constantly growing temperature of the combustion chamber, while the oxygen is not sufficient to break up the fuel particles even at high temperatures. Consequently, unburnt materials occur in the formation of soot. The buildup of the components above contributes to the formation of the deposit. The explanation of the formation of carbon blacks and deposit may be due to the: (1) decomposition of hydrocarbons (this process produces carbon components); and (2) condensation of hydrocarbon (this process is thought to incorporate aromatic hydrocarbons with larger polynuclear to produce the deposits). Two favorable condition for diesel engines including the presence of metal-based catalysis for hydrocarbon decomposition process and the condensation of thermo-physicochemical conditions (Hoang and Pham, 2019).

2.6.1.5 Compression of The Layer

A study made by Nikolakopoulos (2021) which is evaluated the impact on the tribological performance of the lubricant by the geometrical profile of the compression ring, including the friction force, thickness, and pressure of the lubrication film. At piston overturns with a low speed, the new and worn profiles showed considerably inadequate minimum film thickness as shown in Figure 2.8. Nevertheless, with increasing engine speed, the thicker film emerges in the middle of each stroke at the worn ring profile. This can be explained by increasing wedge effects as the lubricant reaches the ring-liner gap, especially at the middle of the strike where the wedge action is prevalent. Overall, the ring-bore clearing is distinguished by the ring shape surface and correspondingly the worst sealing behavior because of the deposit (Nikolakopoulos, 2021).

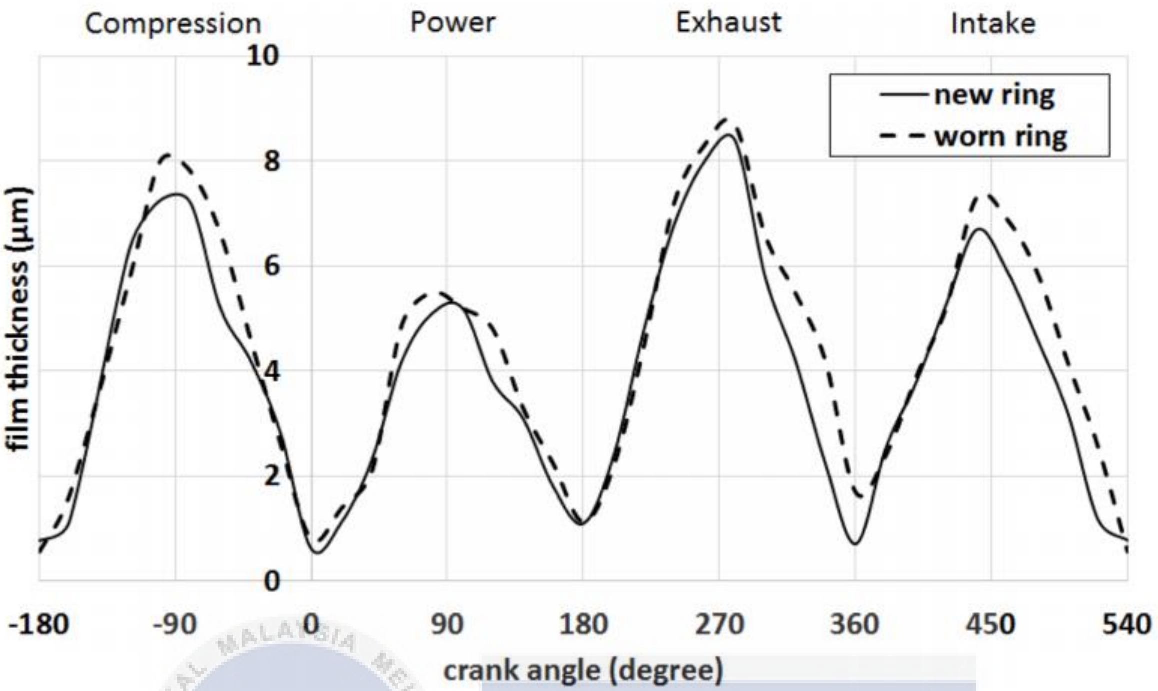

Figure 2. 8: The variation of the new and worn rings for minimum film thickness (Nikolakopoulos, 2021)

2.6.2 Removal Mechanisms

During the formation of deposits in engines, Lepperhoff and Houben (1993) recommended 6 forms of removal mechanisms. The mechanisms for removal are:

1) Soot and hydrocarbon oxidation that cause by deposit and high gas temperature.
2) Volatile fraction evaporation with increasing temperature.
3) Gaseous component desorption primarily due to the rise in temperature.
4) Gaseous component desorption primarily due to the rise in temperature.
5) Low adhesive force that causes abrasion to happen.

6) Break off especially in the porous structure of the deposit that happen due to the shear stress.
7) Wash off when liquid flows are separated from a deposit precursor that is likely to raise the deposit volume.

2.7 Factor of Deposit Mechanism

There are many factors that caused the deposit mechanism such as liquid film formation, wall surface temperature, air/fuel ratio, engine operating conditions, and the fuel and lubricant oil. These factors have been widely researched in previous literature on deposit formation in a combustion chamber of an engine.

2.7.1 Liquid Film Formation

The surface of the oil film fuel is distributed like a continuous circular, wavy-like, fluid-like film with a dry surface area, but it is much less than the dry surface area of the film as shown in Figure 2.9 (Liu et al., 2019). The film spread area on a thicker oil film from the second and third rows can be found, and more fuel is accumulated at the rim of the film. If we looked closely at the second picture in the third line, we found a few isolated droplets scattered across the central region of the film, which was not seen in other conditions. Some of the droplets can penetrate and then be covered by the oil film when it is sprayed in the oil film. The fuel was mixed with the oil film and some of the coated droplets in the impact area will mixed into the mixture with the violent disturbance that are resulting from the spray impingement. The other droplets which are not in the central area of effect when they enter the oil film, are not affected with the impingement, and are not mixed with the mixture. These droplets are forced out as the film spreads and the final droplets form. For formation of the dispersed droplets, some requirement could be found which are low oil film viscosity and high enough incident velocity for the penetration of oil film by the droplets.

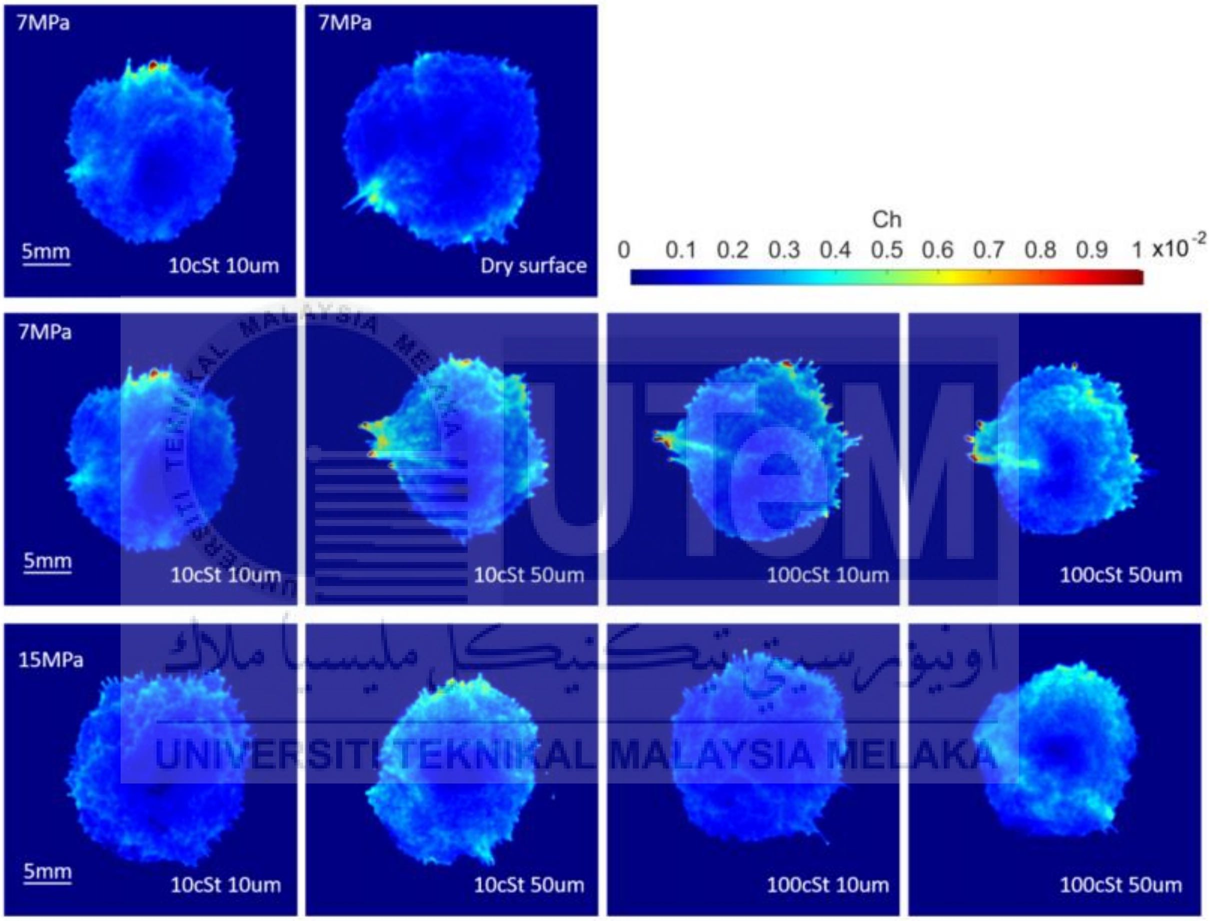

Figure 2. 9: The first line shows the comparation of the morphology between dry surface and oil film; the second and third rows illustrate the effect of the oil film properties on the film morphology under the injection of 7 and 15 MPa separately (Liu et al., 2019)

2.7.2 Wall Temperature Effect

For deposit formation, the wall temperature effect is the most significant factor. In this statement, (Ye et al., 2007) said that the flammable combustion temperatures and the surface temperature of the cylinders are essential factors for the formation of deposits. The flame and combustion chamber that have a high temperature causes significant carbonization of deposits. The combustion chamber contains various sections that will have different wall temperature and it also have different exposure to the deposit able parts. On the edge of the piston bowl where the average temperature is comparatively lower, the thickest deposit layer was found. Due to its higher surface temperature, fewer deposits were found on the intake and exhaust valves.

Temperature and flow rates have been determined as a parameter that can change the amount and nature of deposits (Sadashiva Prabhu et al., 2017). The study of the deposit structure physically under different operating conditions shows the nature of deposits and risk deposit areas. At the respective temperatures, the impact of temperature on deposit formation is clearly distinguished as solid, semisolid, and liquid forms. The flow of fluid film or semisolid urea to successive regions with an increase in air flow rate has also been observed. In Figure 2.10, Figure 2.11, and Figure 2.12, the plot of deposit transformation at different temperatures for different flow rates are shown.

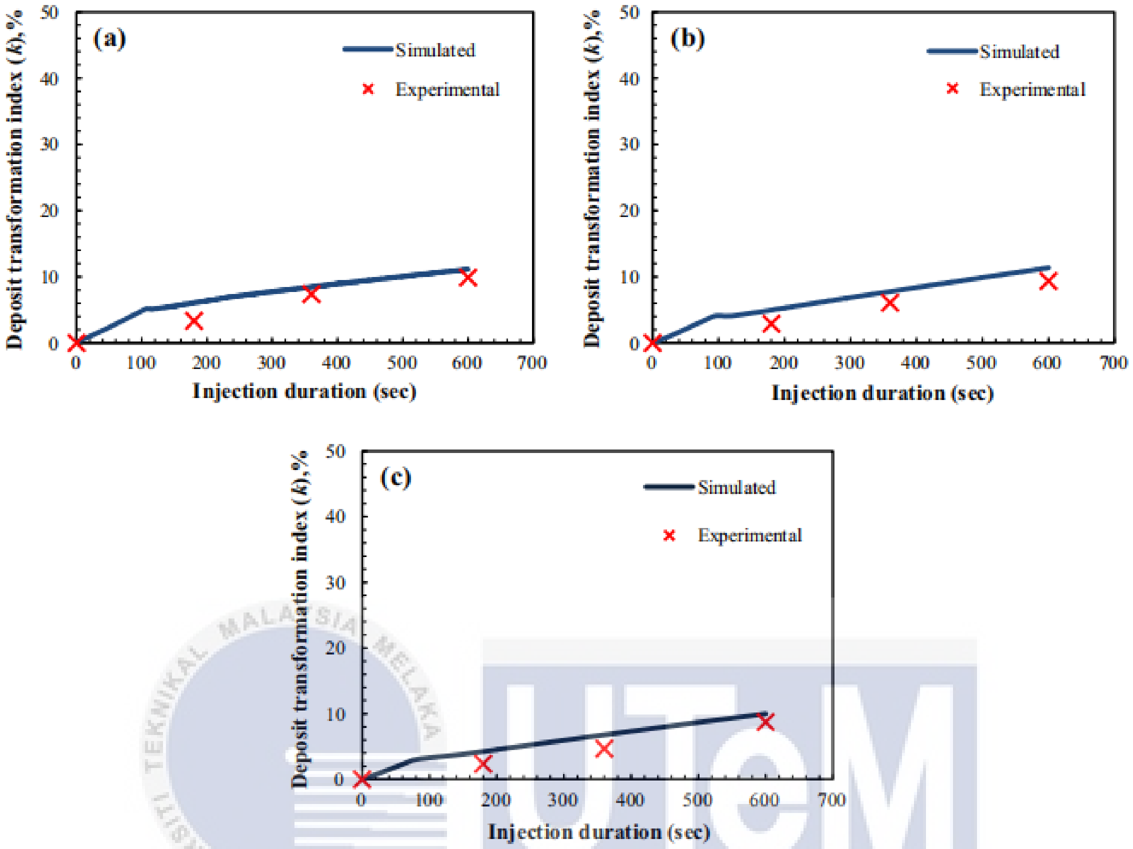

Figure 2. 10: Plot of deposit transformation index (k) vs injection duration at temperature 150 °C for flow rates (a) 34.74 kg/h, (b) 86.86 kg/h and (c) 121.6 kg/h (Sadashiva Prabhu et al., 2017)

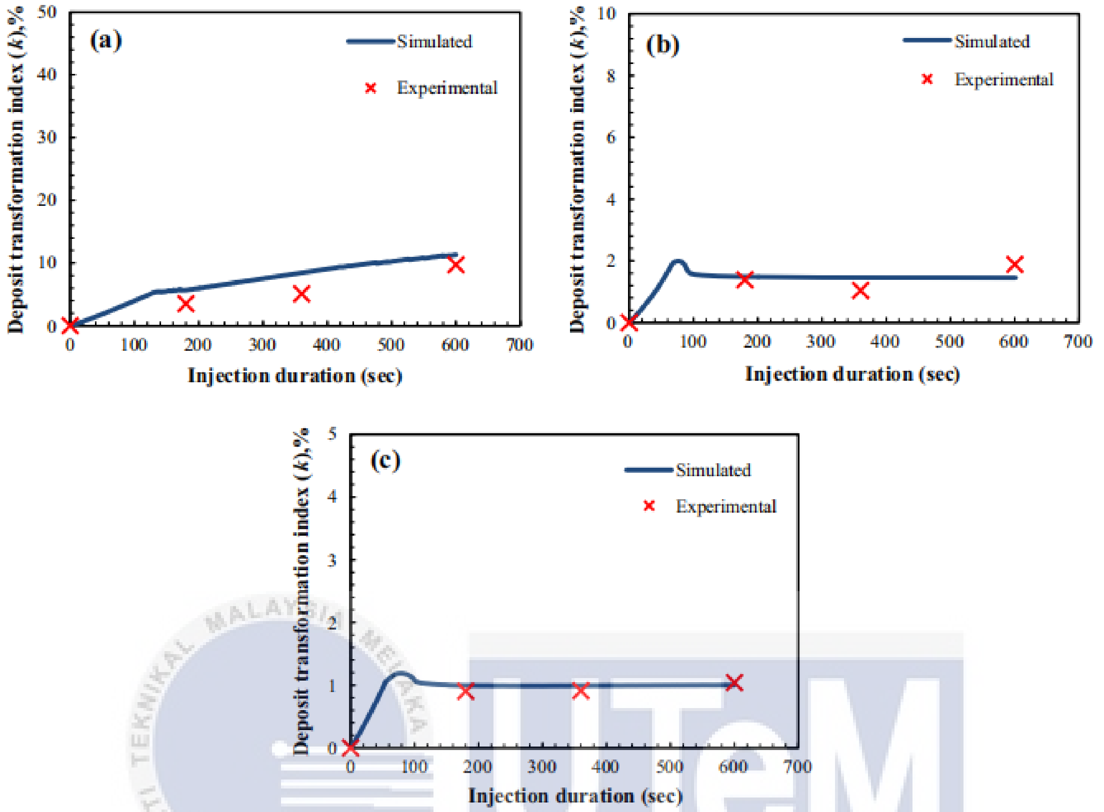

Figure 2. 11: Plot of deposit transformation index (k) vs injection duration at temperature 200 °C for flow rates (a) 34.74 kg/h (b) 86.86 kg/h, and (c) 121.6 kg/h (Sadashiva Prabhu et al., 2017)

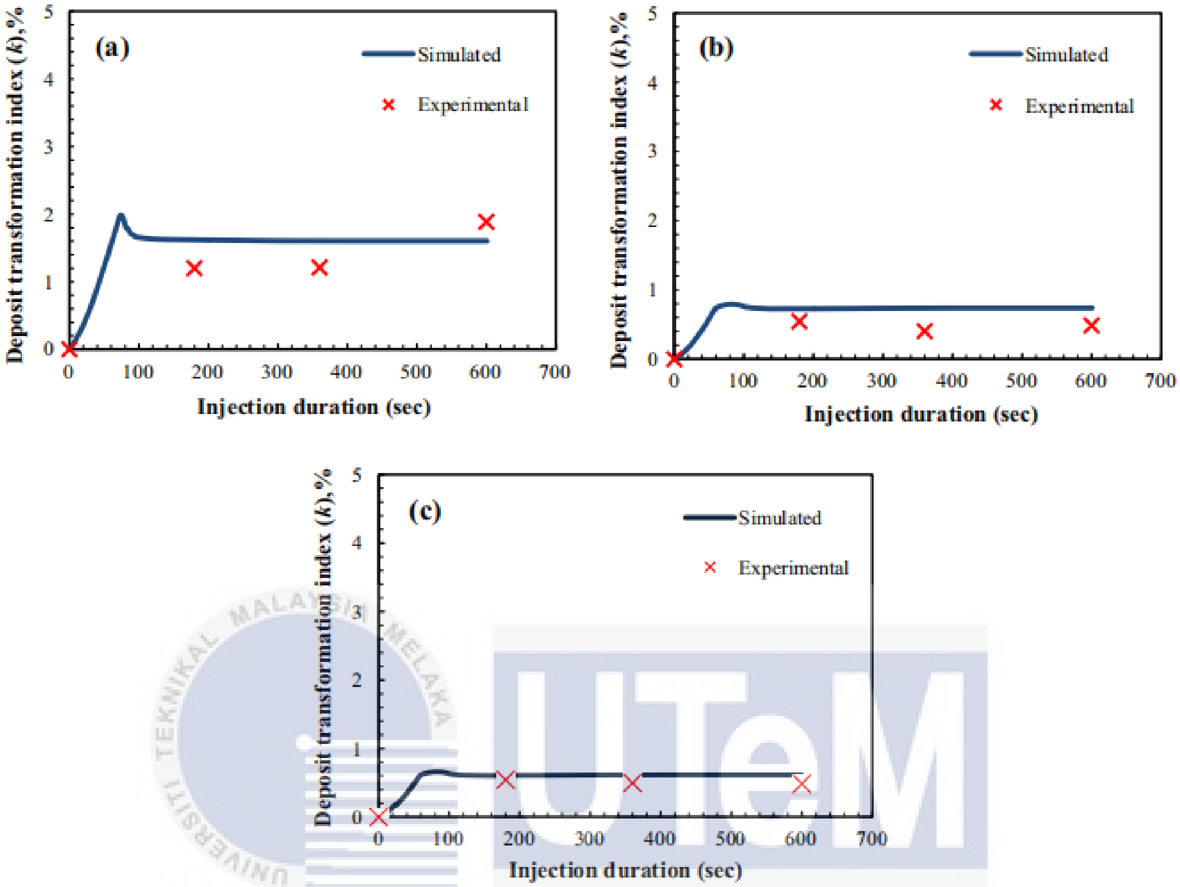

Figure 2. 12: Plot of deposit transformation index (k) vs injection duration at temperature 250 °C for flow rates (a) 34.74 kg/h, (b) 86.86 kg/h and (c) 121.6 kg/h (Sadashiva Prabhu et al., 2017)

2.7.3 Air / Fuel Ratio

Another major factor in the formation of deposits is the air/fuel (A/F) ratio. Ye et al. (2007) used the SI engine bench test in different A/F ratios to test the deposit development in the engines. The study found that, when the A/F ratio mixture was adjusted from an excess of A/F ratios to a stoichiometric A/F ratio as shown in Figure 2.13, the deposit volume accumulated on the sample plug that have been installed in the cylinder head of the engine, dropped. When the A/F mixture reaches a much lower value, the volume of deposit increases again.

As Ye et al. (2007) explained, a rich mixture has a low concentration of oxygen will then contributes to combustion that is incomplete. The incomplete combustion of halfway products tends to accumulate on the exhaust valves, cylinder wall, and piston surface. Because of the high flame and combustion chamber temperature, the carbonization effect is remarkable where, on the wall surface, a significant amount of combustion deposit is accumulated. The increasing of engine power will affect the grows of the combustion deposit on the chamber, within the rich conditions.

As the A/F ratio keeps increasing, there was an excessively lean mixture that will present. Due to the low flame and reaction temperature, halfway products cannot react entirely. Therefore, a certain amount of reaction products will remain on the surface of the combustion chamber, and the other amounts will discharge from the cylinder and enter the exhaust system. Therefore, there will be an increased amount of deposit on the sample plug.

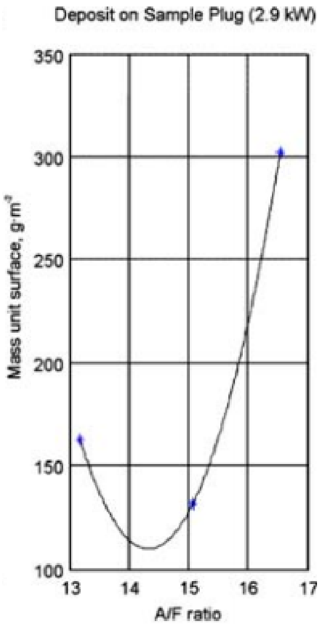

Figure 2. 13: Effect of A/F on deposits (Ye et al., 2007)

2.7.4 Engine Operation Condition

Based on Lepperhoff and Houben (1993), the study mentioned that new deposit formation problems occur in new and existing engines. The problems occur because of changes in operating conditions due to modifications in engine design and/or the operating combustion processes. For example, even in low load operations over a long distance, injection nozzles can be fouled in DI diesel engines. The explanation could be a high-pressure fuel system and narrow spray holes which lead to a rise in temperature inside the injector tip.

Ye et al. (2007) analyzed the effect of deposit, on HC emissions from various cylinder pressure, where, in fact, deposits with low cylinder pressure are more effective than those with high cylinder pressure. To reduce the problem of temperature and deposit formation, a small compression ratio is preferable. Besides that, Hoang and Le (2019), made analyzation which is to evaluate the deposit formation mechanism in diesel engines by focusing on the injector nozzle. Injector geometry affects injection pressure, fuel injection velocity, flow fuel mass, and therefore plays an important role in controlling the formed deposits in the injector.

2.7.5 Fuel and Lubricant Oil

The degradation of the engine shows the accumulation of carbon deposition in cylinders, and the contamination and thickening of lubricant on the engine. The direct use of JO as fuel contributes to the formation of excessive deposits at various internal components (Almutairi et al., 2017). It is apparent that carbon residues filled the piston head's concave and coated the injector nozzle. The volumetric efficiency of the concave piston and the injector function are thus reduced. The formation of carbon deposits is mainly due to the physicochemical characteristics of JO that effect the spray fuel and process of combustion. Akintayo (2004) has shown that the JO's iodine value is 105, which characterized that JO is a Di-unsaturated oil. The greater the value, the less saturated the oil is. Thus, the combustion deteriorates, resulting in longer evaporation time and delays in ignition, affecting the deposition of fuel.

Engine soot deposition is primarily due to partial fuel combustion, improper scavenging, and a deterioration of lube oil (Kumar Patidar and Raheman, 2020). Soot depositions are influenced by engine design, lubricating oil composition, type of fuel and engine operating conditions. Excessive deposits influence the spraying pattern, which in turn alters the mixture of air and fuel, thereby reducing fuel economy and improving the HC and emissions of particulate matter.

Ullmann et al. (2008) analyzed the connection on deposit formation by certain diesel fuel additives. The results from the study show that additives alone do not tend to produce any degradation product and therefore do not develop any deposits. Combinations of certain additives, however, can lead to deposit formation. For instance, gum-like polymetric deposits can be formed by the combinations of typical diesel detergents and di-fatty acids. When formic acid is present, this will be exacerbated.

2.8 Engine Problem Due to Deposits

2.8.1 Heat Transfer in The Combustion Chamber

A rate control factor for deposit formation shall be included the surface condition of the wall of the combustion chamber. Heat and vaporization processes that form deposition on its surface involve unburned fuels adhering to the combustion chamber surface. As a result, the wall of the cylinders that are overheated in the combustion chamber, can cause knock to the engine and degradation of fuel which leads to more deposits forming, increased combustion and exhausted gas temperatures, as stated by (Ye et al., 2007).

The deposit layer serves as thermal insulator in the combustion chamber where it influences the release of heat. Ishii et al. (2001) found that changes in instantaneous surface temperature and heating flux, were caused by the amount of deposit attached to a wall, as shown in Figure 2.14. The larger the number of deposits, created a greater change in the heat flux and surface temperature. Low thermal conductivity of deposits will lead to a reduction in conduction rate and reduces the ability of the combustion chamber to release heat. The surface temperature of the deposits ($T_{Deposit}$) is greater than that of the clean wall (T_{Wall}) as reported in Figures 2.15, because of the thermal isolation effect of the deposit.

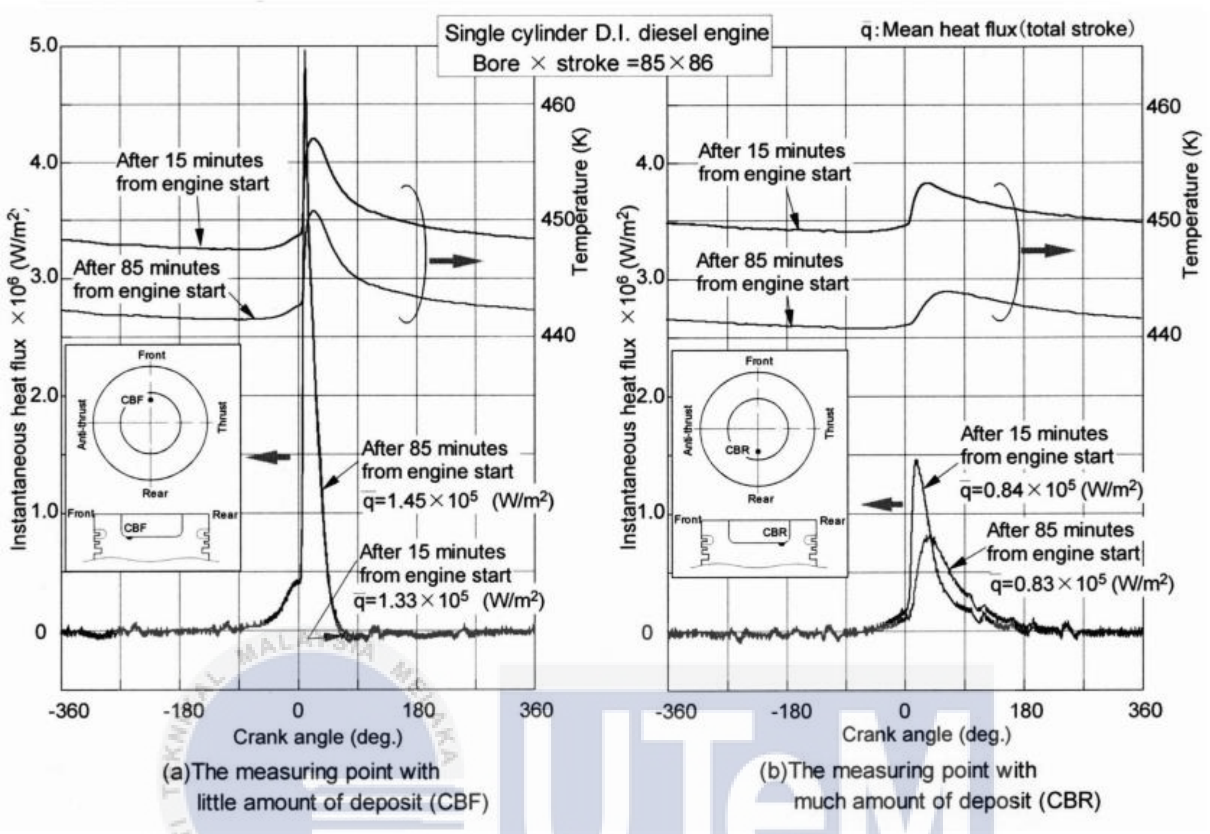

Figure 2. 14: Effect of deposits on instantaneous surface temperature and instantaneous heat flux (1200 rpm, full load) (Ishii et al., 2001)

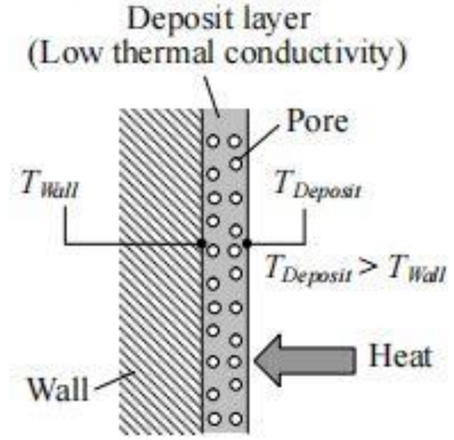

Figure 2. 15: Deposit layer effect on heat transfer (Arifin, 2009)

2.8.2 Engine Performance

There are two root reasons why the engine performance has deteriorated, and the HC emissions are increased: first, the pattern of distorted spraying by injection fouling; second, the forming of deposit at injector tip (Xu et al., 2015). Deviations from optimal spraying patterns, such as spray angle that is adjusted, asymmetrical spray envelope, long distance of penetration and droplet distribution that is increased, have negative impacts on performance and emissions of the engine. Although they do not contribute to a flow rate loss, deposits on the injector tip may influence the engine performance. A fresh mixture during intake and compression strokes is also heated by the engine deposit (Ye et al., 2007).

2.8.3 Engine Emissions

Deposits can collect droplets of liquid fuel and hence, cause combustion diffusion that led to poor emissions (Xu et al., 2015). The use of high-speed imaging in an optical engine has been proved by (Berndorfer et al., 2013). Near the pump, diffusion combustion has been found. Ra et al. (2006) mentioned that soot emissions are intrinsically related to the build-up of a soot deposit on engine surfaces since a part of the soot formed during the process of combustion in cylinder is deposited on the oxidation-protected combustion chamber surfaces. Deposit development may affect the increase in the soot emissions from an engine to some extent. The CCD's effects on HC emissions depend on the mechanisms that dominate on a given engine and operational condition (Caceres et al., 2003).

2.8.4 Engine Damage

Bore polishing leads to engine damage in diesel engines. The formation of the valve seat deposits however contributes to damage to sparking-ignition engines (Lepperhoff and Houben, 1993). As the engines age, wear and degrade of engine parts induces additional oil in the combustion chambers. As a result, more deposits will form as a result of oil and oil additives (Caceres et al., 2003). This could lead to more a serious damage. Moreover, Jiang et al. (2017), study the effect of deposits on the injector pulse width and flow rate. It can be seen that each day of the test, the injection time increases slowly (over a total of 7 days for the 30-h test). This could be because of either a loss of fuel efficiency (therefore a higher amount of fuel is needed to maintain the same engine performance) or a lower injection flow rate because deposits accumulate, which would require compensation for the same amount of fuel with a longer injection duration, or because both effects are combined.

2.9 Deposit Preventive Measures

Formation of depositing in engines relies on many interconnected variables. There is also no clear way to minimize an engine's deposit. Numerous studies however, suggested general preventive measures for different types of engines and operational conditions. The preventive measures suggested here are focused on various aspects and according to their research on real engine deposits.

2.9.1 Engine Parameter

The procedure involves a consistent use of a diesel motor at high loads, to achieve the temperature of cylinder that is sufficiently high to oxidize the deposits (Jonkers et al., 2002). Ye et al. (2007) recommended that the partially burned mixtures and halfway products should be reduced by changing the value of the A/F ratio to reduce the accumulation of deposit.

Besides that, Xu et al. (2015) suggested that using detergents as a one of the way for injector deposit reduction. There are numerous deposit control detergents that are specifically designed for intake valve deposits and combustion chamber deposits. For example, polyether amines, polyolefin amines, and alkenyl succinimides. Detergents are used to protect metal surfaces, disperse precursors of the deposit, and clean the metal surface. In general, fuel detergents have long chain of hydrocarbons at one end of their molecule with polar head groups. There is no polar property in the other group in the fuel detergent molecule. The polar head group can attach themselves easily to a metal surface, to form a protective surface and thus prevent the deposition precursor from being deposited on the metal surface. This process is called as ‘protection’. The polar head group can also attach to the deposit precursors. By doing that, it keeps the deposit precursors to be dispersed in the liquid, and this process is called as ‘dispersion’. For deposits that already exist on the metal surface, the polar-headed detergent collects deposits and helps to remove them from the metal surface. The detergents break up and take a certain amount of the deposit along with the detergent. This process is called as 'detergency'.

2.9.2 Engine Design

The design of an engine can be modified to manage deposit problems. However, by redesigning, it can lead to new deposit characteristics (Caceres et al., 2003). And so, Ye et al. (2007) proposed that by reducing the surface-to-volume ratio, deposit formation can be minimized to decrease the surface area that are subjected to engine deposits. Caceres et al. (2003) stressed the importance of increasing the durability of the engine components to reduce the introduction of oil in the engine cylinder, to reduce CCD formation resulting from lubricant oil. Besides that, Xu et al. (2015) suggested that the increased pressure for fuel injections has proved to be an efficient way to reduce the formation of deposits. A higher injection pressure will suppress the formation of the injector deposit by increasing the deposit removal rate. Thus, reduce the Particulate Matter (PM) emissions in Gasoline Direct Injection (GDI) engines.

2.9.3 Deposit Mechanism Considerations

Lepperhoff and Houben (1993) proposed that the wall surface should cover liquid and the liquid flow should be sufficiently high to constantly wash all particles to avoid the accumulation of deposits that caused by the liquid flow (e.g., intake valves, injector tips and injector holes). As the initial deposits accumulate, a deposit growth continues to grow on a wall surface in a combustion chamber, until the processes of removal and formation are in equilibrium. Therefore, deposits can be prevented totally only by avoiding the deposit formation mechanisms induction process. Either the components can be washed away, or the liquid surface layer can be prevented, the preventive of deposit formation can be achieved.

Ye et al. (2007) explained that the deposit formation may be reduced because of maximizing the deposit ratio of release rate (evaporation, reaction) ratio with the condensing rate among engine deposits (e.g., high votality). When the deposit rate is faster than produced, deposits are gradually reduced.

2.9.4 Wall Temperature Control

Xu et al. (2015) found the nozzle temperature to be lower than the T90 fuel temperature to suppress deposits in the nozzle holes. From this, the residual fuel in the nozzle hole will be in a liquid state thus, the deposit precursor can be washed away by the fuel injection. The deposit formation in the nozzle hole was therefore restrained.

2.9.5 Fuel and Lubricant Formulation

Ullmann et al. (2008) mentioned that the best option to prevent the new kind of injector deposits is using lubricity additive chemistries. This is because the lubricity additive chemistries do not further react with other fuel compounds. If practicable, acid-based additives will be replaced by neutral chemistries to prevent these types of deposits while retaining the protection afforded by diesel detergents. Deposit problems at different locations can be handled by developing special fuel and/or lubricant compounds and/or additives (Lepperhoff and Houben, 1993).

CHAPTER 3

METHODOLOGY

3.1 Introduction

The methodology that is used in this project will be described in this chapter. This study is based on the formation of deposit that occurs because of the fuel droplets that evaporate on the surface that is heated to a certain temperature. Experiments are performed according to the variables that have been set which are the type of fuel, the surface temperature, and the time interval between each droplet. The deposit result is obtained through a picture showing the deposit present on the hot surface and the total mass of deposit formed. The flow of the project will be summarized in a flow chart as shown in Figure 3.1.

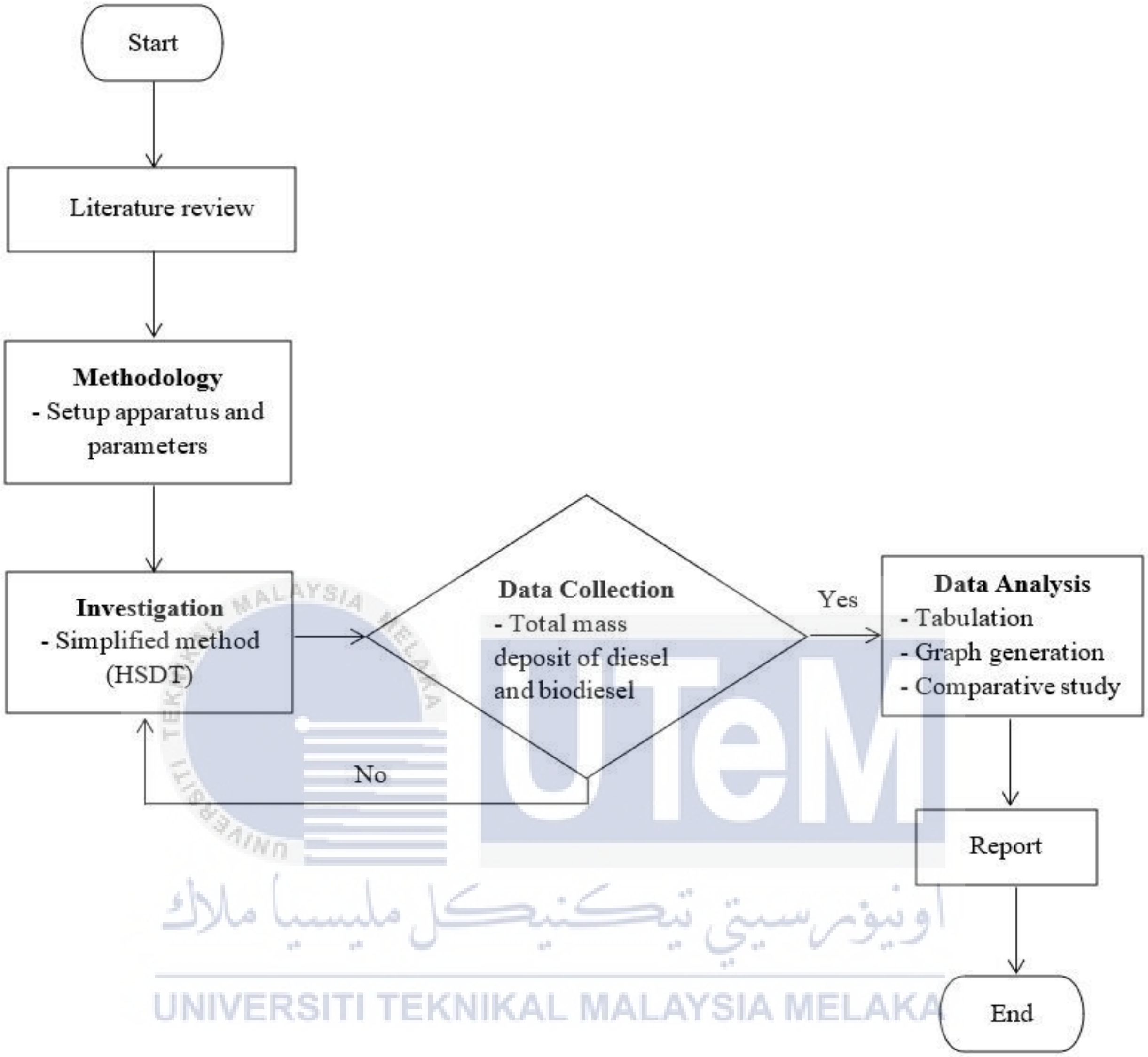

Figure 3. 1: Flow chart of methodology

3.2 Introduction of The Hot Surface Deposition Test (HSDT)

A significant number of fuel droplets are involved during atomization in real engines. In the combustion chamber, the droplets evaporate and burn. However, in the combustion chamber, some of the droplets find way as shown in Figure 3.2 to impinge the wall surface. The interaction of a fuel spray with a surface within an engine results in the deposition of film liquid fuel. One of the causes of deposits on the wall surface in the combustion chamber was this liquid film formation.

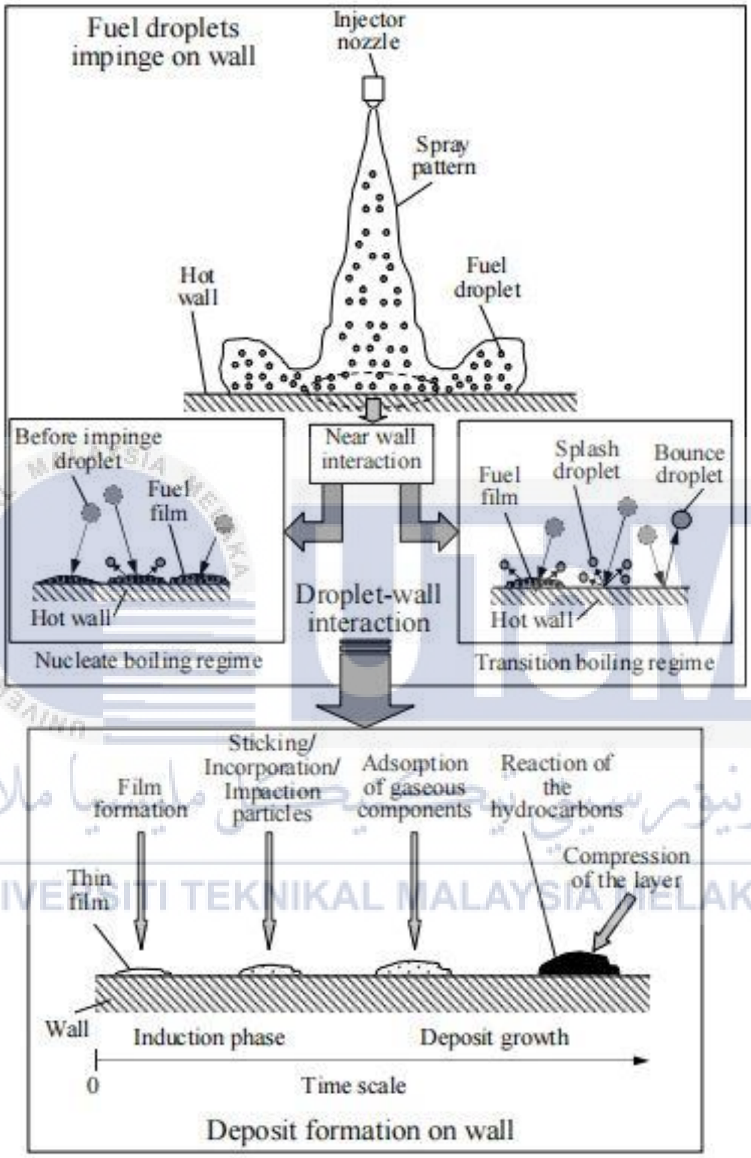

Figure 3. 2: Mechanism of deposit formation in an engine (Arifin et al., 2008)

As the fuel spray impinges the wall surface of an engine, liquid fuel films are formed on the surface. The variation of wall surface temperature will affect the volume of fuel film attached to the wall. The temperature of the wall influences the volume of non-volatile or heavy molecular fuel components. This molecular will remain in the wall and the contact between the droplet and the surface during impingement. Less liquid film is probably attached to the wall for high surface temperatures and even when the interaction is under the boiling regime of transition. In the regime, there will be more droplets, as secondary droplets that will be impinged in the other combustion chamber surfaces or released from the engine during the exhaust stroke. The liquid fuel film which adhered to the surface of the wall, will further experience physical processes (evaporation, particle impaction, etc.) and chemical processes (polymerization, thermal decomposition, etc.) due to the temperature of the heated wall surface. As shown in Figure 3.2, the development of deposit on the wall in the combustion chamber is presented.

During the combustion, the formation of deposits is more severe due to high temperature of gases and flames, in particular carbonaceous deposit formation, which enhance the carbonization process. In addition, soot particles are also attached during the process. The high temperature and the flame in a real engine caused some of the deposits to burn and oxidize quickly on the wall surface, resulting in a reduction in the deposit. The drop in deposits of an engine can also be caused by other factors such as the flow of gas, piston movement and vibration, as the deposits are physically removed and released from the engine during the engine exhaust stroke.

Next, the impingement spray will impinge the surface of the deposit layer which is formed by the previous impingement. As described above, the deposit forming processes continue until the engine has ended. The deposit layers often stowed up and coated the wall of the combustion chamber during engine operation. In a real engine, however, the amount of deposit accumulated on the surface stabilizes after a certain period, when the rate of deposit development and the rate of deposit removal reaches a balance condition.

The formation of deposits in an engine is a complex phenomenon and deposit development and mechanisms in a real engine are difficult to observe. Therefore, in this study, a simpler approach called a Hot Surface Deposition Test (HSDT), is suggested. The fundamental concept of this simplified technique is the repeat of fuel droplets on a hot surface that leads to a piled-up deposition on the wall surface. Figure 3.2 illustrates the processes of repeating and piling of deposits on a hot wall surface. In the figure, a droplet of fuel is released from a tip of needle to form a fuel film on the surface of the hot wall surface. Volatile fuel film components will vaporize and then leave the non-volatile fuel components on the surface of the heat wall. In addition, these non-volatile fuel components oxidize slowly before transforming into carbonaceous deposits. Like an engine, the volume of non-volatile fuel on the hot wall surface varies, that depend on the wall surface temperature, using this simplified process. The higher the surface temperature, the less the non-volatile fuel and deposits.

At the same impingement point, the next droplet is continuously impinged on the surface at a constant impingement interval. However, due to the formation of a deposit layer form previous impingement, the surface may have changed. Again, volatile fuels components will vaporize and leave non-volatile fuel components, which will also become into deposits. This will lead to the formation of new deposit layer at the impingement point. The deposit amount is increased because of non-volatile fuel components, that does not vaporize and remained after the impingement. The accumulated deposit also grows with each repetition. The process of droplets impinging on the surface occurs repeatedly. The addition of non-volatile fuel components that impinge on the wall surface and the stacking process of deposits continues to repeat throughout the experiment.

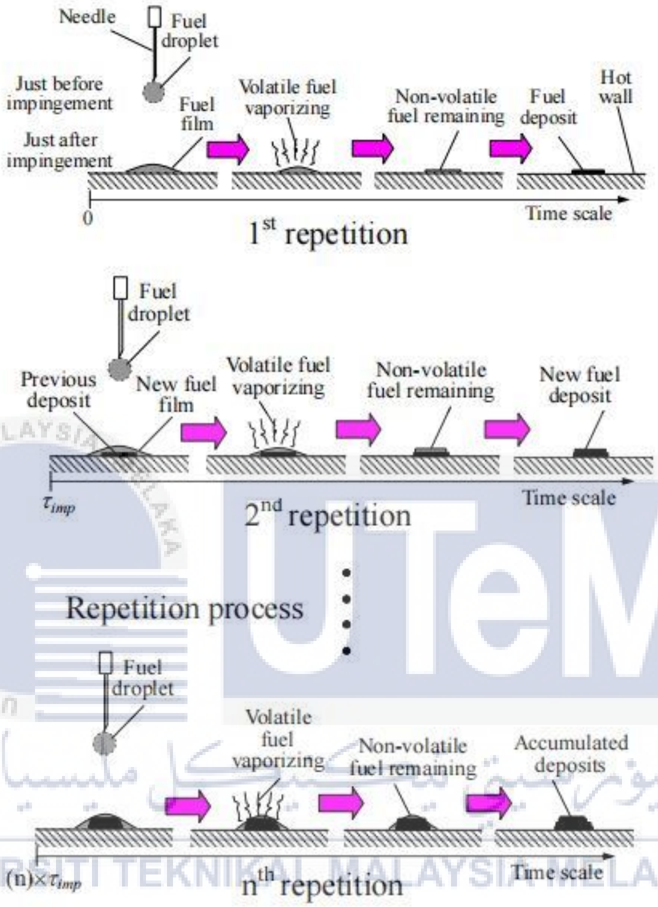

Figure 3. 3: Repetition process of deposit formation on a hot wall surface (Arifin et al., 2008)

In this simplified form, repeating and piling-up deposition processes are same as the deposition process due to spray impingements in an engine on wall surfaces, as illustrated in Figure 3.2 previously. The process of repeating for the engine was represented with the simpler method by repeating fuel droplets which were constantly impinged on the hot wall surface. The piled-up deposit process in an engine was therefore represented by HSDT method through non-volatile fuel components, which remain and then become a carbonaceous deposit layer for each droplet impingement.

The repeat and stacking-up processes of deposit in an engine are described by using the simplified technique referred to in this study as a hot surface deposition test (HSDT). The aim of HSDT is thus to simulate the deposition on the wall in the combustion chamber of an engine and to analyze the development of deposit, mechanisms and factors which affect formation of deposit.

3.3 Experimental Apparatus

Each equipment and apparatus to be used should be provided and placed in a suitable area. This study involves the production of smoke due to evaporation of fuel, therefore the experimental area should have a good ventilation system (do not have an air conditioning system) and no smoke detection system. A hot surface deposition test (HSDT) is conducted.

3.3.1 Apparatus and Equipment

A photograph of this single droplet repetition apparatus required for this HSDT is shown in Figure 3.4. The schematic diagram of HSDT is shown in Figure 3.5 and the apparatus consists of 1) hot surface plate; 2) heater; 3) droplet detector; 4) needle; 5) pinch cock; 6) fuel tube; 7) fuel tank; 8) thermocouple; 9) temperature controller; 10) detector system; 11) pulse generator; 12) pulse conditioner and 13) universal counter.

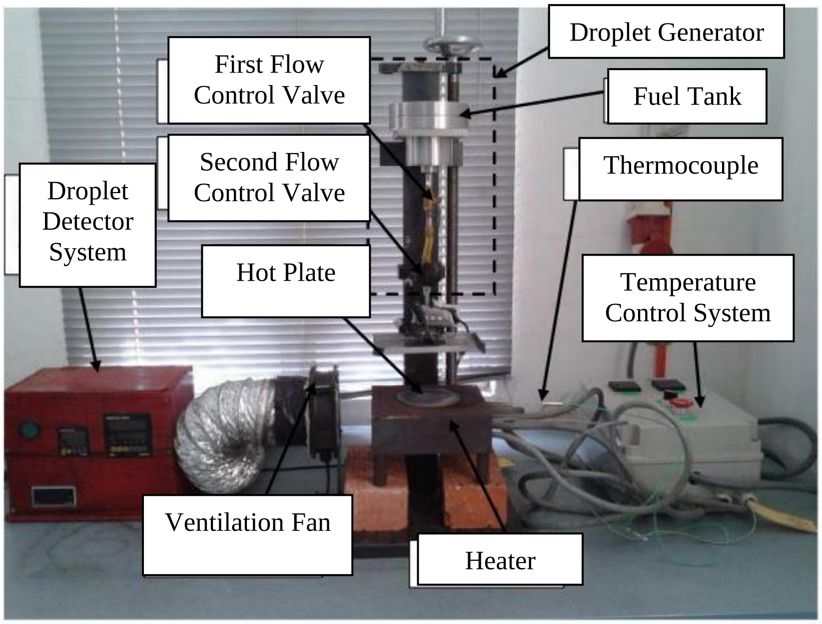

Figure 3. 4: Photograph of HSDT bench

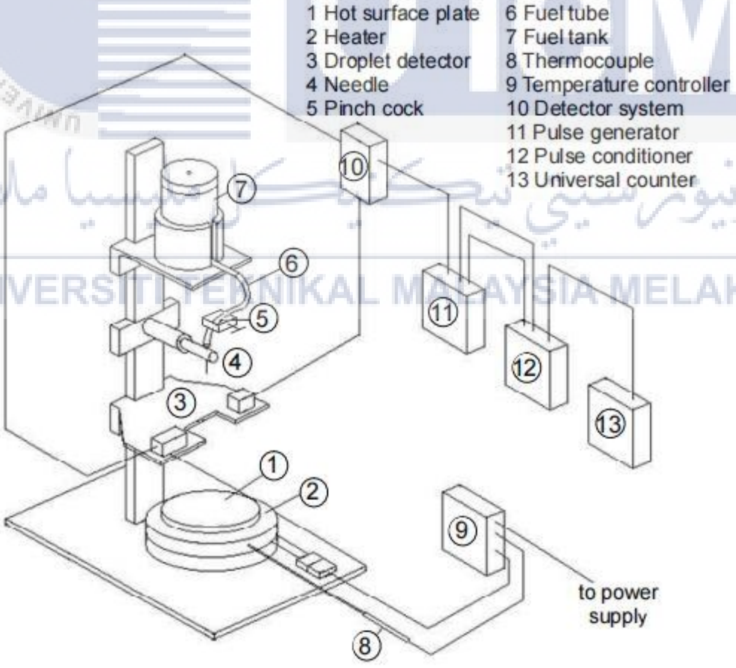

Figure 3. 5: Schematic diagram of single droplet repetition apparatus (Arifin et al., 2008)

3.3.1.1 Fuel

Fuel is an important thing that should be in this study because this experiment aims to see the results of the fuel residue that is sediment for each type of fuel. There are two types of fuels used in this experiment, namely diesel fuel (DF), and as well as a mixture of both diesel and bio-diesel fuels, namely B20. The letter B stands for biodiesel and its subsequent value indicates the percentage value of the biodiesel used in the mixture of the two fuels.

3.3.1.2 Aluminum Alloy Sheets

Hot surfaces are areas where fuel droplets evaporate, and the formation of deposit occurs during experiments. Aluminum alloy sheets with a curved surface are used as the hot surface plat. The nature of aluminum alloy which has a high melting point of 660 °C allows it to not melt when reaching the highest temperature of the experiment conducted. Furthermore, the process of washing the deposit found on the hot surface plate is easy and convenient because the plate will be reused for further testing. The lightweight aluminum alloy sheet makes it easy to lift during the process of weighing the amount of deposit formation formed.

3.3.1.3 Temperature Control Set

While the experiment is in progress, the temperature used should be constant in the duration of the experiment. The temperature control system along with the heater set and thermocouple set is used as a set of temperature controller. Through the temperature control system, an electric current is converted into heat through an iron rod connected to the heater set and it will heat up. The thermocouple will measure the temperature reading and will show on a digital display on the temperature control system. The desired temperature value will be obtained by setting the desired value on the temperature control system. The step to heat the aluminum surface at the experimental temperature is by entering the desired temperature value on the temperature control panel as shown in Figure 3.6 using the provided button. The temperature value entered is 100 °C first and leave until the temperature display panel shows the same value. This step is repeated until it reaches the desired experimental temperature value. Once the experiment is complete, the temperature value on the control panel is reduced to 30 °C (room temperature) before both the ON/OFF switch and the emergency switch are closed.

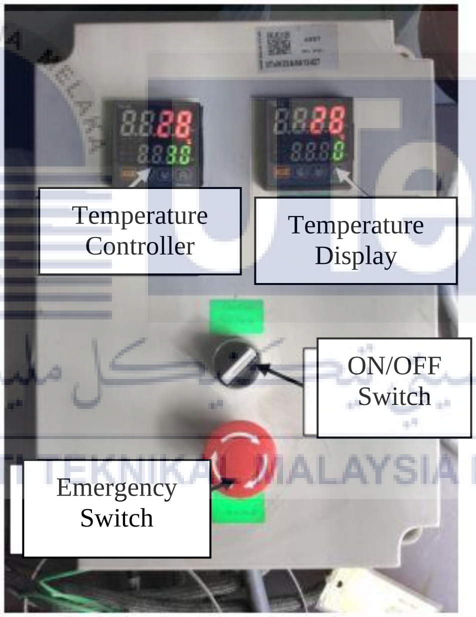

Figure 3. 6: Temperature control system

3.3.1.4 Droplet Generator

The resulting drop should be at a fixed interval rate for each drop that falls according to the desired situation; dry or wet conditions so that the experiments carried out achieve the desired objectives. The fuel tank is to be refilled and stored before the fuel is drained using fuel tube during the test. The first flow control valve aims to control the downstream flow path of the fuel, whether it will be fully opened or completely closed to receive the downward flow of fuel or vice versa. The second flow control valve, on the other hand, is to control the time interval of the resulting droplet through the drip needle.

3.3.1.5 Needle

Drops are produced through a needle that is mounted under a second flow control valve with a rubber tube connection and located between the detectors. Figure 3.7 shows the needle to be used during the experiment and the size of this needle is fixed for the whole experiment. The size of the needle used is 21G x 1” (length = 25.4mm, outer diameter = 0.8mm), resulting in a suitable droplet size for this study.

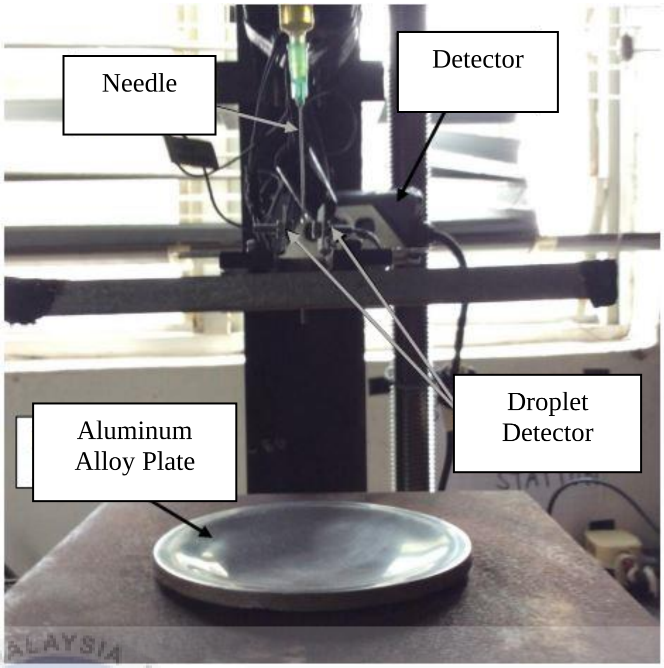

Figure 3. 7: Needle

3.3.1.6 Droplet Generator Holder

The droplet generator should be placed parallel to the hot surface so that the resulting droplets continue to fall on the middle part of the surface. The droplet generator holder was specially designed for this study. Through this holder, the height of the droplet generator can be adjusted so that the distance between the needle and the hot surface can be set as desired. At the surface of the droplet generator holder, the droplet generator and the heater set are in parallel position.

3.3.1.7 Droplet Detector System

The total number of fuel droplets for one experiment is 3000 drops. For every 500 drops, the experiment will be stopped to take the mass readings on the hot surface plate. The droplet detector is used to calculate the amount of each droplet that has been produced and the time interval between each fuel droplet as shown in Figure 3.8.

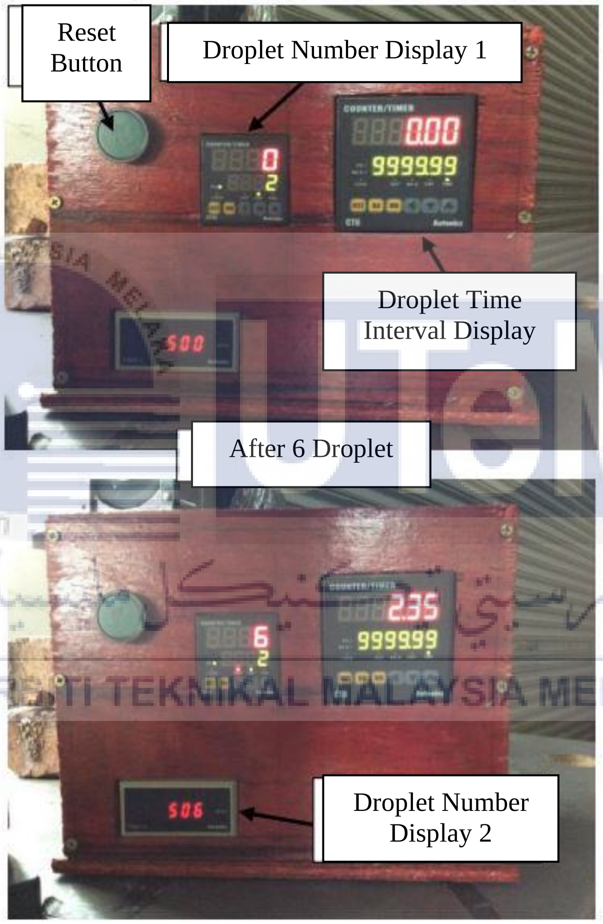

Figure 3. 8: Droplet detector system

The reset button on the droplet detector system allows the resulting readings to display the number of droplets 1. The droplet interval display can be reset to zero so that the reading can be started at the proper conditions. Figure 3.8 shows the reset button has been pressed causing the display of the number of droplets 1 and the time interval of the droplets to show a zero value. After a few drops have been dropped, the droplet count control panel shows 6 drops of fuel have been produced with an interval between each drop is 2.35 seconds. The second flow control valve should be adjusted little by little while pressing the reset button to get the proper time interval. The number 2 drop view will be set to zero after the required time interval has been obtained by using the small reset button that is found on the side of the display panel.

3.3.1.8 Ventilation Fan

Vaporization of fuel at high temperatures produces gas or smoke and it needs to be sucked out of the laboratory so that the ventilation in the laboratory is not disturbed by the smoke. The ventilation fan as shown in Figure 3.9, is used to extract the smoke and heat coming from the heater. The distance between the fan and the heater should be kept safe so that the fan is not damaged or melted due to the high heat temperature.

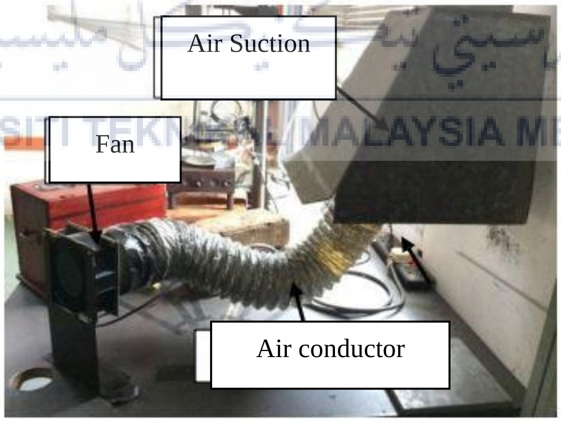

Figure 3. 9: A ventilation fan

3.3.1.9 Hot Plate Holder and Microbalance

Once the number of droplets reach 500, and the hot pieces need to be weighed, lifting the hot plate by hand even with the wearing of gloves is certainly risky as the hot plate have been heated at high temperatures by the heater. The hot plate holder shown in Figure 3.10 has been designed to lift the hot plate for weighing or to be placed on a special rack for the cooling process of the hot plate. Microbalance is used to measure the resulting deposit mass because the scale has a high sensitivity that able to measure small masses up to 1 microgram as shown in Figure 3.11. The hot plate should be cooled first before putting it into the microbalance. The microbalance is tightly closed so that the effect of the hot plate temperature and wind does not affect the resulting reading value. The mass readings of hot plate are taken three times and taking the average data to ensure the reliability of the data.

Figure 3. 10: A hot plate holder

Figure 3. 11: A microbalance

3.3.2 HSDT Procedure

The temperature of the hot plate surface is use as an indicated temperature (T_i °C) and surface temperature (T_S °C). In this case, the first is measured using a thermocouple and the latter is measured using an infrared thermocouple. Before each ET and HSDT was started, a linear correlation has been calculated for both temperatures. The general correlation of the two different temperatures is shown in Figure 3.12. From the correlations, it can be used for an actual surface temperature approximation.

At various impingement intervals, the fuel droplets have repeatedly been impinged on the hot surface of aluminum alloy. Deposits were measured for each 500 droplets and deposits were photographed. Due to the microbalance sensitivity, the hot surface needed to be cooled down before the total deposit amount was measured at 500 droplets. Between the saturated and

Leidenfrost temperatures, the hot surface temperature for the deposition test was chosen which are the wet conditions are located within this temperature range.

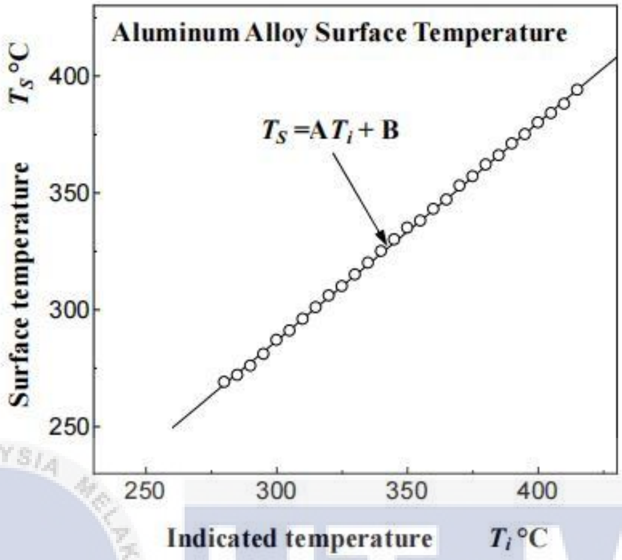

Figure 3. 12: Temperature correlation (Arifin et al., 2008)

Using an infrared thermometer for the analysis of the heat transfer effect on deposition, the data for maximum and minimum surface temperatures of deposits (T_d) in impingement interval was collected. The measurement of the surface deposit temperature with the use of the infrared thermometer is shown in Figure 3.13. A minimum deposit surface temperature means the deposit surface temperature has been measured at the point of impingement immediately after the fuel droplet impinged on the deposit surface.

However, the maximum surface temperature of a deposit means that, immediately before the next droplets impinges the deposit surface, the deposit surface temperature was measured at the impingement point. To evaluate the droplet lifetime for deposition tests, the maximum surface temperature of the deposit and the evaporation characteristics of fuels was used.

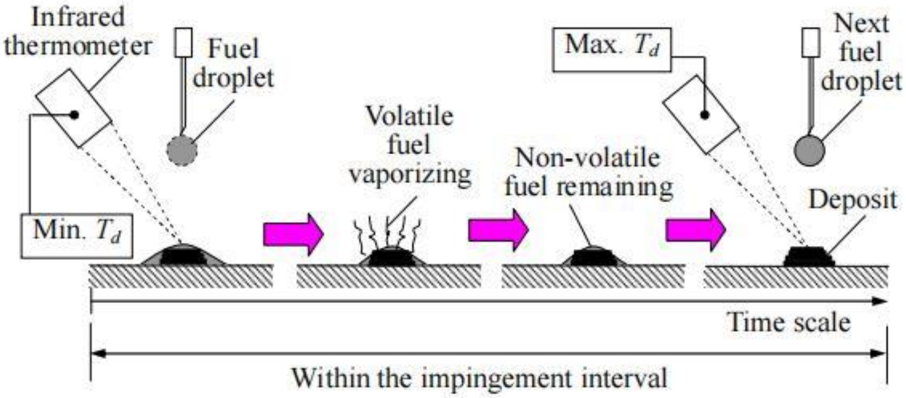

Figure 3. 13: Deposit surface temperature measurement (Arifin et al., 2008)

During the experiment is being carried out, the ventilation fan is used so that it can extract the smoke out of the laboratory room that is resulting from the process of evaporation of fuel to prevent the smoke from spreading in the room.

Based on the study variables mentioned earlier, Table 3.1 shows test condition for HSDT. The results of the experiments performed are based on the amount of deposit formation that occurs by taking reading of the total mass of deposit produced at 500 drops for a total number of drops of 3000 drops.

Table 3. 1: HSDT condition

Type of Fuel	**Surface Temperature (°C)**	**Time interval between each droplet (s)**
DF	250, 357, 450 and 600	1 and 5
B20	250, 357, 450 and 600	1 and 5

Each type of fuel will be dropped on a hot surface at a set temperature at each droplet interval. For example, for diesel fuels, experiments will be performed at 250 °C with an interval of 1 second and 5 seconds, 357 °C with an interval of 1 second and 5 seconds, 450 °C with an interval of 1 second and 5 seconds, and 600 °C with 1 second and 5 second intervals. For B20 fuel, it will be carried out using the same method.

CHAPTER 4

RESULTS AND DISCUSSION

4.1 Introduction

The aim of this chapter is to investigate and analyze the deposit formation of diesel and different blends of bio-diesel fuels droplets that impinge on a hot surface of an aluminum alloy. The deposit formation of diesel fuel will be used as a reference to compare with the deposit formation of different blends of bio-diesel fuel. The types of fuel that will be used in this experiment are diesel fuel, and bio-diesel fuels blended with diesel fuel which referred as bio-blended diesel fuel (B20). The hot surface temperature for the aluminum alloy will be set at various temperature which are 250 °C, 357 °C, 450 °C and 600 °C with impingement interval of 1 and 5 seconds.

4.2 Preliminary Results

4.2.1 Characteristics of Diesel and Bio-Diesel Fuels

Each fuel has different density value. Throughout this study, several characteristics of diesel and B20 fuel are recorded. Firstly, a 100 ml of diesel fuel is put on a petri dish and the mass is recorded using a microbalance. Beforehand, the mass of the empty petri dish, m_p is recorded and then, the total mass of petri dish with a 100 ml of diesel, m_T is subtracted with the empty petri dish, m_p to obtain the mass of fuel as shown in Eq. (4.1). After that, the density of a diesel fuel droplet is obtained using Eq. (4.2) as the mass of diesel fuel and volume of diesel fuel have been obtained. Then, to get the diameter of a diesel fuel droplet, 10 droplets of diesel fuel is put on a petri dish and recorded using a microbalance. Then, the total mass of petri dish with 10 droplets of diesel, is subtracted with the empty petri dish, m_p and divided by 10 to obtain the mass of a diesel fuel droplet, m_d. Using Eq. (4.2) again, as the density of a diesel fuel droplet, ρ and mass of a diesel fuel droplet, m_d have been obtained previously, volume of a diesel fuel droplet, V_d can be obtained. The diameter of a diesel fuel droplet, d is determined using the sphere equation as shown in Eq. (4.3). Why Eq. (4.3) is used because, the shape of a fuel droplet is similar to the shape of a sphere when the droplet leaves the nozzle. All these steps are repeated to get the characteristics for B20 fuel.

$$m_T - m_p = m_d \tag{4.1}$$

$$\rho = \frac{m_d}{V_d} \tag{4.2}$$

$$V_d = \frac{4\pi(\frac{d}{2})^3}{3} \tag{4.3}$$

Where,

m_T = Total mass of petri dish with fuel droplet

m_p = Mass of the empty petri dish

m_d = Mass of a fuel droplet

V_d = Volume of a fuel droplet

d = Diameter of a fuel droplet

ρ = Density of a fuel droplet

Table 4. 1: Density, mass, and diameter of a droplet for different type of fuels

Fuel	**Density of A Fuel Droplet, ρ (kg/m^3)**	**Mass of A Fuel Droplet, m_d (mg)**	**Diameter of A Fuel Droplet, d (mm)**
DF	784.00	5.71	2.400
B20	816.00	5.90	2.421

4.2.2 Dry and Wet Condition

Throughout the experiment, there are two impingement intervals between the fuel droplets that will be used which are 1 and 5 seconds. These intervals are appropriate to simulate between wet and dry condition, respectively. The dry condition means all volatile components of the first fuel droplet are vaporized or all non-volatile components of the first fuel droplet formed into deposits before the next impingement of the second fuel droplet occur. As for the wet condition, the second impingement of the fuel droplet occurs when the volatile components of the first fuel droplet are not completely vaporized, creating an overlapped state.

4.2.3 Surface Temperature

The surface temperature that are used in this experiment are 250 °C, 357 °C, 450 °C and 600 °C. In this temperature range, the deposit formation and characteristic between diesel and B20 fuel can be identified in this study.

4.2.4 Deposition of Diesel and Bio-diesel Fuels

The mass of the fuel deposit for diesel and B20 bio-diesel fuels will be recorded using a microbalance for every 500 droplets until a maximum of 3000 droplets. All the data have been recorded and tabulated for mass of fuel deposit, M_D (mg) and ratio of fuel deposit, $\frac{M_D}{m_D}$ at different surface temperature of aluminum alloy which are 250 °C, 357 °C, 450 °C and 600 °C.

4.2.4.1 Diesel Fuel (DF)

Table 4. 2: Total mass of diesel fuel deposit (mg) at wet condition (time interval = $1s$) and surface temperature of 250 °C

Amount of Droplet	**Mass of Fuel Deposit, M_D (mg)**				**Ratio of Fuel Deposit, $\frac{M_D}{m_D}$**
	1	**2**	**3**	**Average**	
500	110.1864	110.188	110.187	110.1871	19.2972
1000	110.296	110.2962	110.2963	110.2962	19.3163
1500	110.381	110.3831	110.3833	110.3825	19.3314
2000	110.7143	110.7162	110.7172	110.7159	19.3898
2500	111.0505	111.0497	111.0494	111.0499	19.4483
3000	111.3638	111.3636	111.3634	111.3636	19.5033

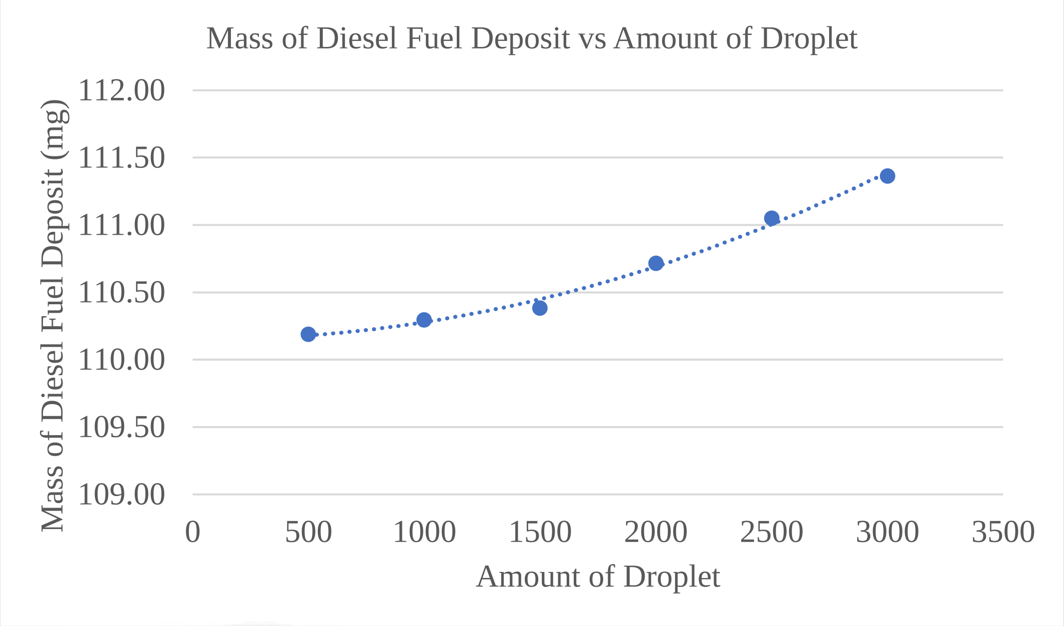

Figure 4. 1: Mass of diesel fuel deposit, M_D at wet condition (time interval = 1s) and surface temperature of 250 °C

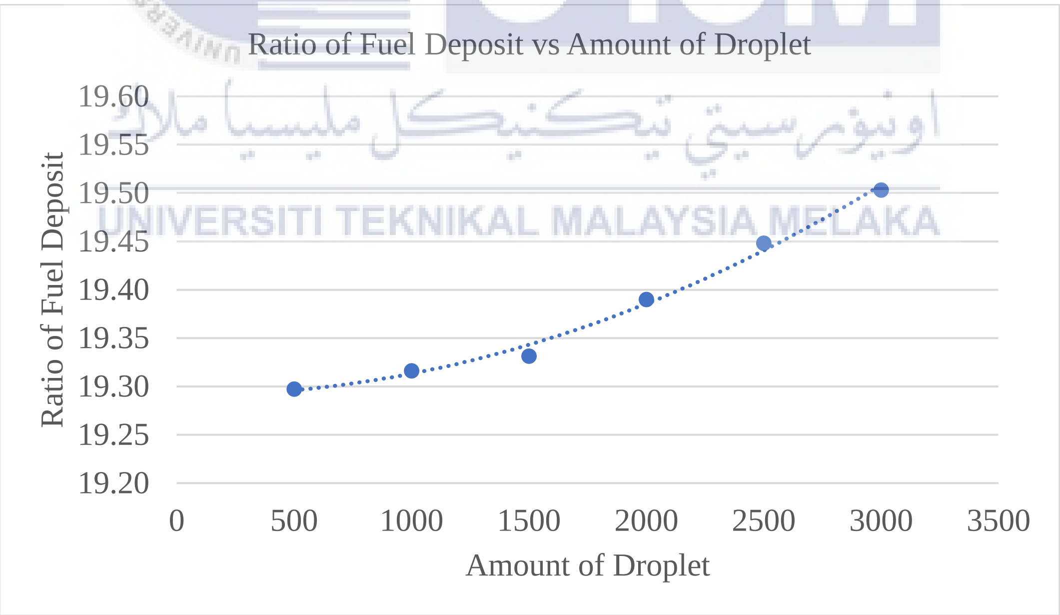

Figure 4. 2: Ratio of fuel deposit, $\frac{M_D}{m_D}$ at wet condition (time interval = 1s) and surface temperature of 250 °C

Table 4. 3: Total mass of diesel fuel deposit (mg) at wet condition (time interval = $1s$) and surface temperature of 357 °C

Amount of Droplet	**Mass of Fuel Deposit, M_D (mg)**				**Ratio of Fuel Deposit, $\frac{M_D}{m_D}$**
	1	**2**	**3**	**Average**	
500	110.1494	110.1496	110.1497	110.1496	19.2906
1000	110.151	110.1514	110.1517	110.1514	19.2910
1500	110.1533	110.153	110.1533	110.1532	19.2913
2000	110.1551	110.1551	110.1559	110.1554	19.2917
2500	110.1578	110.1576	110.1578	110.1577	19.2921
3000	110.1586	110.1586	110.1592	110.1588	19.2923

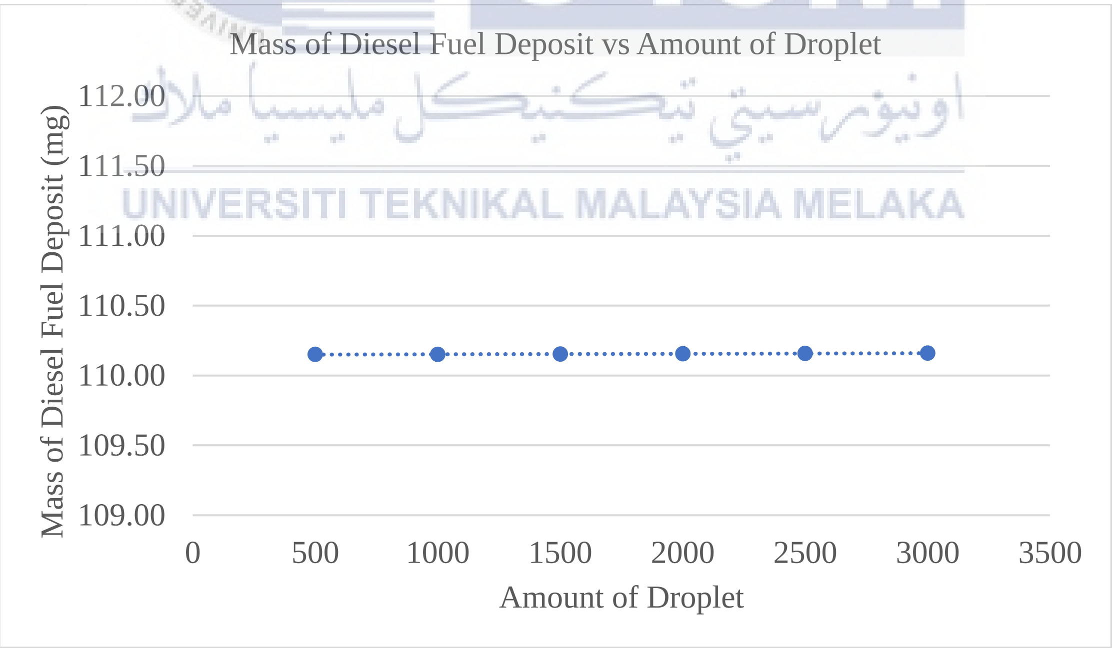

Figure 4. 3: Mass of diesel fuel deposit, M_D at wet condition (time interval = $1s$) and surface temperature of 357 °C

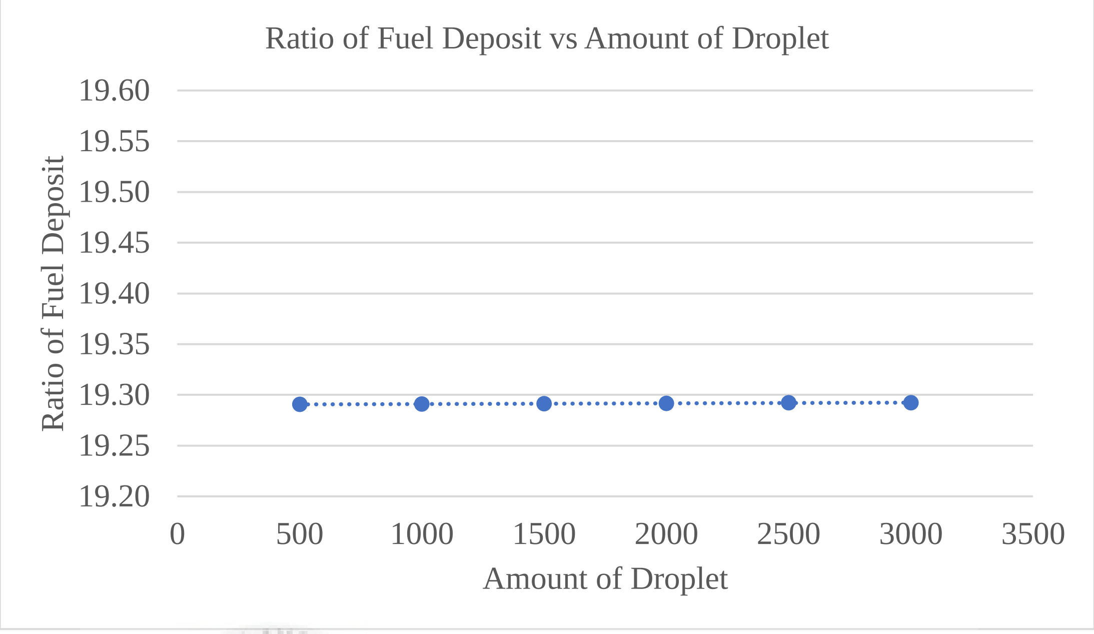

Figure 4. 4: Ratio of fuel deposit, $\frac{M_D}{m_D}$ at wet condition (time interval = $1s$) and surface temperature of 357 °C

Table 4. 4: Total mass of diesel fuel deposit (mg) at wet condition (time interval = $1s$) and surface temperature of 450 °C

Amount of Droplet	**Mass of Fuel Deposit, M_D (mg)**				**Ratio of Fuel Deposit, $\frac{M_D}{m_D}$**
	1	**2**	**3**	**Average**	
500	110.1184	110.1186	110.1181	110.1184	19.2852
1000	110.1198	110.1197	110.1195	110.1197	19.2854
1500	110.1202	110.1204	110.1203	110.1203	19.2855
2000	110.1214	110.1215	110.1216	110.1215	19.2857
2500	110.123	110.1229	110.1228	110.1229	19.2860
3000	110.1256	110.1258	110.1255	110.1256	19.2864

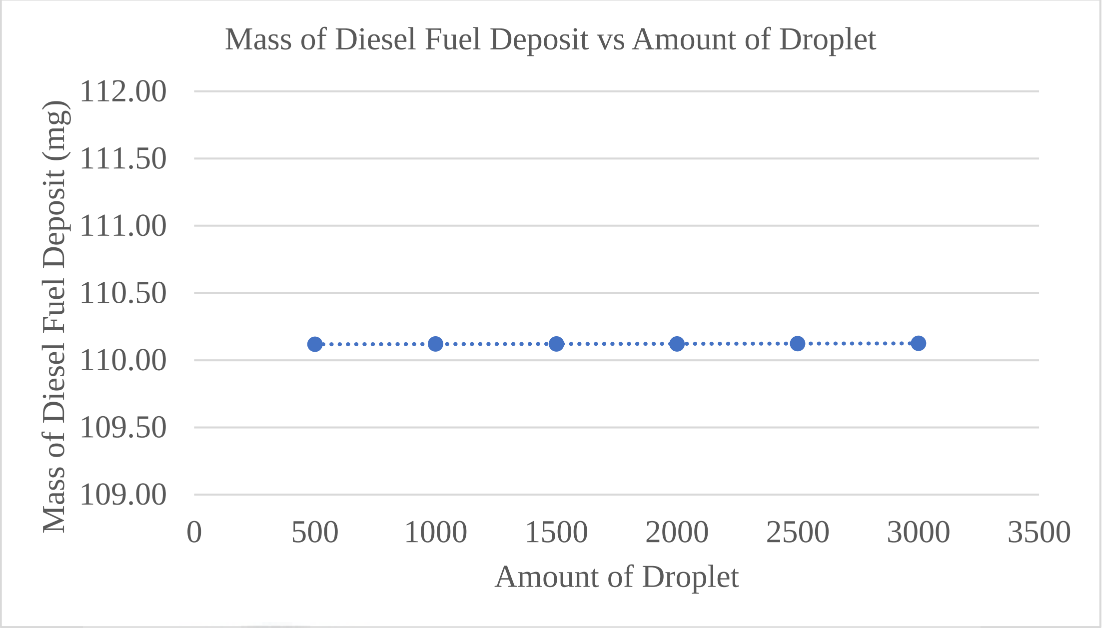

Figure 4. 5: Mass of diesel fuel deposit, M_D at wet condition (time interval = $1s$) and surface temperature of 450 °C

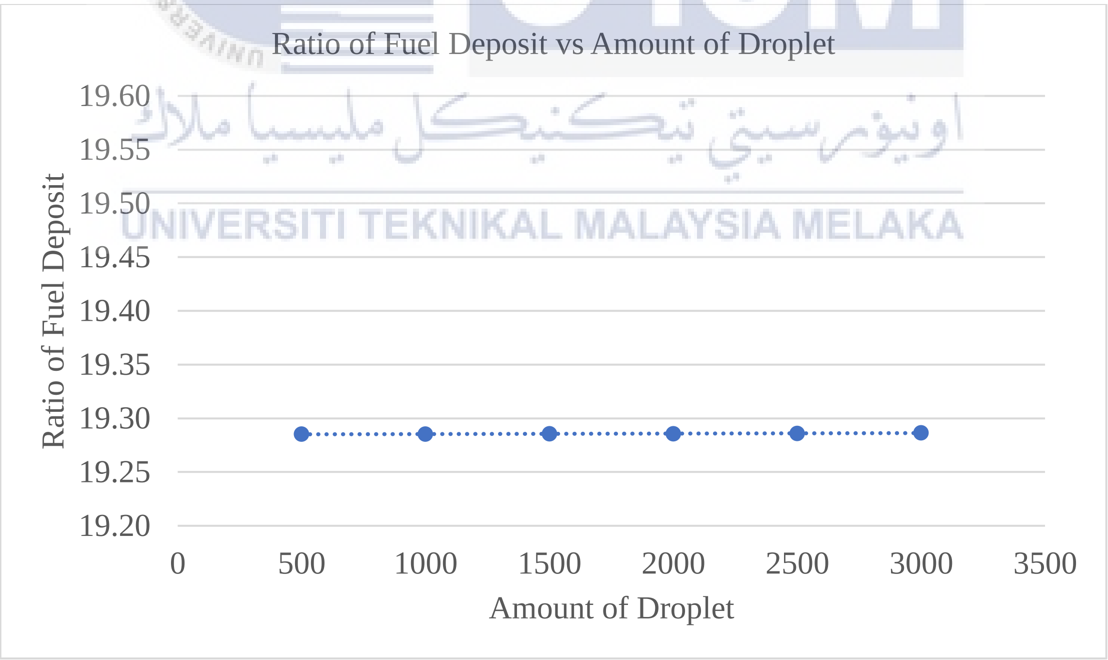

Figure 4. 6: Ratio of fuel deposit, $\frac{M_D}{m_D}$ at wet condition (time interval = $1s$) and surface temperature of 450 °C

Table 4. 5: Total mass of diesel fuel deposit (mg) at wet condition (time interval = 1s) and surface temperature of 600 °C

Amount of Droplet	**Mass of Fuel Deposit, M_D (mg)**				**Ratio of Fuel Deposit, $\frac{M_D}{m_D}$**
	1	**2**	**3**	**Average**	
500	110.1105	110.1105	110.1102	110.1104	19.2838
1000	110.1111	110.1113	110.1116	110.1113	19.2839
1500	110.1124	110.1121	110.1123	110.1123	19.2841
2000	110.1134	110.1131	110.1133	110.1133	19.2843
2500	110.1146	110.1147	110.1149	110.1147	19.2845
3000	110.1162	110.1154	110.1152	110.1156	19.2847

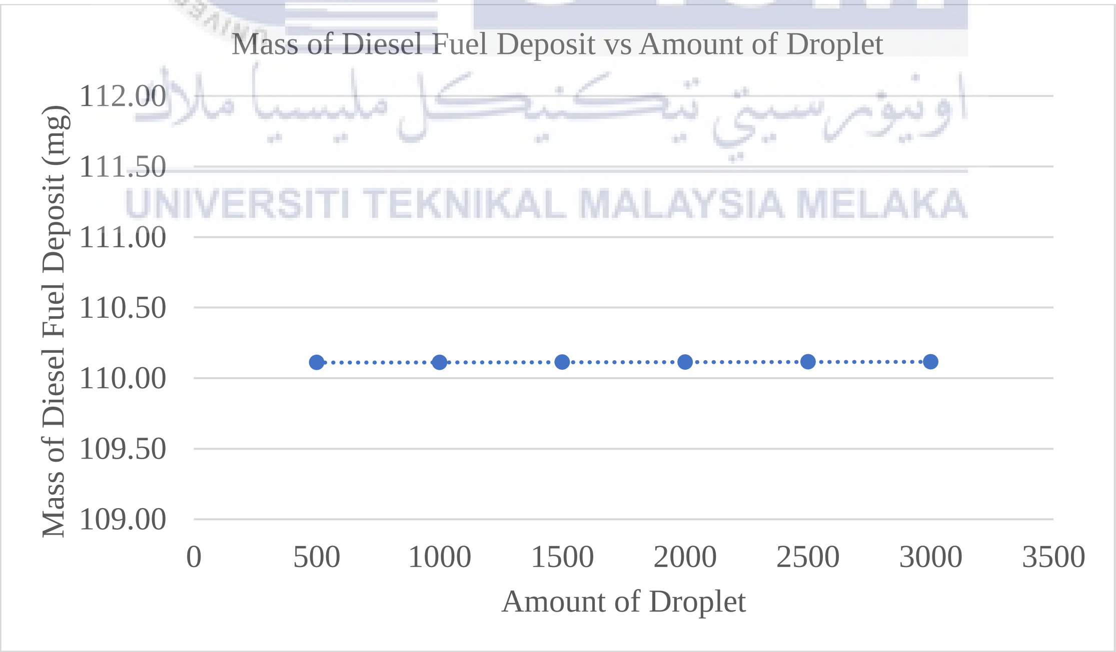

Figure 4. 7: Mass of diesel fuel deposit, M_D at wet condition (time interval = 1s) and surface temperature of 600 °C

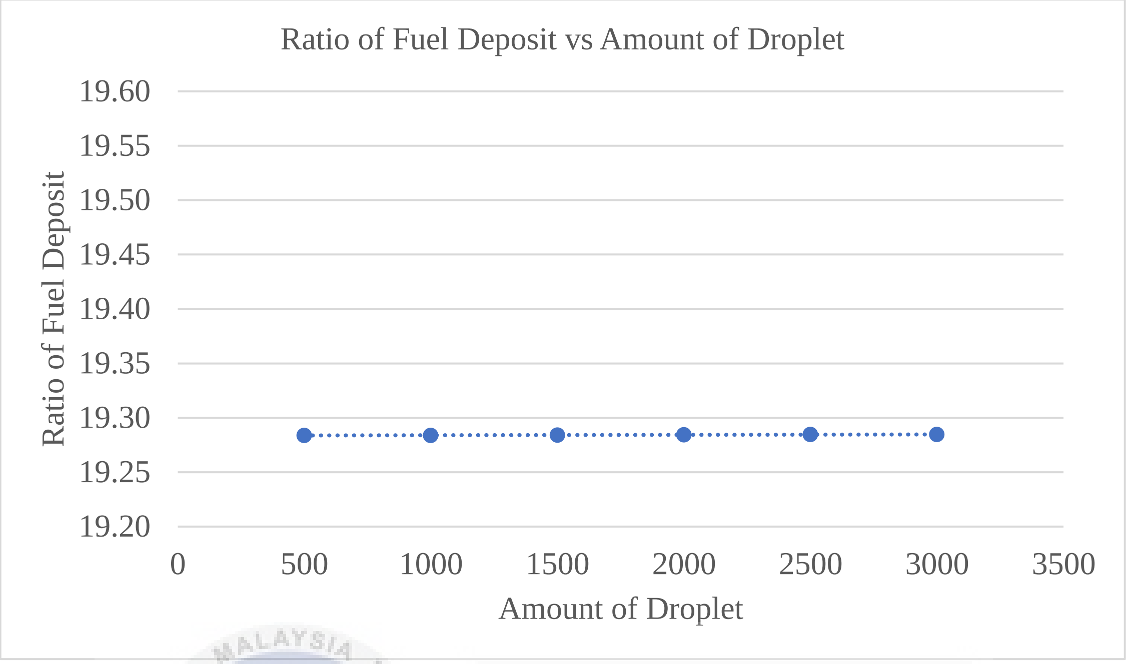

Figure 4. 8: Ratio of fuel deposit, $\frac{M_D}{m_D}$ at wet condition (time interval = $1s$) and surface temperature of 600 °C

Table 4. 6: Total mass of diesel fuel deposit (mg) at dry condition (time interval = $5s$) and surface temperature of 250 °C

Amount of Droplet	**Mass of Fuel Deposit, M_D (mg)**				**Ratio of Fuel Deposit, $\frac{M_D}{m_D}$**
	1	**2**	**3**	**Average**	
500	110.1177	110.1107	110.1169	110.1151	19.2846
1000	110.1565	110.1564	110.1563	110.1564	19.2918
1500	110.2957	110.2958	110.296	110.2958	19.3163
2000	110.3388	110.3582	110.3587	110.3519	19.3261
2500	110.4186	110.418	110.4176	110.4181	19.3377
3000	110.4527	110.4528	110.4523	110.4526	19.3437

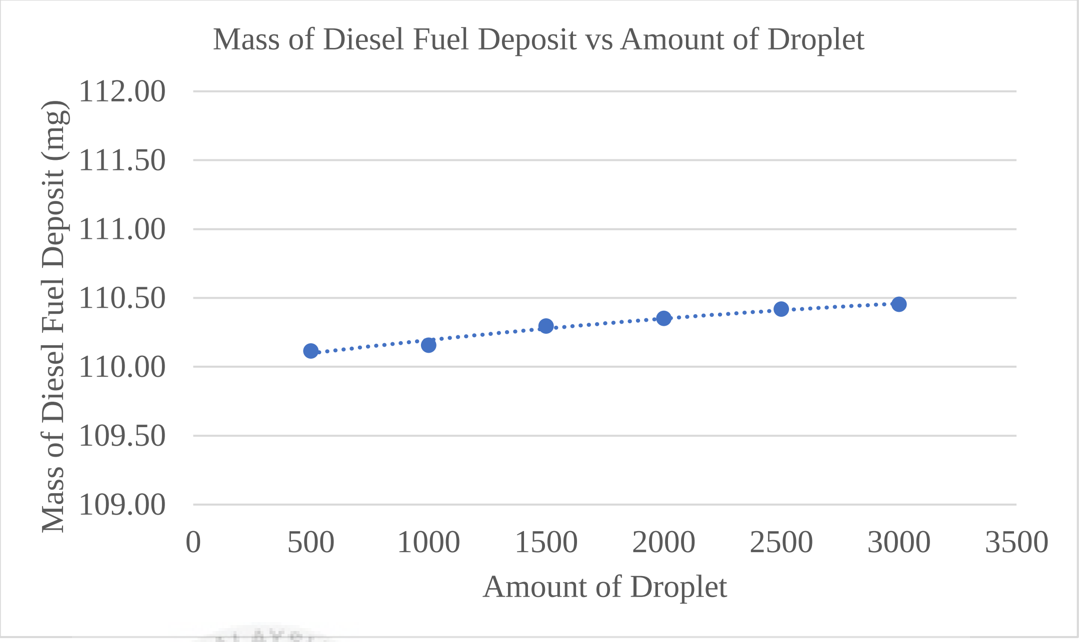

Figure 4. 9: Mass of diesel fuel deposit, M_D at dry condition (time interval = $5s$) and surface temperature of 250 °C

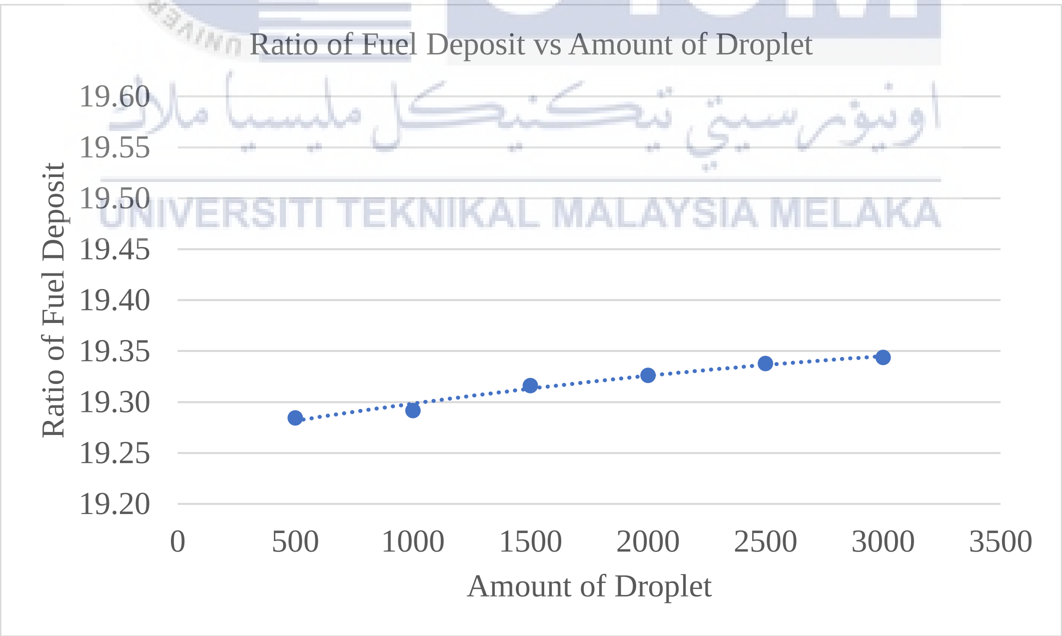

Figure 4. 10: Ratio of fuel deposit, $\frac{M_D}{m_D}$ at dry condition (time interval = $5s$) and surface temperature of 250 °C

Table 4. 7: Total mass of diesel fuel deposit (mg) at dry condition (time interval = $5s$) and surface temperature of 357 °C

Amount of Droplet	**Mass of Fuel Deposit, M_D (mg)**				**Ratio of Fuel Deposit, $\frac{M_D}{m_D}$**
	1	**2**	**3**	**Average**	
500	110.0816	110.082	110.0818	110.0818	19.2788
1000	110.0823	110.0817	110.0822	110.0821	19.2788
1500	110.0825	110.0825	110.0827	110.0826	19.2789
2000	110.0831	110.083	110.0829	110.083	19.2790
2500	110.0839	110.084	110.0839	110.0839	19.2791
3000	110.0842	110.0843	110.0842	110.0842	19.2792

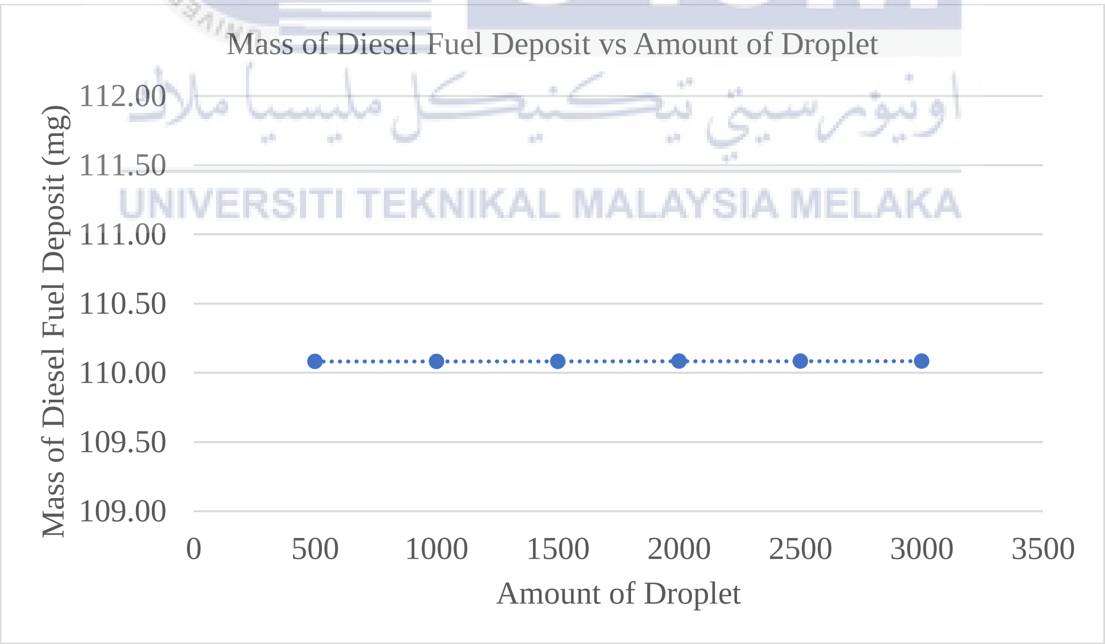

Figure 4. 11: Mass of diesel fuel deposit, M_D at dry condition (time interval = $5s$) and surface temperature of 357 °C

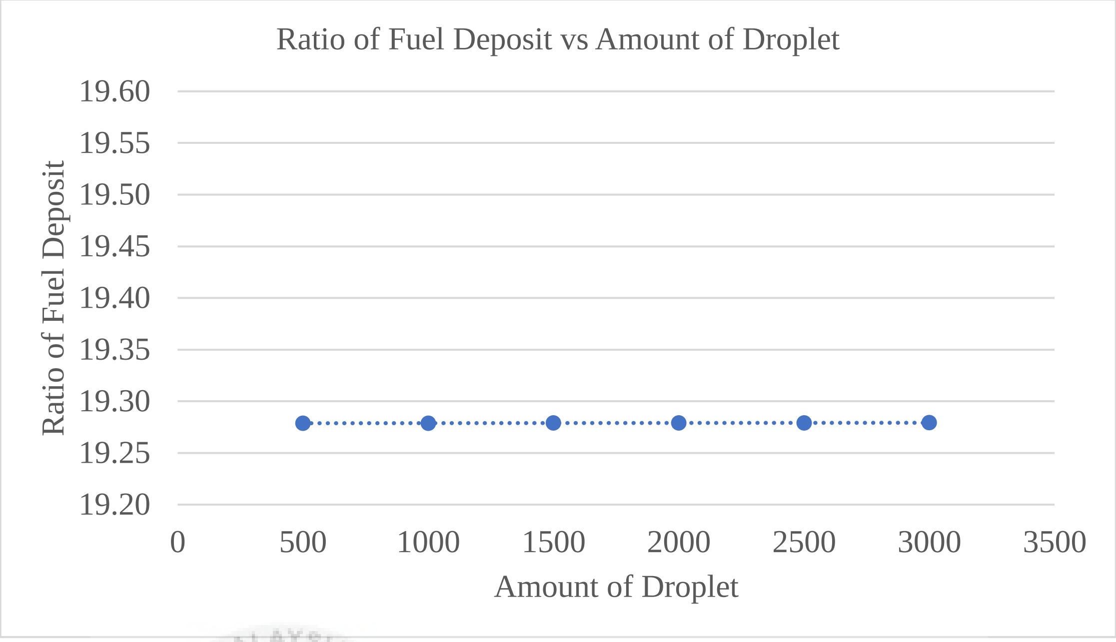

Figure 4. 12: Ratio of fuel deposit, $\frac{M_D}{m_D}$ at dry condition (time interval = $5s$) and surface temperature of 357 °C

Table 4. 8: Total mass of diesel fuel deposit (mg) at dry condition (time interval = $5s$) and surface temperature of 450 °C

Amount of Droplet	**Mass of Fuel Deposit, M_D (mg)**				**Ratio of Fuel Deposit, $\frac{M_D}{m_D}$**
	1	**2**	**3**	**Average**	
500	110.0612	110.0613	110.0614	110.0613	19.2752
1000	110.0617	110.0618	110.0619	110.0618	19.2753
1500	110.0621	110.0623	110.0624	110.0623	19.2754
2000	110.0626	110.0627	110.0627	110.0627	19.2754
2500	110.0634	110.0635	110.0634	110.0634	19.2756
3000	110.0638	110.064	110.0637	110.0638	19.2756

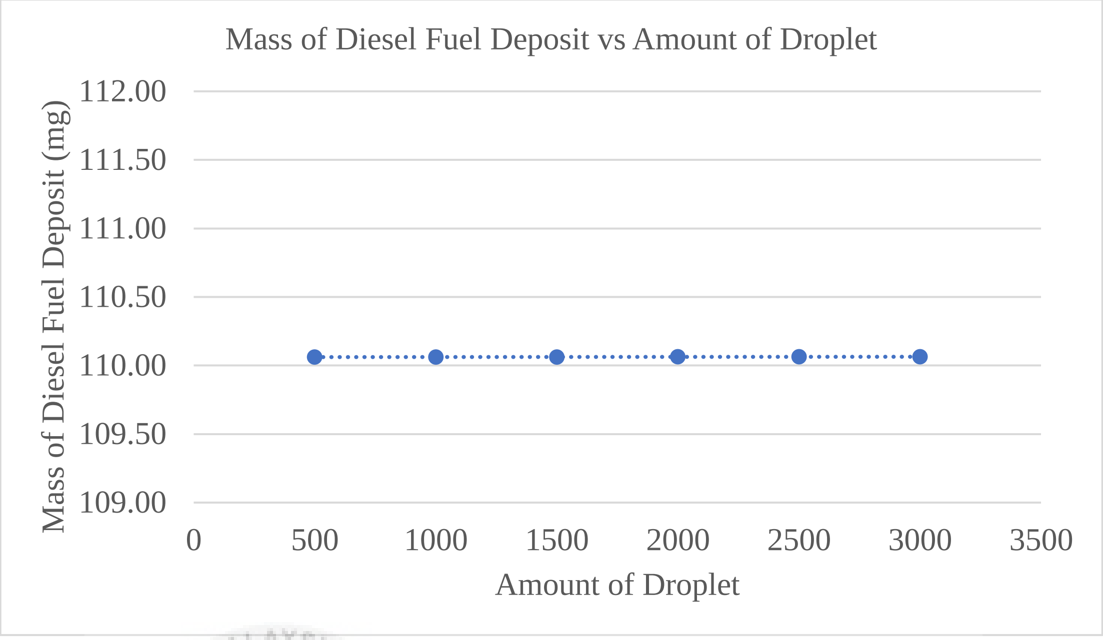

Figure 4. 13: Mass of diesel fuel deposit, M_D at dry condition (time interval = $5s$) and surface temperature of 450 °C

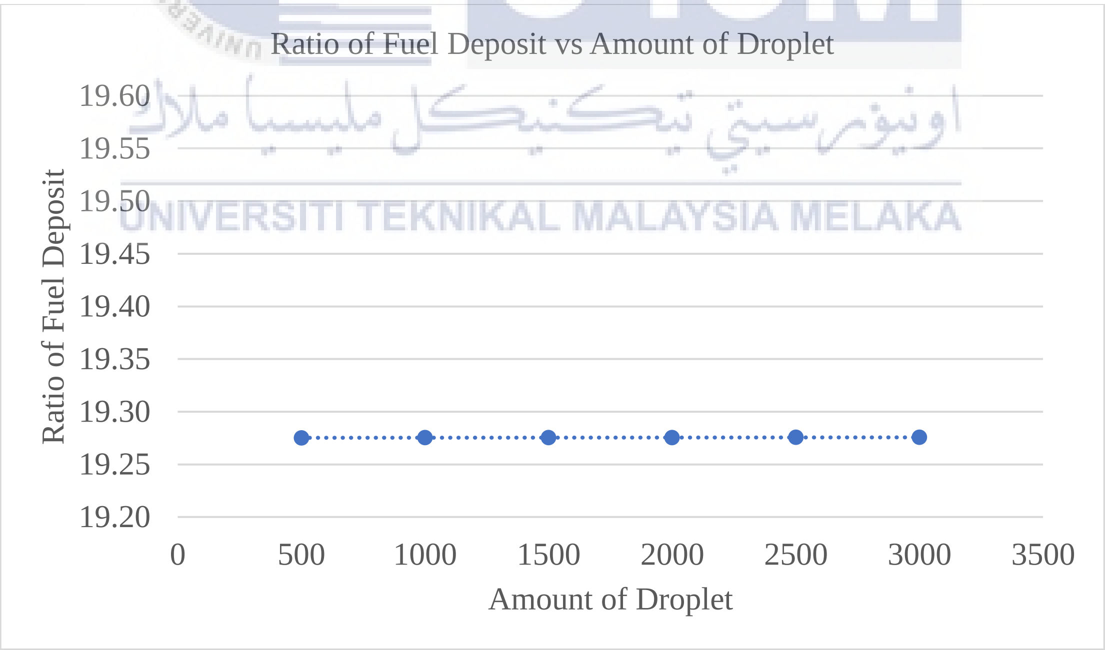

Figure 4. 14: Ratio of fuel deposit, $\frac{M_D}{m_D}$ at dry condition (time interval = $5s$) and surface temperature of 450 °C

Table 4. 9: Total mass of diesel fuel deposit (mg) at dry condition (time interval = $5s$) and surface temperature of 600 °C

Amount of Droplet	**Mass of Fuel Deposit, M_D (mg)**				**Ratio of Fuel Deposit, $\frac{M_D}{m_D}$**
	1	**2**	**3**	**Average**	
500	110.0411	110.041	110.0412	110.0411	19.2716
1000	110.0418	110.0418	110.0417	110.0418	19.2718
1500	110.0423	110.0424	110.0423	110.0423	19.2719
2000	110.0428	110.0427	110.0426	110.0427	19.2719
2500	110.0435	110.0433	110.0431	110.0433	19.2720
3000	110.044	110.0439	110.0438	110.0439	19.2721

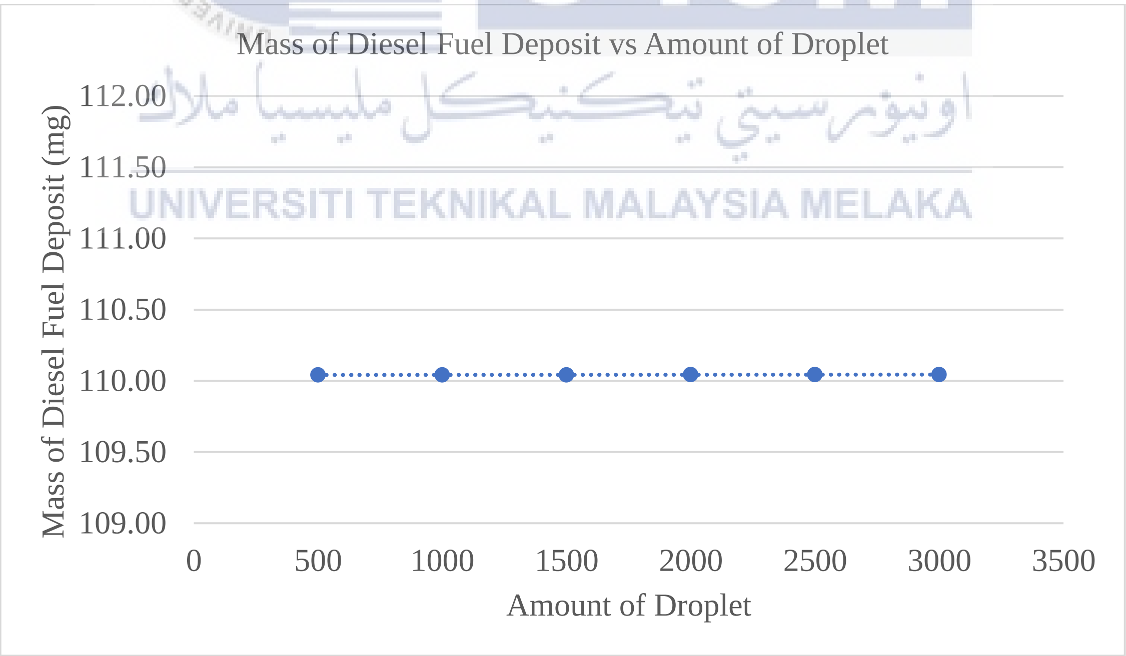

Figure 4. 15: Mass of diesel fuel deposit, M_D at dry condition (time interval = $5s$) and surface temperature of 600 °C

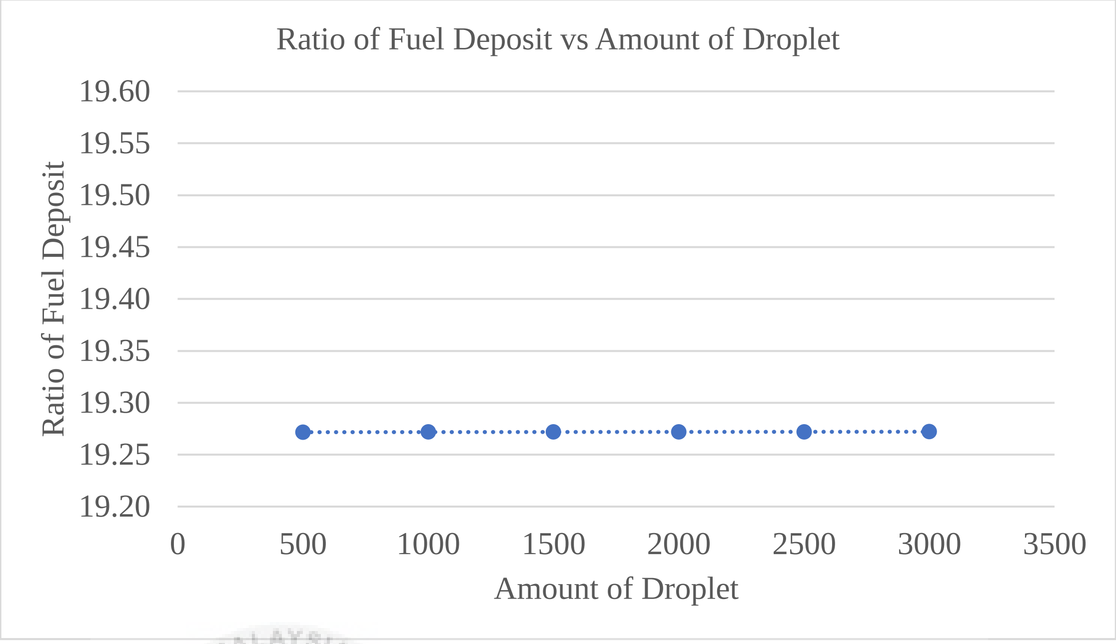

Figure 4. 16: Ratio of fuel deposit, $\frac{M_D}{m_D}$ at dry condition (time interval = $5s$) and surface temperature of 600 °C

4.2.4.2 Bio-diesel Fuel (B20)

Table 4. 10: Total mass of B20 fuel deposit (mg) at wet condition (time interval = $1s$) and surface temperature of 250 °C

Amount of Droplet	**Mass of Fuel Deposit, M_D (mg)**				**Ratio of Fuel Deposit, $\frac{M_D}{m_D}$**
	1	**2**	**3**	**Average**	
500	109.6604	109.6602	109.6603	109.6603	18.5865
1000	109.6695	109.6688	109.669	109.6691	18.5880
1500	109.6871	109.6875	109.6873	109.6873	18.5911
2000	109.7446	109.7447	109.7445	109.7446	18.6008
2500	109.8266	109.8268	109.8261	109.8265	18.6147
3000	109.929	109.9297	109.9292	109.9293	18.6321

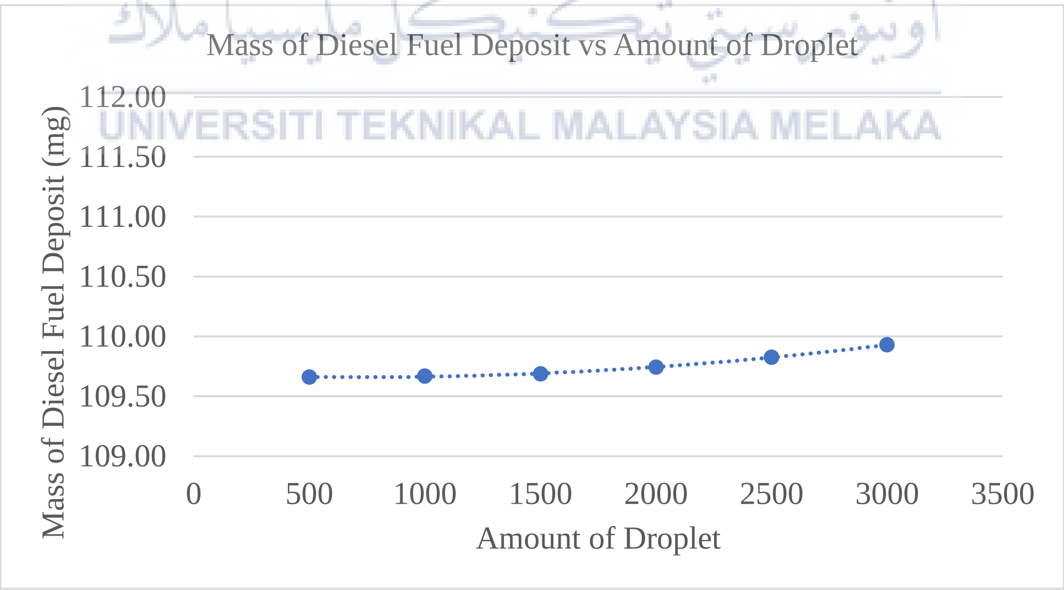

Figure 4. 17: Mass of B20 fuel deposit, M_D at wet condition (time interval = $1s$) and surface temperature of 250 °C

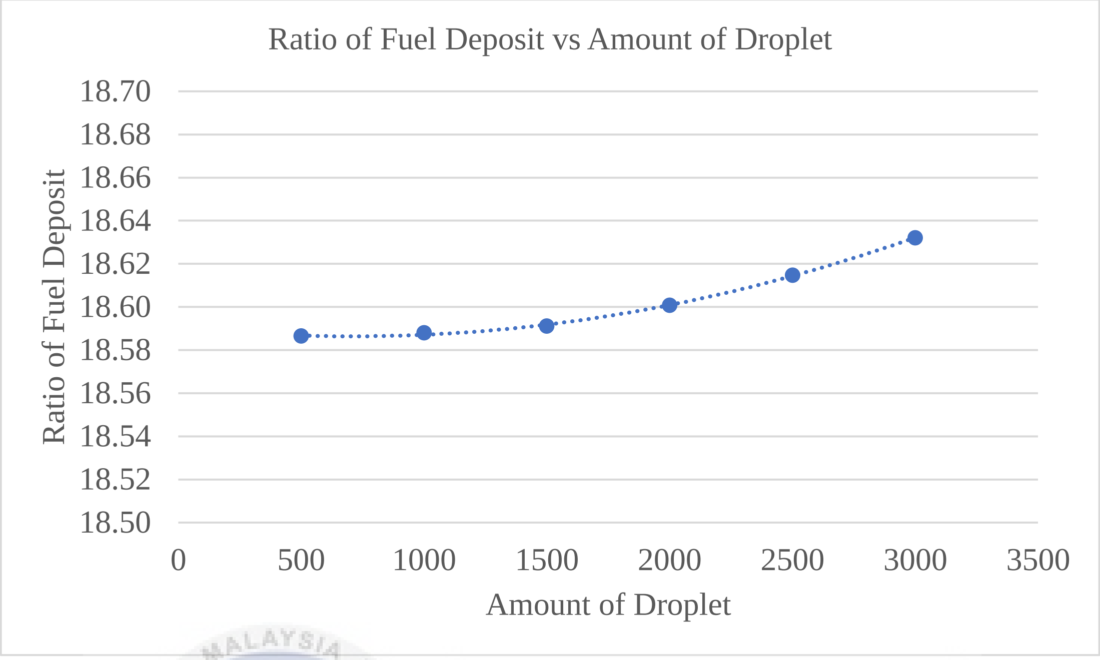

Figure 4. 18: Ratio of fuel deposit, $\frac{M_D}{m_D}$ at wet condition (time interval = $1s$) and surface temperature of 250 °C

Table 4. 11: Total mass of B20 fuel deposit (mg) at wet condition (time interval = $1s$) and surface temperature of 357 °C

Amount of Droplet	**Mass of Fuel Deposit, M_D (mg)**				**Ratio of Fuel Deposit, $\frac{M_D}{m_D}$**
	1	**2**	**3**	**Average**	
500	109.6326	109.6327	109.6325	109.6326	18.5818
1000	109.6338	109.6341	109.6337	109.6339	18.5820
1500	109.6355	109.6356	109.6355	109.6355	18.5823
2000	109.6363	109.6365	109.6369	109.6366	18.5825
2500	109.6379	109.638	109.6378	109.6379	18.5827
3000	109.6394	109.6393	109.6395	109.6394	18.5829

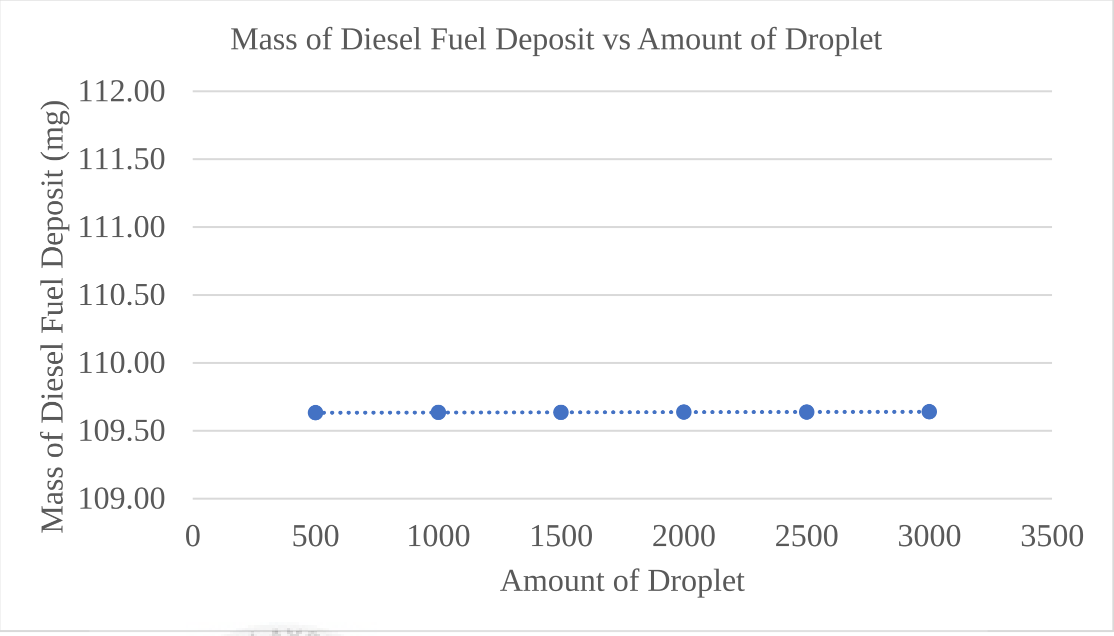

Figure 4. 19: Mass of B20 fuel deposit, M_D at wet condition (time interval = 1s) and surface temperature of 357 °C

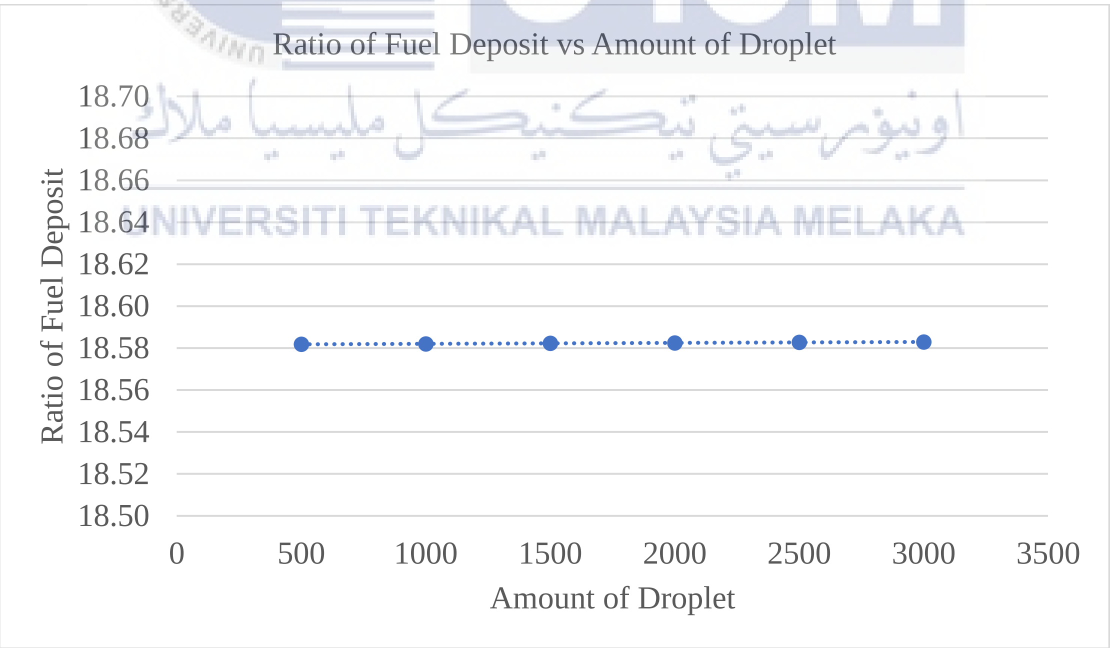

Figure 4. 20: Ratio of fuel deposit, $\frac{M_D}{m_D}$ at wet condition (time interval = 1s) and surface temperature of 357 °C

Table 4. 12: Total mass of B20 fuel deposit (mg) at wet condition (time interval = $1s$) and surface temperature of 450 °C

Amount of Droplet	**Mass of Fuel Deposit, M_D (mg)**				**Ratio of Fuel Deposit, $\frac{M_D}{m_D}$**
	1	**2**	**3**	**Average**	
500	109.5915	109.5914	109.5913	109.5914	18.5748
1000	109.5918	109.5919	109.5918	109.5918	18.5749
1500	109.5923	109.5922	109.5922	109.5922	18.5749
2000	109.5928	109.5927	109.5928	109.5928	18.5751
2500	109.5931	109.5932	109.5931	109.5931	18.5751
3000	109.5938	109.5938	109.5939	109.5938	18.5752

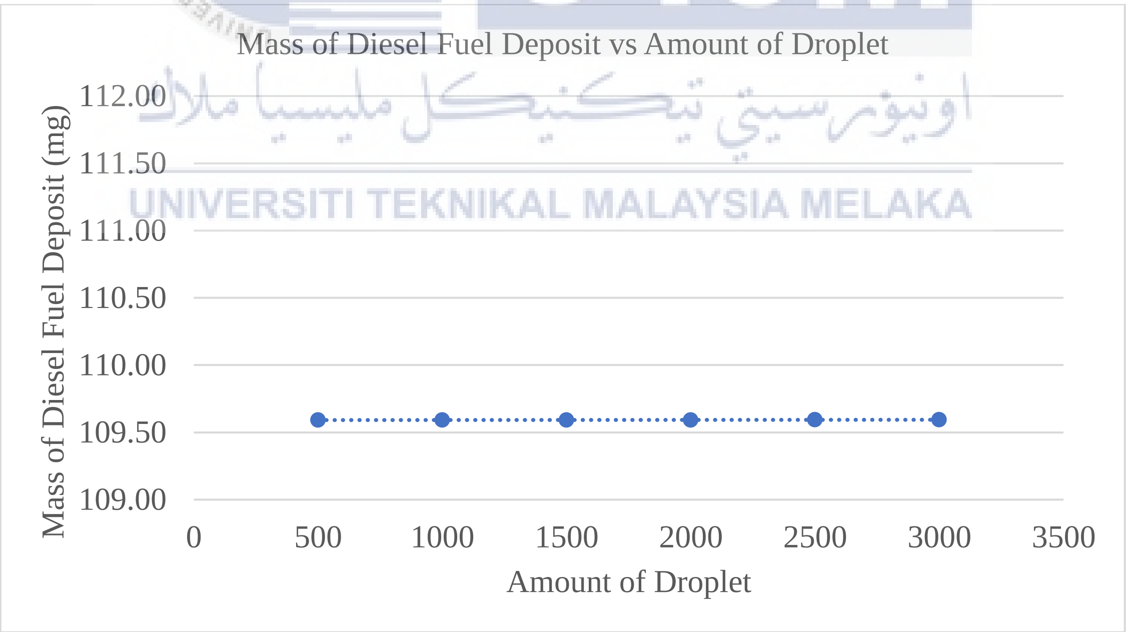

Figure 4. 21: Mass of B20 fuel deposit, M_D at wet condition (time interval = $1s$) and surface temperature of 450 °C

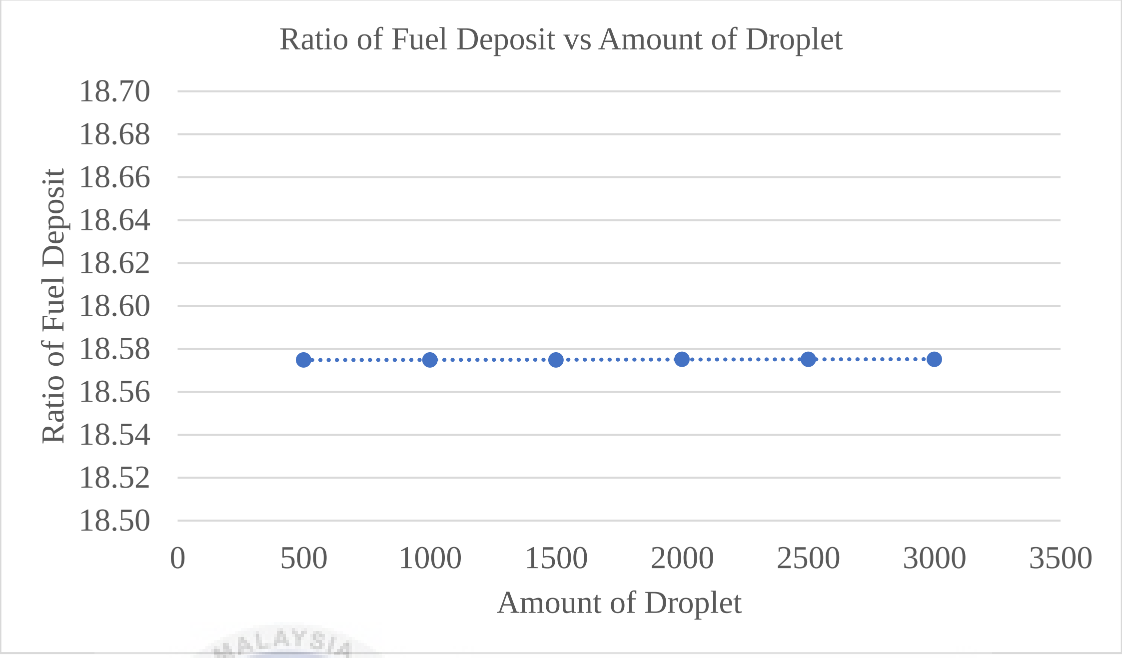

Figure 4. 22: Ratio of fuel deposit, $\frac{M_D}{m_D}$ at wet condition (time interval = $1s$) and surface temperature of 450 °C

Table 4. 13: Total mass of B20 fuel deposit (mg) at wet condition (time interval = $1s$) and surface temperature of 600 °C

Amount of Droplet	**Mass of Fuel Deposit, M_D (mg)**				**Ratio of Fuel Deposit, $\frac{M_D}{m_D}$**
	1	**2**	**3**	**Average**	
500	109.5651	109.5653	109.5651	109.5652	18.5704
1000	109.5652	109.5653	109.5654	109.5653	18.5704
1500	109.5654	109.5654	109.5655	109.5654	18.5704
2000	109.5656	109.5655	109.5657	109.5656	18.5704
2500	109.5659	109.5658	109.5658	109.5658	18.5705
3000	109.5659	109.5661	109.5656	109.5659	18.5705

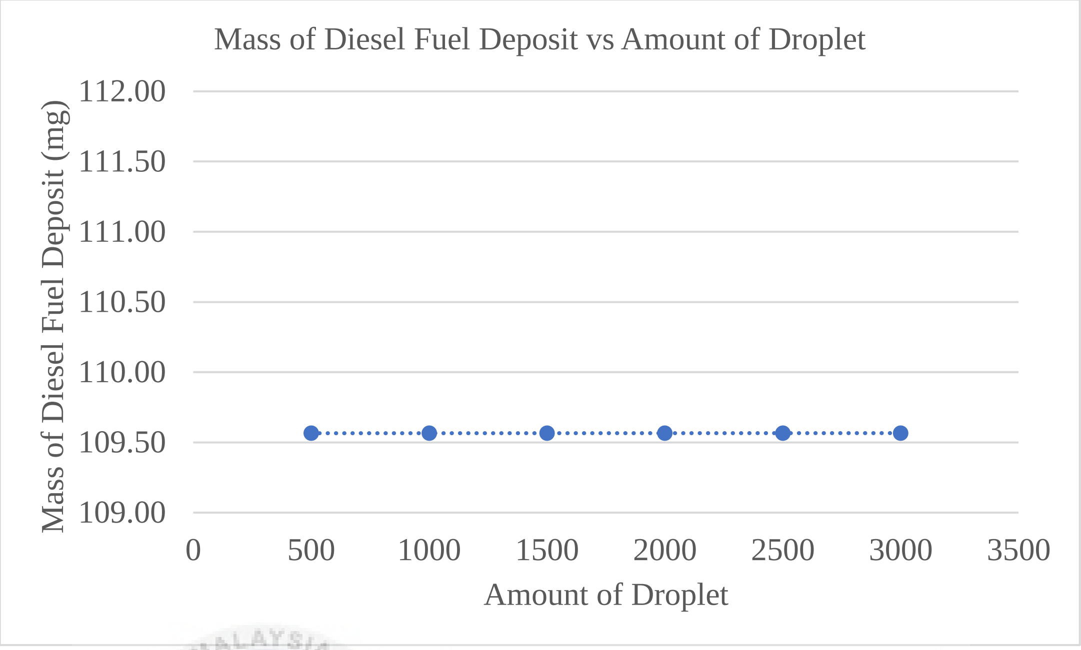

Figure 4. 23: Mass of B20 fuel deposit, M_D at wet condition (time interval = $1s$) and surface temperature of 600 °C

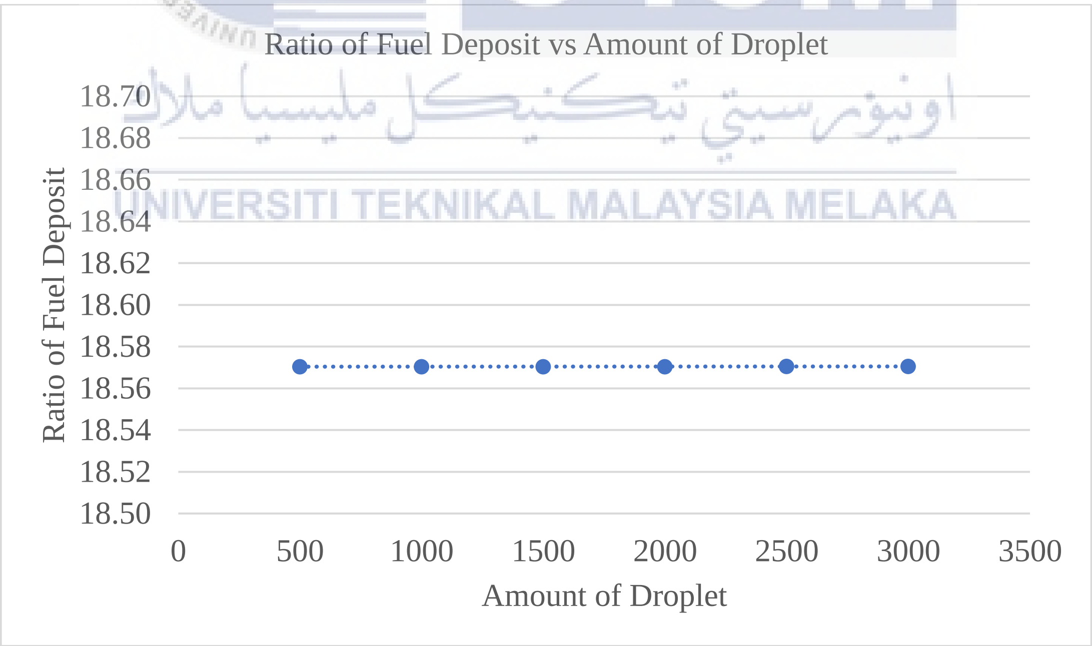

Figure 4. 24: Ratio of fuel deposit, $\frac{M_D}{m_D}$ at wet condition (time interval = $1s$) and surface temperature of 600 °C

Table 4. 14: Total mass of B20 fuel deposit (mg) at dry condition (time interval = $5s$) and surface temperature of 250 °C

Amount of Droplet	**Mass of Fuel Deposit, M_D (mg)**				**Ratio of Fuel Deposit, $\frac{M_D}{m_D}$**
	1	**2**	**3**	**Average**	
500	109.577	109.5773	109.5772	109.5772	18.5724
1000	109.5921	109.5922	109.5919	109.5921	18.5749
1500	109.6995	109.6994	109.6999	109.6996	18.5932
2000	109.8356	109.8358	109.8354	109.8356	18.6162
2500	109.9216	109.9218	109.9217	109.9217	18.6308
3000	109.9523	109.9523	109.952	109.9522	18.6360

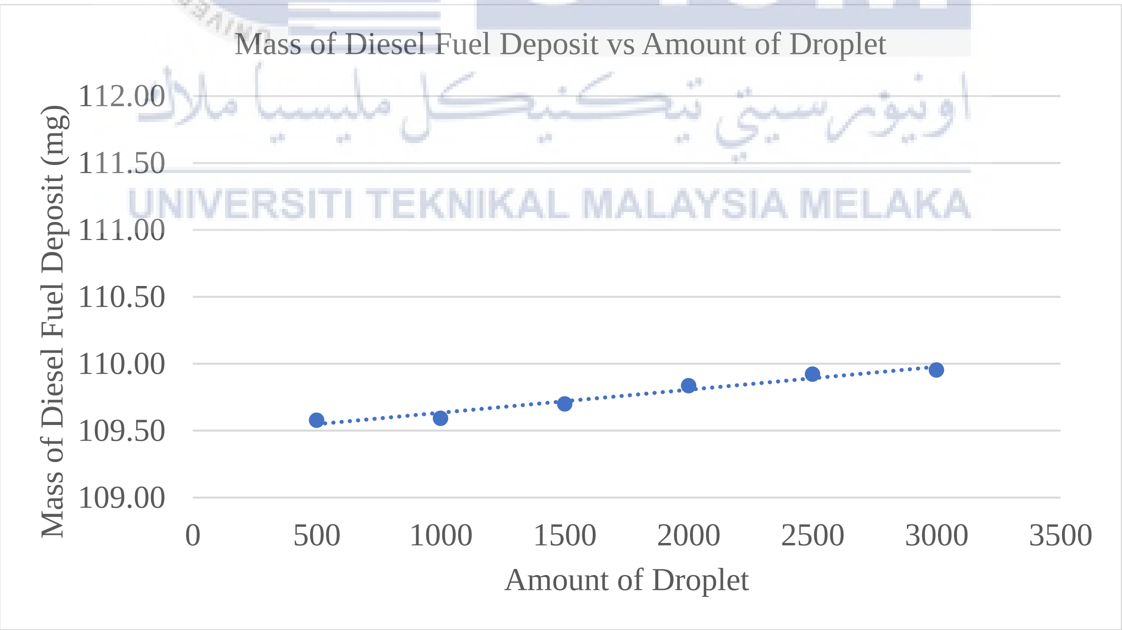

Figure 4. 25: Mass of B20 fuel deposit, M_D at dry condition (time interval = $5s$) and surface temperature of 250 °C

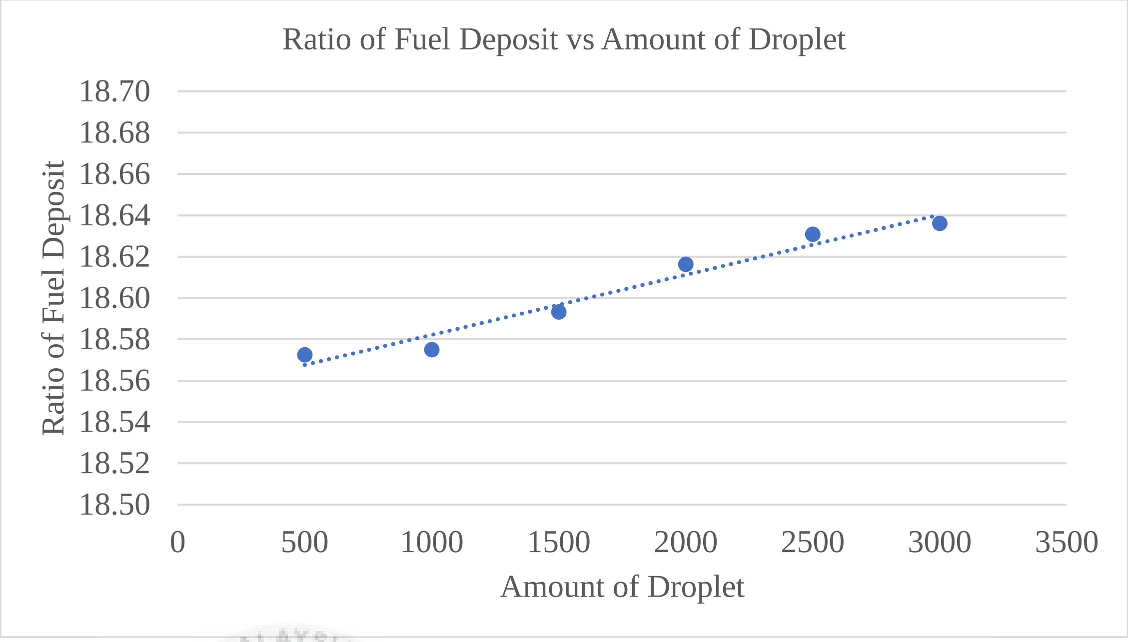

Figure 4. 26: Ratio of fuel deposit, $\frac{M_D}{m_D}$ at dry condition (time interval = $5s$) and surface temperature of 250 °C

Table 4. 15: Total mass of B20 fuel deposit (mg) at dry condition (time interval = $5s$) and surface temperature of 357 °C

Amount of Droplet	**Mass of Fuel Deposit, M_D (mg)**				**Ratio of Fuel Deposit, $\frac{M_D}{m_D}$**
	1	**2**	**3**	**Average**	
500	109.5223	109.5225	109.5225	109.5224	18.5631
1000	109.5231	109.5232	109.5231	109.5231	18.5632
1500	109.5243	109.5245	109.5244	109.5244	18.5635
2000	109.5268	109.5271	109.527	109.527	18.5639
2500	109.5281	109.528	109.5281	109.5281	18.5641
3000	109.5292	109.5291	109.5292	109.5292	18.5643

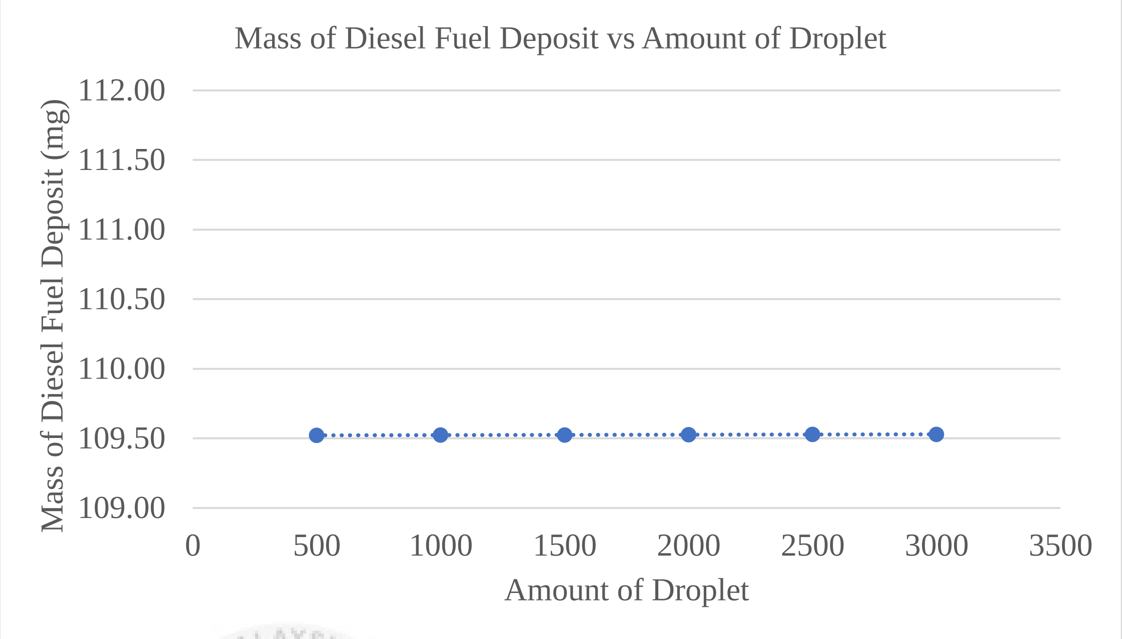

Figure 4. 27: Mass of B20 fuel deposit, M_D at dry condition (time interval = $5s$) and surface temperature of 357 °C

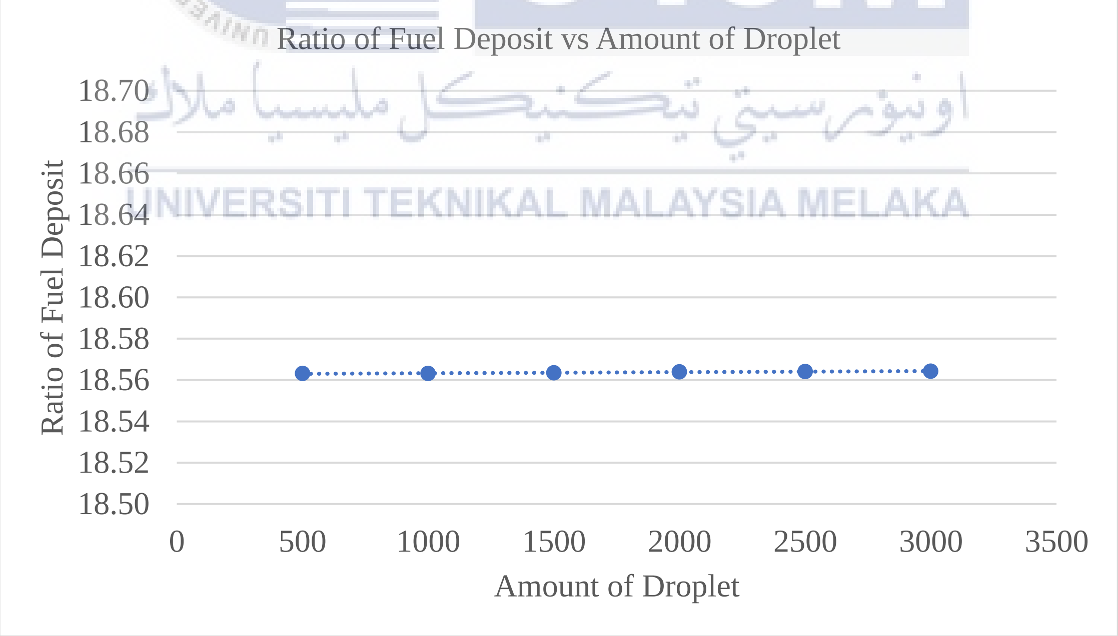

Figure 4. 28: Ratio of fuel deposit, $\frac{M_D}{m_D}$ at dry condition (time interval = $5s$) and surface temperature of 357 °C

Table 4. 16: Total mass of B20 fuel deposit (mg) at dry condition (time interval = 5s) and surface temperature of 450 °C

Amount of Droplet	**Mass of Fuel Deposit, M_D (mg)**				**Ratio of Fuel Deposit, $\frac{M_D}{m_D}$**
	1	**2**	**3**	**Average**	
500	109.4759	109.4757	109.4758	109.4758	18.5552
1000	109.4763	109.4763	109.4764	109.4763	18.5553
1500	109.4768	109.4766	109.4769	109.4768	18.5554
2000	109.4773	109.4771	109.4772	109.4772	18.5555
2500	109.4775	109.4777	109.4776	109.4776	18.5555
3000	109.4779	109.4779	109.4778	109.4779	18.5556

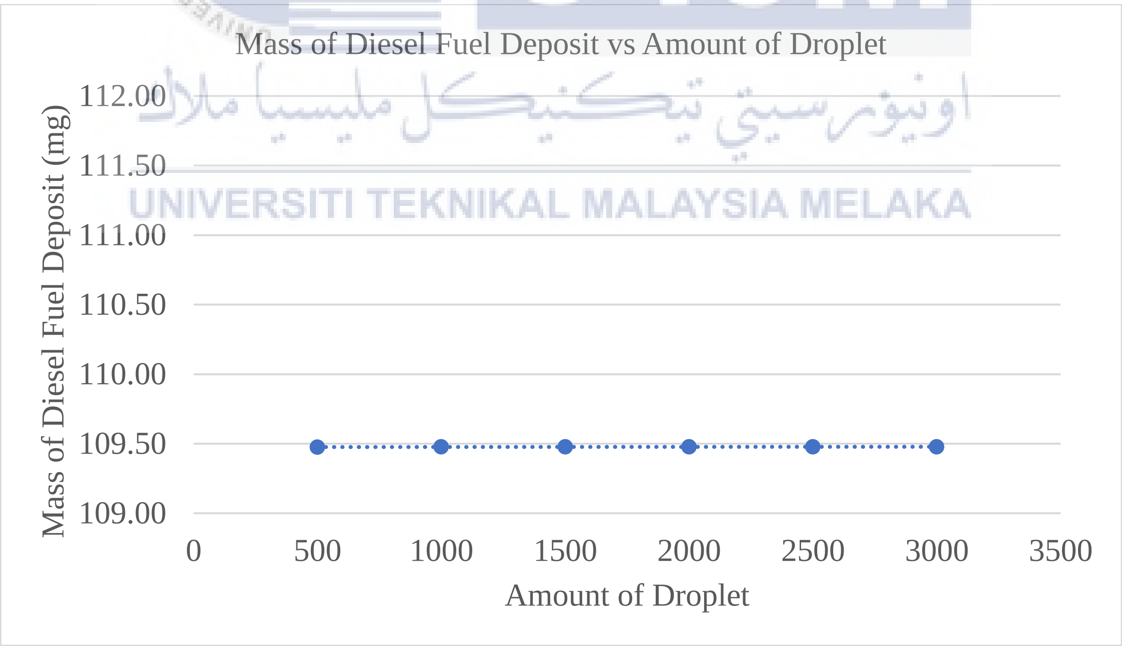

Figure 4. 29: Mass of B20 fuel deposit, M_D at dry condition (time interval = 5s) and surface temperature of 450 °C

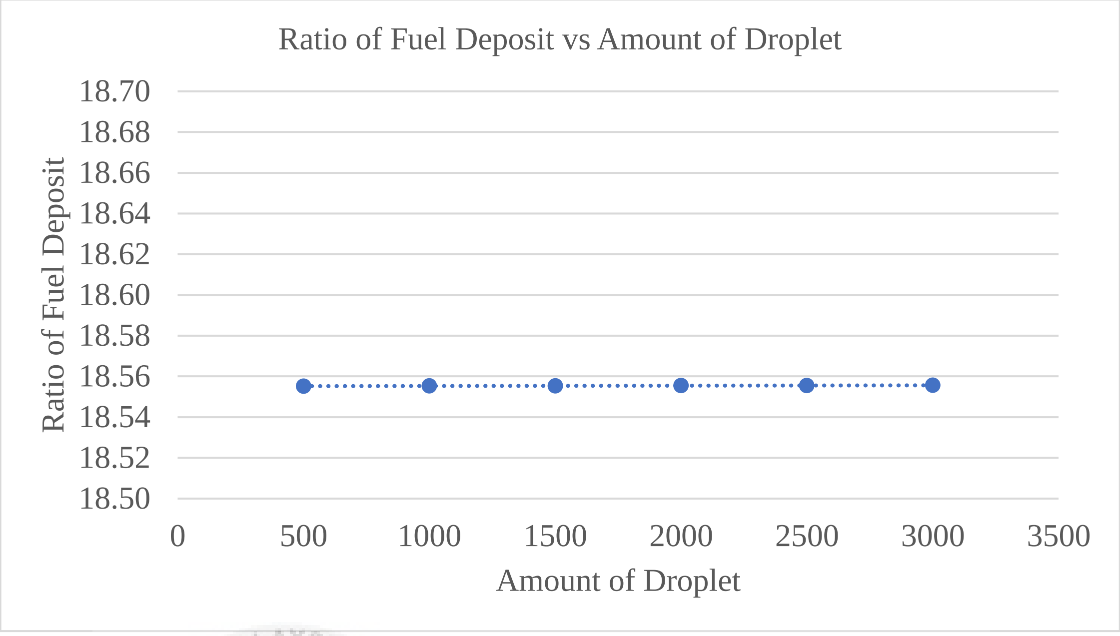

Figure 4. 30: Ratio of fuel deposit, $\frac{M_D}{m_D}$ at dry condition (time interval = $5s$) and surface temperature of 450 °C

Table 4. 17: Total mass of B20 fuel deposit (mg) at dry condition (time interval = $5s$) and surface temperature of 600 °C

Amount of Droplet	**Mass of Fuel Deposit, M_D (mg)**				**Ratio of Fuel Deposit, $\frac{M_D}{m_D}$**
	1	**2**	**3**	**Average**	
500	109.4441	109.444	109.4441	109.4441	18.5498
1000	109.4443	109.4442	109.4443	109.4443	18.5499
1500	109.4445	109.4444	109.4444	109.4444	18.5499
2000	109.4446	109.4446	109.4445	109.4446	18.5499
2500	109.4447	109.4449	109.4448	109.4448	18.5500
3000	109.4449	109.445	109.4451	109.445	18.5500

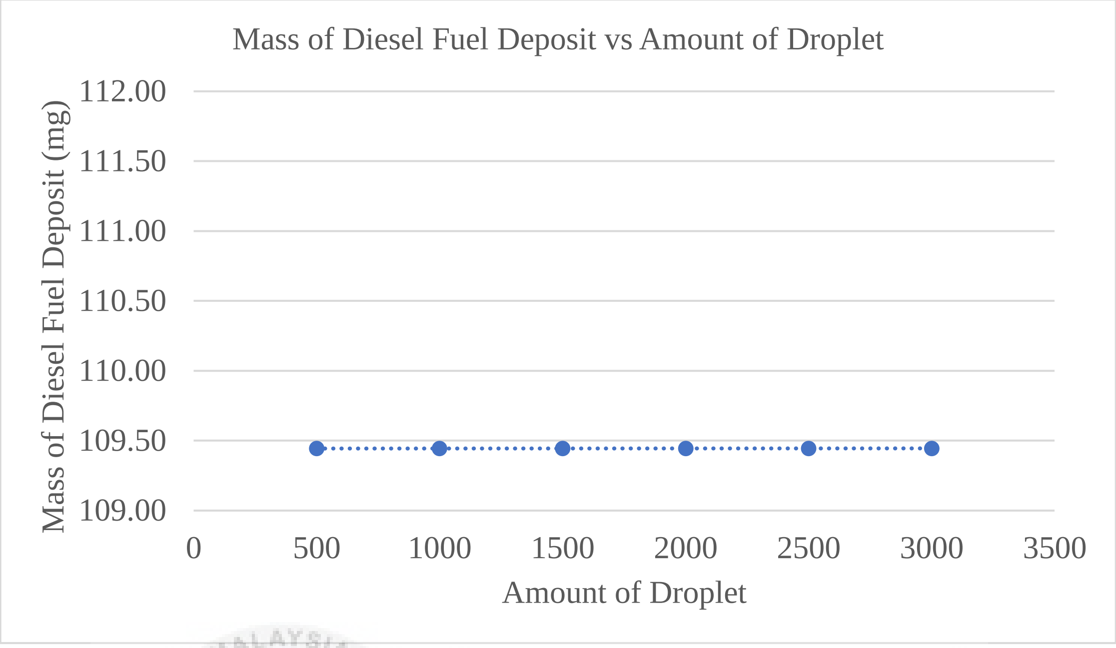

Figure 4. 31: Mass of B20 fuel deposit, M_D at dry condition (time interval = $5s$) and surface temperature of 600 °C

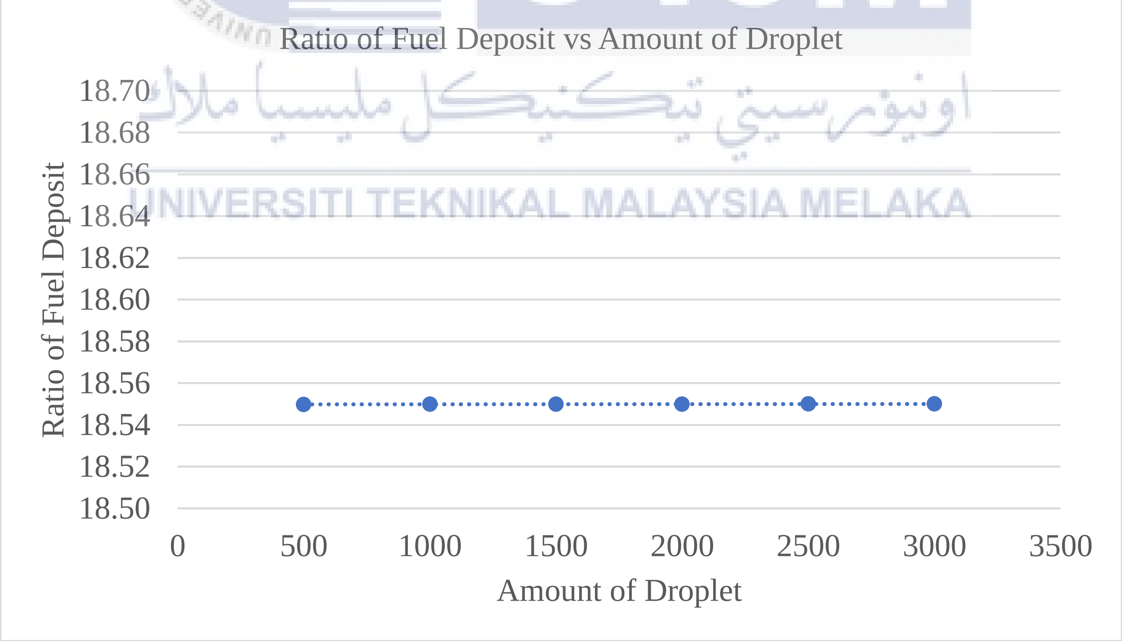

Figure 4. 32: Ratio of fuel deposit, $\frac{M_D}{m_D}$ at dry condition (time interval = $5s$) and surface temperature of 600 °C

4.2.5 Ratio of Fuel Deposit for Diesel and Bio-diesel Fuel Deposit

The results from the Table 4.2 to Table 4.17 can be summarized further by plotting graph of ratio of fuel deposit, $\frac{M_D}{m_D}$ for diesel and bio-diesel fuel deposit at different surface temperatures after 3000 droplets. The surface temperatures are 250 °C, 357 °C, 450 °C and 600 °C.

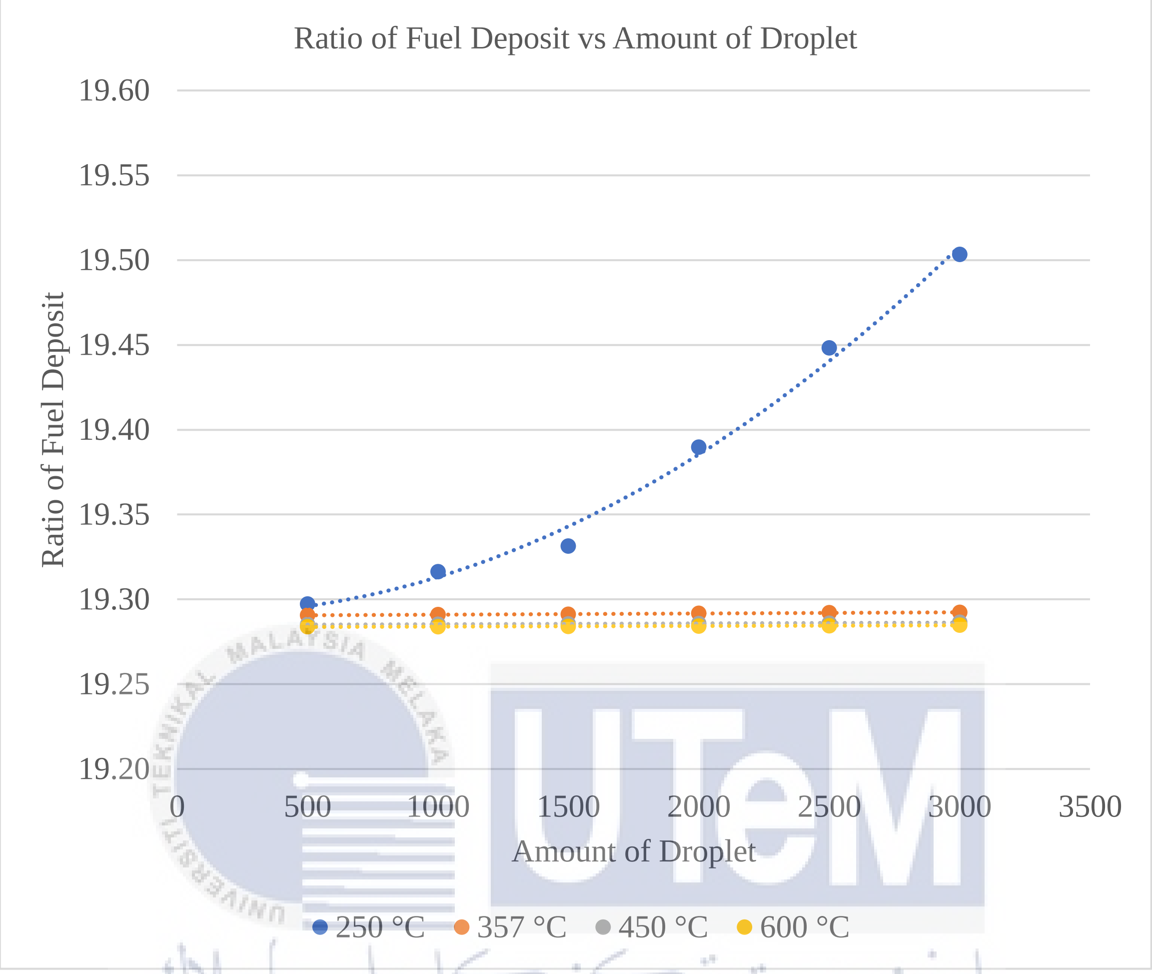

Figure 4. 33: Ratio of fuel deposit, $\frac{M_D}{m_D}$ of diesel fuel at wet condition and surface temperature of 250 °C, 357 °C, 450 °C and 600 °C

Based on graph 4.33, at wet condition, the ratio of fuel deposit, $\frac{M_D}{m_D}$ of diesel fuel deposit at 250 °C surface temperature is increasing with the amount of droplet, N_D. Diesel fuel deposit at 250 °C have the highest $\frac{M_D}{m_D}$, followed by diesel fuel deposit at 357 °C and 450 °C. The lowest $\frac{M_D}{m_D}$ is diesel fuel deposit at surface temperature of 600 °C.

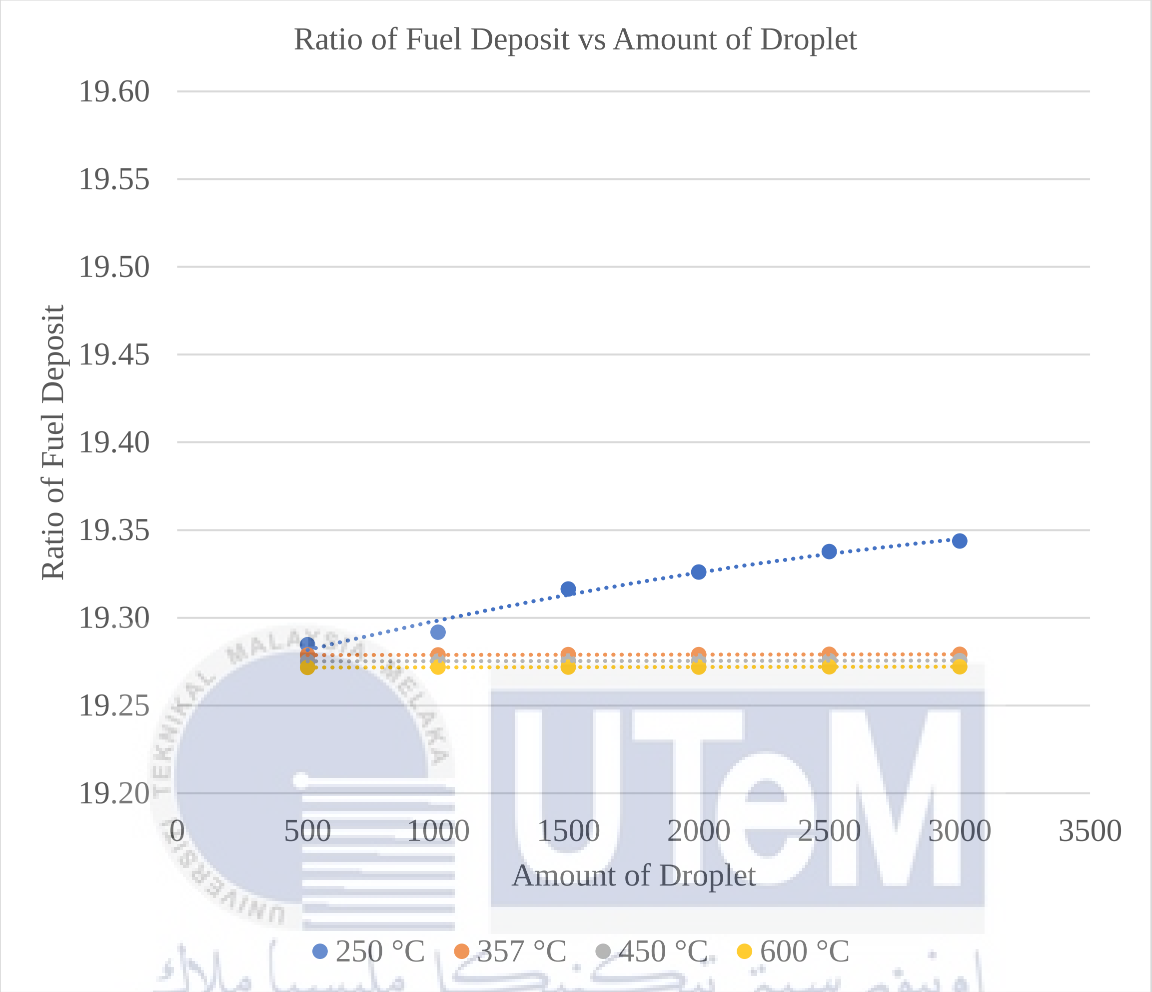

Figure 4. 34: Ratio of fuel deposit, $\frac{M_D}{m_D}$ of diesel fuel at dry condition and surface temperature of 250 °C, 357 °C, 450 °C and 600 °C

Based on graph 4.34, at dry condition, the ratio of fuel deposit, $\frac{M_D}{m_D}$ of diesel fuel deposit at 250 °C surface temperature is increasing with the amount of droplet, N_D. Diesel fuel deposit at 250 °C have the highest $\frac{M_D}{m_D}$, followed by diesel fuel deposit at 357 °C and 450 °C. The lowest $\frac{M_D}{m_D}$ is diesel fuel deposit at surface temperature of 600 °C.

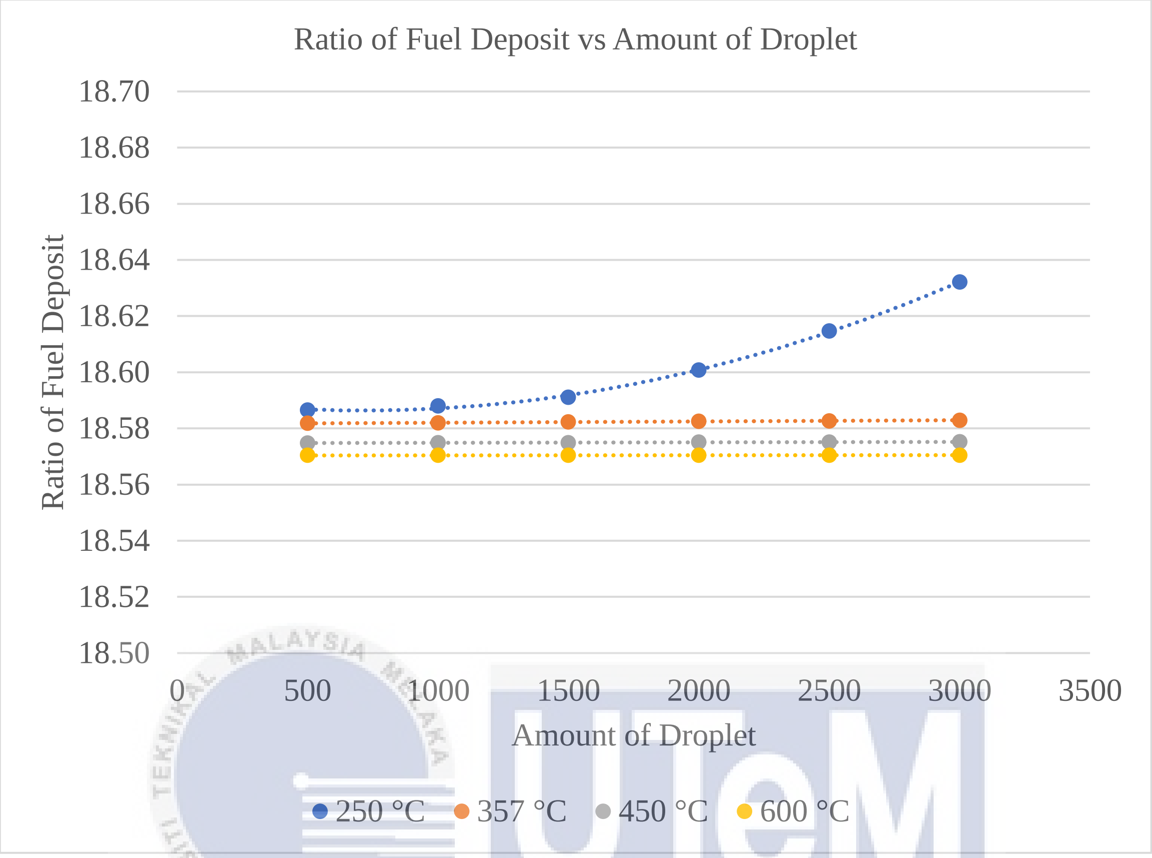

Figure 4. 35: Ratio of fuel deposit, $\frac{M_D}{m_D}$ of B20 fuel at wet condition and surface temperature of 250 °C, 357 °C, 450 °C and 600 °C

Based on graph 4.35, at wet condition, the ratio of fuel deposit, $\frac{M_D}{m_D}$ of B20 fuel deposit at 250 °C surface temperature is increasing with the amount of droplet, N_D. Diesel fuel deposit at 250 °C have the highest $\frac{M_D}{m_D}$, followed by diesel fuel deposit at 357 °C and 450 °C. The lowest $\frac{M_D}{m_D}$ is B20 fuel deposit at surface temperature of 600 °C.

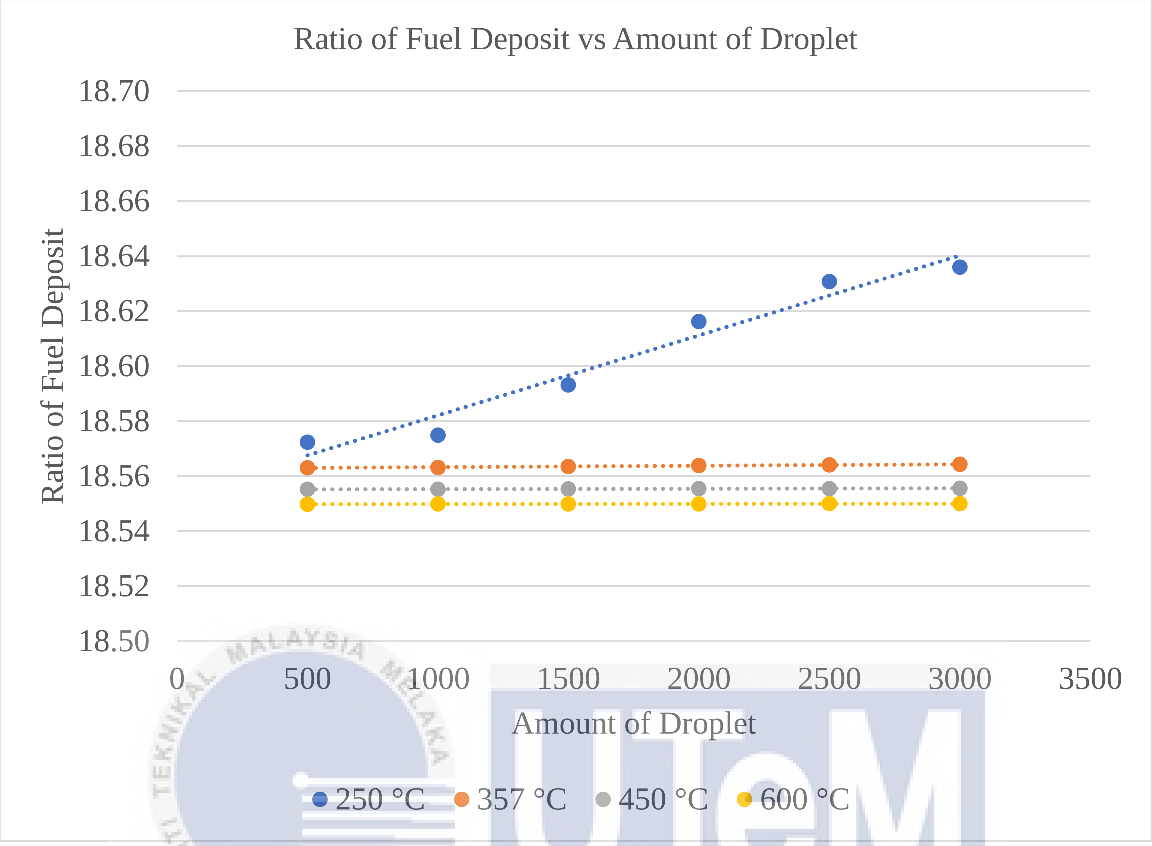

Figure 4. 36: Ratio of fuel deposit, $\frac{M_D}{m_D}$ of B20 fuel at dry condition and surface temperature of 250 °C, 357 °C, 450 °C and 600 °C

Based on graph 4.36, at dry condition, the ratio of fuel deposit, $\frac{M_D}{m_D}$ of B20 fuel deposit at 250 °C surface temperature is increasing with the amount of droplet, N_D. Diesel fuel deposit at 250 °C have the highest $\frac{M_D}{m_D}$, followed by diesel fuel deposit at 357 °C and 450 °C. The lowest $\frac{M_D}{m_D}$ is B20 fuel deposit at surface temperature of 600 °C.

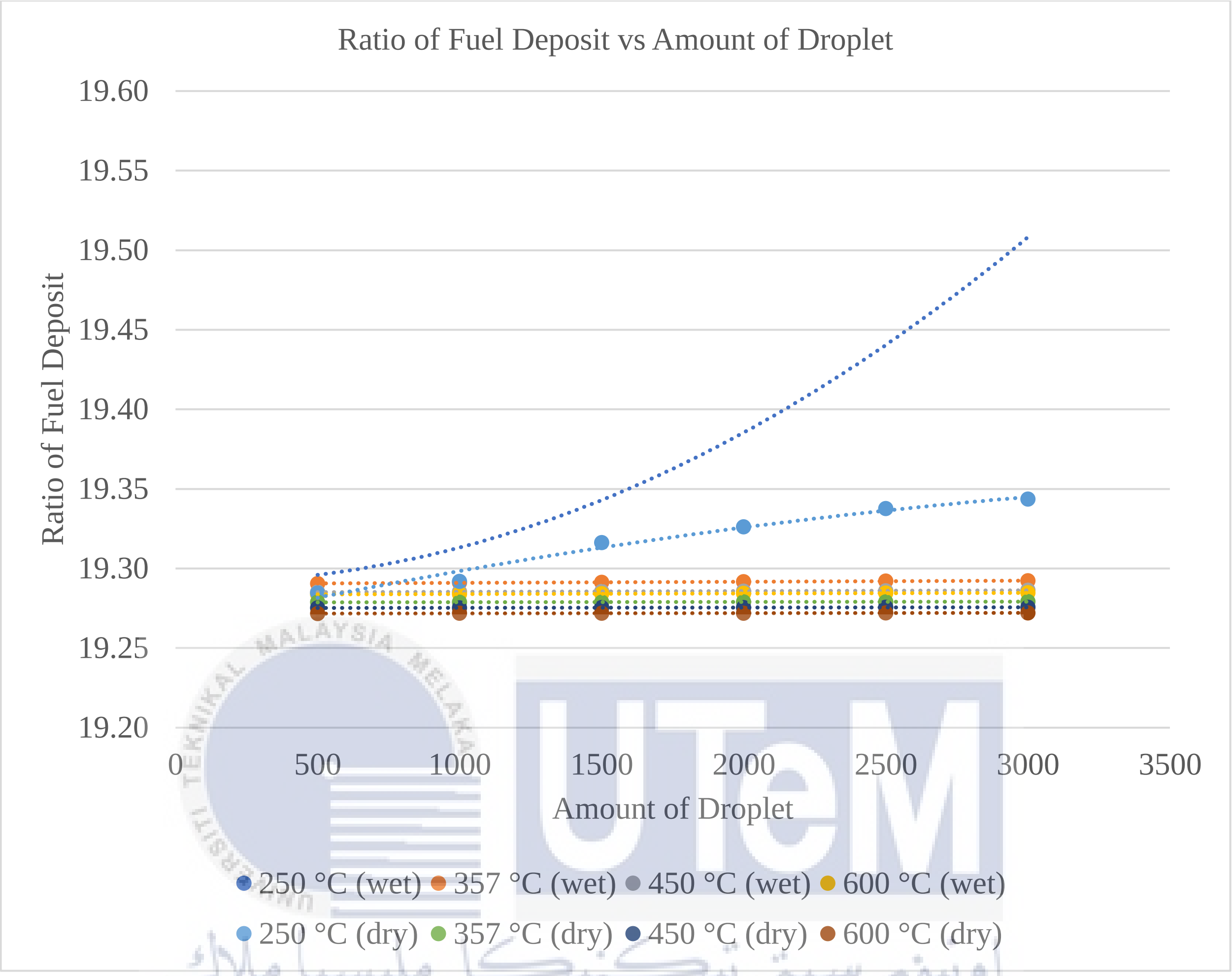

Figure 4. 37: Ratio of fuel deposit, $\frac{M_D}{m_D}$ of diesel fuel at wet and dry condition, and surface temperature of 250 °C, 357 °C, 450 °C and 600 °C

Based on graph 4.37, the ratio of fuel deposit, $\frac{M_D}{m_D}$ of diesel fuel deposit at wet and dry condition for 250 °C surface temperature is increasing with the amount of droplet, N_D. Diesel fuel deposit at 250 °C have the highest $\frac{M_D}{m_D}$ at wet condition compared to dry condition, followed by diesel fuel at 357 °C (wet condition), 450 °C (wet condition), 600 °C (wet condition), 357 °C (dry condition), and 450 °C (dry condition). The lowest $\frac{M_D}{m_D}$ is diesel fuel deposit at surface temperature of 600 °C (dry condition).

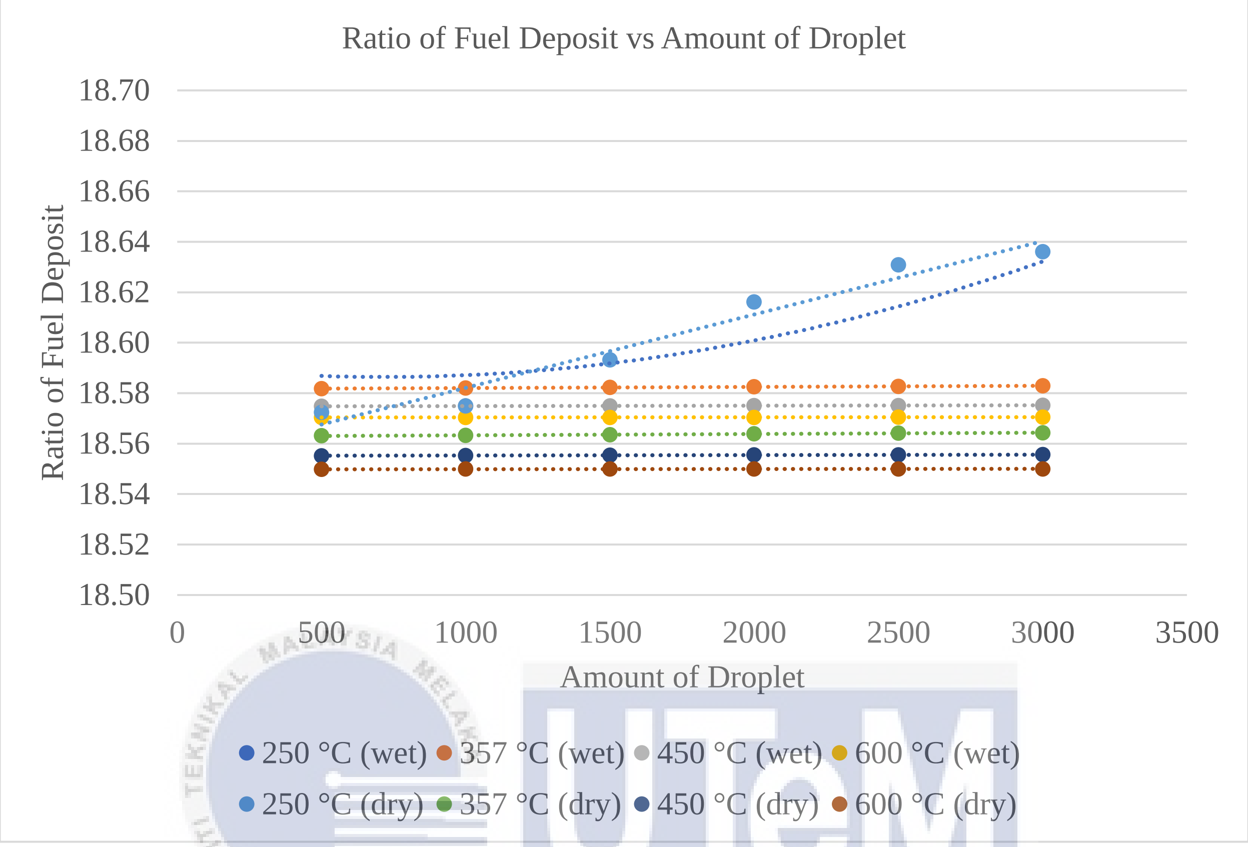

Figure 4. 38: Ratio of fuel deposit, $\frac{M_D}{m_D}$ of B20 fuel at wet and dry condition, and surface temperature of 250 °C, 357 °C, 450 °C and 600 °C

Based on graph 4.38, the ratio of fuel deposit, $\frac{M_D}{m_D}$ of B20 fuel deposit at wet and dry condition for 250 °C surface temperature is increasing with the amount of droplet, N_D. B20 fuel deposit at 250 °C have the highest $\frac{M_D}{m_D}$ at dry condition compared to wet condition, followed by B20 fuel at 357 °C (wet condition), 450 °C (wet condition), 600 °C (wet condition), 357 °C (dry condition), and 450 °C (dry condition). The lowest $\frac{M_D}{m_D}$ is B20 fuel deposit at surface temperature of 600 °C (dry condition).

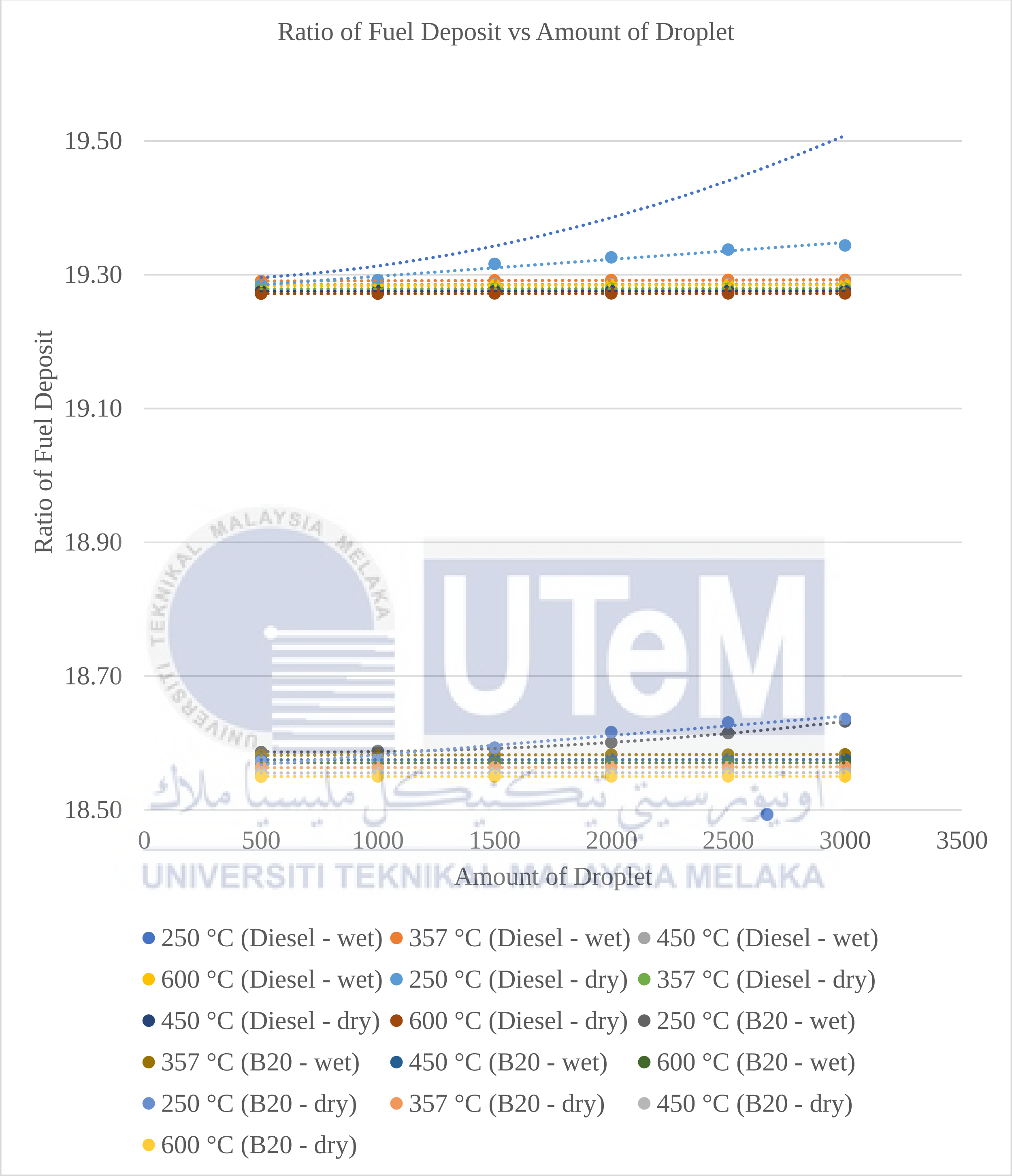

Figure 4. 39: Ratio of fuel deposit, $\frac{M_D}{m_D}$ of diesel and B20 fuel at wet and dry condition, and surface temperature of 250 °C, 357 °C, 450 °C and 600 °C

Based on graph 4.39, the ratio of fuel deposit, $\frac{M_D}{m_D}$ of B20 fuel deposit at wet and dry condition for 250 °C, 357 °C, 450 °C, and 600 °C surface temperature is lower compared to diesel fuel deposit at wet and dry condition for 250 °C, 357 °C, 450 °C, and 600 °C surface temperature. For diesel fuel deposit, the ratio of fuel deposit, $\frac{M_D}{m_D}$ at wet and dry condition for 250 °C surface temperature is increasing with the amount of droplet, N_D. Diesel fuel deposit at 250 °C have the highest $\frac{M_D}{m_D}$ at wet condition compared to dry condition, followed by diesel fuel at 357 °C (wet condition), 450 °C (wet condition), 600 °C (wet condition), 357 °C (dry condition), and 450 °C (dry condition). The lowest $\frac{M_D}{m_D}$ for diesel fuel deposit is at surface temperature of 600 °C (dry condition). For B20 fuel deposit, the ratio of fuel deposit, $\frac{M_D}{m_D}$ at wet and dry condition for 250 °C surface temperature is increasing with the amount of droplet, N_D. B20 fuel deposit at 250 °C have the highest $\frac{M_D}{m_D}$ at dry condition compared to wet condition, followed by B20 fuel at 357 °C (wet condition), 450 °C (wet condition), 600 °C (wet condition), 357 °C (dry condition), and 450 °C (dry condition). The lowest $\frac{M_D}{m_D}$ is B20 fuel deposit at surface temperature of 600 °C (dry condition). As the temperature increases to the point where the Leidenfrost effect is more prominent, the higher oxygen content in B20 fuel molecule aids in better fuel combustion thus, lesser deposit is formed compared to diesel fuel deposit.

This finding can be support by another study made by Mulyono et al., (2018) that use fuel droplet method on a plate to compare the characteristics and mechanisms of deposit formation between different blends of bio-diesel fuel which are B20 FAME (Fatty Acid Methyl Ester), B30 FAME and B30 HVO (Hydrotreated Vegetable Oil). The fuel deposit mass growth on a plate at different surface temperature for B20 FAME, B30 FAME, and B30 HVO are shown in Figure 4.40, Figure 4.41, and Figure 4.42.

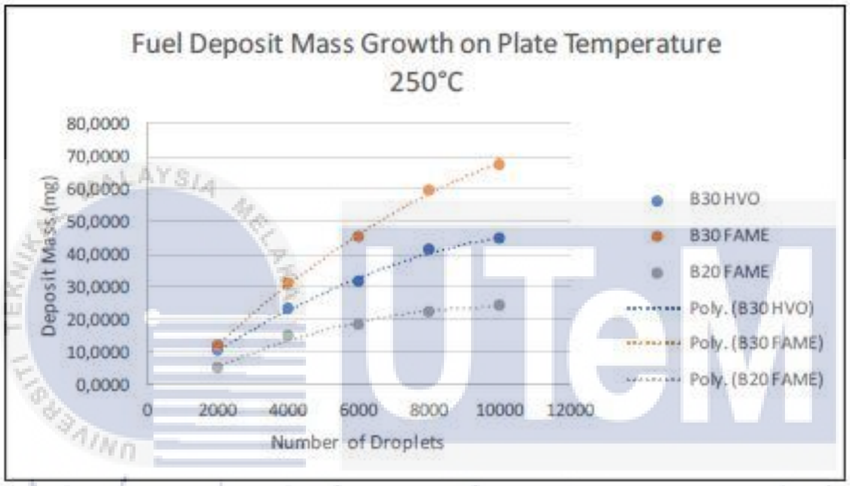

Figure 4. 40: Fuel deposit mass growth on plate temperature of 250 °C (Mulyono et al., 2018)

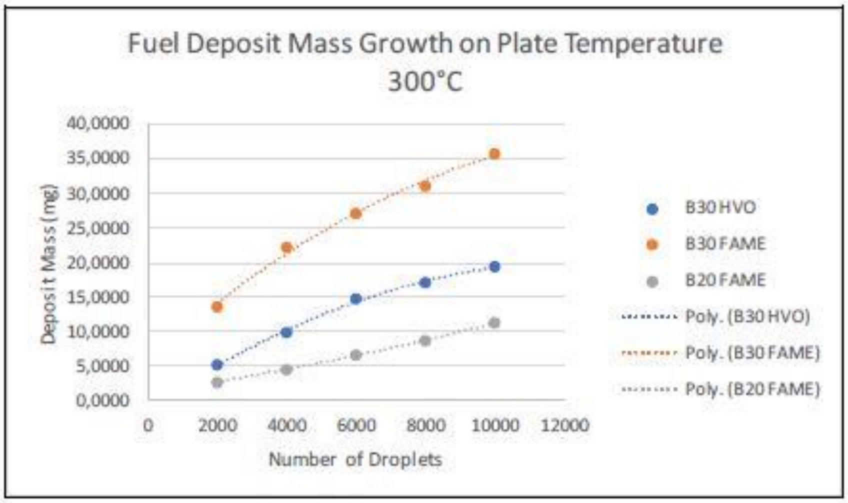

Figure 4. 41: Fuel deposit mass growth on plate temperature of 300 °C (Mulyono et al., 2018)

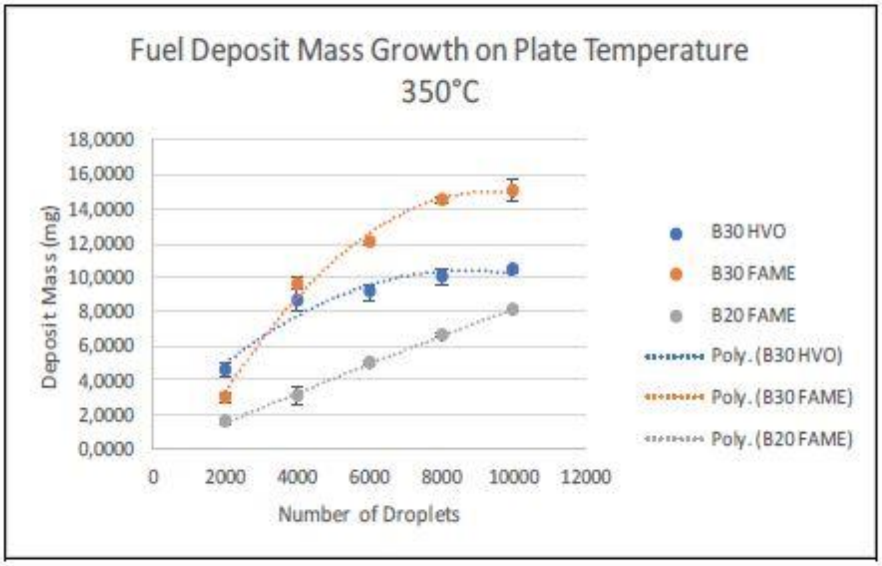

Figure 4. 42: Fuel deposit mass growth on plate temperature of 350 °C (Mulyono et al., 2018)

Based on Figure 4.40, Figure 4.41, and Figure 4.42, the decreasing trend for total deposit mass (mg) after 10,000 number of droplets can be seen as the surface temperature increase from 250 °C to 350 °C. The total deposit mass (mg) for B30 FAME decrease from approximately 68,000 mg at surface temperature 250 °C to approximately 15,000 mg at surface temperature 350 °C. As for B30 HVO, at surface temperature 250 °C, the total deposit mass (mg) decreases from approximately 45,000 mg to approximately 10,200 mg at surface temperature of 350 °C. Lastly, the total deposit mass (mg) for B20 FAME decrease from approximately 24,000 mg at surface temperature 250 °C to approximately 8,100 mg at surface temperature 350 °C. The highest total mass deposit (mg) for all surface temperature is B30 FAME and the lowest total mass deposit (mg) for all surface temperature is B20 FAME.

Besides that, another study that support this finding is made by Kumar Patidar and Raheman (2020), that conduct experiments using a short-run engine test in order to evaluate combustion, performance and emissions using different blend of water emulsified biodiesel-diesel fuel blend which are PB20S10W (89% v/v B20 + 10% v/v water + 1% v/v surfactants), B20 (20% v/v palm biodiesel + 80% v/v diesel) and HSD (High Speed Diesel). Based on this study, the cylinder head and piston crown pictures after completion of each 100-hour engine long-run phase using PB20S10W, B20 and HSD are captured, and compared with the cleaned cylinder head and piston crown before starting the engine long-run phase as shown in Figure 4.43 and Figure 4.44. From these figures, it can be clearly seen from these figures that the soot deposits on top parts of the engine were lower compared to HSD when operated using PB20S10W and B20. After 100-hour operation, the lowest amount of soot deposits is shown by B20 bio-diesel blend operated engine compared to PB20S10W and HSD. This is maybe due the extra oxygen available in B20 blend that led to better combustion characteristics in the B20 engine. The highest amount of soot deposits is shown by HSD operated engine which is 14.45-32.20 % higher soot deposit compared to PB20S10W and B20 on the cylinder head and piston crown.

(a) Clean cylinder head (b) PB20S10W

(c) B20 (d) HSD

Figure 4. 43: Soot deposits on cylinder head of the diesel engine (Kumar Patidar and Raheman, 2020)

(a) Clean cylinder head

(b) PB20S10W

(c) B20

(d) HSD

Figure 4. 44: Soot deposits on piston crown of the diesel engine (Kumar Patidar and Raheman, 2020)

CHAPTER 5

CONCLUSION AND RECOMMENDATIONS FOR FUTURE RESEARCH

5.1 Conclusion

The investigation of diesel and B20 fuel deposits on a hot wall surface temperature using a simplified method which is Hot Surface Deposition Test (HSDT) is presented in this report. In terms of deposit development and soot fraction in deposits, HSDT was able to achieve results similar to the Engine Deposit Test (EDT). In addition, the HSDT test conditions are similar to some real conditions of diesel engine such as the wall surface temperature, wetting condition, and part of the deposit mechanisms.

In the development of deposits on a hot surface, the temperature of the hot surface is an important factor which can be manipulated to reduce deposits in an engine. Surface temperatures close to the Maximum Evaporation Rate Point (MEP) temperature clearly tend to slow the development of deposits with less accumulated deposits. Various sub-cooled temperatures from the MEP temperatures have shown various droplet-surface interactions, evaporation lifetime and wet-dry conditions, with different deposit development characteristics. The non-overlapping and dry condition of deposit results in less overall deposit amount, which is considered to be a slow development. Based on the results, the amount of mass fuel deposit, M_D of diesel fuel deposit is higher compared to B20 fuel deposit and the highest M_D is produced at surface temperature of 250 ℃, followed by 357 ℃, 450 ℃ and 600 ℃. As the temperature increases to the point where the Leidenfrost effect is more prominent, the higher oxygen content in B20 fuel molecule aids in better fuel combustion thus, lesser deposit is formed compared to diesel fuel deposit.

Initial non-overlapping/overlapping and wet/dry conditions are determined by the impingement interval and surface temperature. It is important that the impingement interval longer than the lifetime of the droplet to make the non-overlapping cases to happen. However, the conditions for a dry deposit can be maintained when the impingement interval is long enough to ensure that the non-volatile fuel components that is not oxidize yet on the hot surface are fully transformed into deposits. Contradictory, conditions for overlapping only occurs when the impingements interval is shorter than the lifetime of the droplet. The wet dry conditions and overlapping are co-existent. In this study, we use the impingement interval of droplets from 1 to 5 seconds. Impingement interval of 1 second is used for wet condition and 5 seconds is used for dry conditions.

5.2 Recommendation for Future Work

For future work, the difference between the height of the hot surface plate and the tip of the droplet needle can be used as a manipulated variable for the next study and it can be compared with the results from previous studies related to the behavior of droplets on hot surfaces. The impingement interval of droplets can also be changed from 1 to 10. The main purpose of this study was to study the deposition of diesel and bio-diesel fuel on a hot surface using HSDT method to correlate with the effect of fuel deposition in actual diesel engines. Experiments that are performed in an area where the air pressure can be controlled, and the droplet method can be replaced by spray method are likely to produce results that are closely to the actual situation in a diesel engine.

REFERENCES

Agarwal, A. K., & Agarwal, D. (2021). Field-Testing of Biodiesel (B100) and Diesel-Fueled Vehicles: Part 3—Wear Assessment of Liner and Piston Rings, Engine Deposits, and Operational Issues. *Journal of Energy Resources Technology*. https://doi.org/10.1115/1.4048309

Akintayo, E. T. (2004). Characteristics and composition of Parkia biglobbossa and Jatropha curcas oils and cakes. *Bioresource Technology*, *92*(3), 307–310. https://doi.org/10.1016/S0960-8524(03)00197-4

Ali, O. M., Mamat, R., Abdullah, N. R., & Abdullah, A. A. (2015). Analysis of blended fuel properties and engine performance with palm biodiesel-diesel blended fuel. *Renewable Energy*, *86*, 59–67. https://doi.org/10.1016/j.renene.2015.07.103

Almutairi, A., Wu, D., Guo, B., Roskilly, A. P., & Ottley, C. (2017). Characterization of Lubricant Degeneration and Component Deterioration on Diesel Engine Fueling with Straight Plant Oil. *Energy Procedia*, *105*, 636–641. https://doi.org/10.1016/j.egypro.2017.03.368

Anjaneyulu, B., Kaki, S. S., Kanjilal, S., Reddy, J. R. C., Ravinder, T., Prasad, R. B. N., & Rao, B. V. S. K. (2017). Physico-chemical characterization and biodiesel preparation from Ailanthus excelsa seed oil. *Energy Sources, Part A: Recovery, Utilization and Environmental Effects*, *39*(8), 811–816. https://doi.org/10.1080/15567036.2016.1266419

Arifin, Y. M. (2009). *Diesel and Bio-diesel Fuel Deposits on a Hot Wall Surface*. *August*.

Arifin, Y. M., Furuhata, T., Saito, M., & Arai, M. (2008). Diesel and bio-diesel fuel deposits on a hot surface. *Fuel*, *87*(8–9), 1601–1609. https://doi.org/10.1016/j.fuel.2007.07.030

Berndorfer, A., Breuer, S., Piock, W., & Von Bacho, P. (2013). Diffusion combustion phenomena in GDi engines caused by injection process. *SAE Technical Papers*, *2*. https://doi.org/10.4271/2013-01-0261

Caceres, D., Reisel, J. R., Sklyarov, A., & Poehlman, A. (2003). Exhaust emission deterioration and combustion chamber deposit composition over the life cycle of small utility engines. *Journal of Engineering for Gas Turbines and Power*, *125*(1), 358–364. https://doi.org/10.1115/1.1496773

Daly, D. T., Bannon, S. A., Fog, D. A., & Harold, S. M. (1994). Mechanism of combustion chamber deposit formation. *SAE Technical Papers*, *412*. https://doi.org/10.4271/941889

F. Jorand, M. Brun, N. B.-S. & K. S. (2000). *Combustion Science and Technology Formation of Combustion Chamber Deposits during Ignition Delay Formation of Combustion Chamber Deposits during Ignition Delay*. *November 2012*, 37–41.

Güralp, O., Hoffman, M., Assanis, D., Filipi, Z., Kuo, T. W., Najt, P., & Rask, R. (2006). Characterizing the effect of combustion chamber deposits on a gasoline HCCI engine. *SAE Technical Papers*. https://doi.org/10.4271/2006-01-3277

Hoang, A. T., & Le, A. T. (2019). A review on deposit formation in the injector of diesel engines running on biodiesel. *Energy Sources, Part A: Recovery, Utilization and Environmental Effects*, *41*(5), 584–599. https://doi.org/10.1080/15567036.2018.1520342

Hoang, A. T., & Pham, V. V. (2019). A study of emission characteristic, deposits, and lubrication oil degradation of a diesel engine running on preheated vegetable oil and diesel oil. *Energy Sources, Part A: Recovery, Utilization and Environmental Effects*, *41*(5), 611–625. https://doi.org/10.1080/15567036.2018.1520344

Husnawan, M., Masjuki, H. H., Mahlia, T. M. I., & Saifullah, M. G. (2009). Thermal analysis of cylinder head carbon deposits from single cylinder diesel engine fueled by palm oil-diesel fuel emulsions. *Applied Energy*, *86*(10), 2107–2113. https://doi.org/10.1016/j.apenergy.2008.12.031

Ishii, H., Emi, M., Yamada, Y., Kimura, S., Shimano, K., & Enomoto, Y. (2001). Heat loss to the combustion chamber wall with deposit adhering to the wall surface in D.I. diesel engine first report: Influence of deposit on instantaneous heat flux into the piston surfaces. *SAE Technical Papers*, *724*. https://doi.org/10.4271/2001-01-1811

Jiang, C., Xu, H., Srivastava, D., Ma, X., Dearn, K., Cracknell, R., & Krueger-Venus, J. (2017). Effect of fuel injector deposit on spray characteristics, gaseous emissions and particulate matter in a gasoline direct injection engine. *Applied Energy*, *203*, 390–402. https://doi.org/10.1016/j.apenergy.2017.06.020

Jonkers, R. K., Bardon, M. F., & Gardiner, D. P. (2002). Techniques for predicting combustion chamber deposits in a direct injection diesel engine. *SAE Technical Papers, 724*. https://doi.org/10.4271/2002-01-2673

Kalam, M. A., & Masjuki, H. H. (2004). Emissions and deposit characteristics of a small diesel engine when operated on preheated crude palm oil. *Biomass and Bioenergy*. https://doi.org/10.1016/j.biombioe.2004.01.009

Karmakar, A., Karmakar, S., & Mukherjee, S. (2010). Properties of various plants and animals feedstocks for biodiesel production. *Bioresource Technology, 101*(19), 7201–7210. https://doi.org/10.1016/j.biortech.2010.04.079

Kumar Patidar, S., & Raheman, H. (2020). Performance and durability analysis of a single-cylinder direct injection diesel engine operated with water emulsified biodiesel-diesel fuel blend. *Fuel, 273*(September 2019), 117779. https://doi.org/10.1016/j.fuel.2020.117779

Lepperhoff, G., & Houben, M. (1993). Mechanisms of deposit formation in internal combustion engines and heat exchangers. *SAE Technical Papers, 412*. https://doi.org/10.4271/931032

Liu, Y., Pei, Y., Wang, C., Guo, R., & Xu, B. (2019). Characteristics of the deposited fuel liquid film when GDI spray impacts viscous oil film. *Energy, 188*. https://doi.org/10.1016/j.energy.2019.116011

Mulyono, A. B., Sugiarto, B., Suryantoro, M. T., Setiapraja, H., Yubaidah, S., Attharik, M. I., Ariestiawan, M. R., & Cohen, A. (2018). Effect of hydrotreating in biodiesel on the growth of deposits in the combustion chamber as a solution for the deposits reduction in the usage of biodiesel. *E3S Web of Conferences*, *67*. https://doi.org/10.1051/e3sconf/20186702014

Nikolakopoulos, P. G. (2021). Simulation of deposits effect on cylinder liner and influence on new and worn compression ring of a turbocharged DI engine. *Simulation Modelling Practice and Theory*, *106*(August 2020), 102195. https://doi.org/10.1016/j.simpat.2020.102195

Ra, Y., Reitz, R. D., Jarrett, M. W., & Shyu, T. P. (2006). Effects of piston crevice flows and lubricant oil vaporization on diesel engine deposits. *SAE Technical Papers*, *2006*(724). https://doi.org/10.4271/2006-01-1149

Razak, I. F. A., Fatah, A. Y. A., Aqma, W. M. N. W. S., & Rahman, A. H. A. (2017). Razak School of Engineering and Advanced Technology Universiti Teknologi Malaysia Jalan Sultan Yahya. *Energy*. https://doi.org/10.1016/j.energy.2017.10.044

Sadashiva Prabhu, S., Nayak, N. S., Kapilan, N., & Hindasageri, V. (2017). An experimental and numerical study on effects of exhaust gas temperature and flow rate on deposit formation in Urea-Selective Catalytic Reduction (SCR) system of modern automobiles. *Applied Thermal Engineering*, *111*(x), 1211–1231. https://doi.org/10.1016/j.applthermaleng.2016.09.134

Senda, J., Yamada, K., Fujimoto, H., & Miki, H. (1988). HEAT-TRANSFER CHARACTERISTICS OF A SMALL DROPLET IMPINGING UPON A HOT SURFACE. *JSME International Journal, Series B: Fluids and Thermal Engineering*. https://doi.org/10.1299/jsmeb1988.31.1_105

Slavchov, R. I., Mosbach, S., Kraft, M., Pearson, R., & Filip, S. V. (2018). An adsorption-precipitation model for the formation of injector external deposits in internal combustion engines. *Applied Energy*, *228*(April), 1423–1438. https://doi.org/10.1016/j.apenergy.2018.06.130

Stanuch, I., Sozańska, M., Biegańska, J., Cebula, J., & Nowak, J. (2020). Fluctuations of the elemental composition in the layers of mineral deposits formed on the elements of biogas engines. *Scientific Reports*, *10*(1), 1–12. https://doi.org/10.1038/s41598-020-61212-x

Suryantoro, M. T., Setiapraja, H., Yubaidah, S., Sugiarto, B., Mulyono, A. B., Attharik, M. I., Halomoan, T., & Ariestiawan, M. R. (2019). Effect of temperature to diesel (B0) and biodiesel (B100) fuel deposits forming. *AIP Conference Proceedings*, *2062*(January), 0–6. https://doi.org/10.1063/1.5086591

Ullmann, J., Geduldig, M., Stutzenberger, H., Caprotti, R., & Balfour, G. (2008). Investigation into the formation and prevention of internal diesel injector deposits. *SAE Technical Papers*, *2008*(724). https://doi.org/10.4271/2008-01-0926

Xu, H., Wang, C., Ma, X., Sarangi, A. K., Weall, A., & Krueger-Venus, J. (2015). Fuel injector deposits in direct-injection spark-ignition engines. *Progress in Energy and Combustion Science*, *50*, 63–80. https://doi.org/10.1016/j.pecs.2015.02.002

Ye, Z., Meng, Q., Mohamadian, H. P., Wang, J. T., Chen, L., & Zhu, L. (2007). Investigation of deposit formation mechanisms for engine In-cylinder combustion and exhaust systems Using quantitative analysis and sustainability study. *International Journal of Thermophysics*, *28*(3), 1056–1066. https://doi.org/10.1007/s10765-007-0228-5

Zerda, T. W., Yuan, X., & Moore, S. M. (2001). Effects of fuel additives on the microstructure of combustion engine deposits. *Carbon*, *39*(10), 1589–1597. https://doi.org/10.1016/S0008-6223(00)00287-6

APPENDIX

1. Gantt Chart

FINAL YEAR PROJECT SEMESTER 1														
Week Work	1	2	3	4	5	6	7	8	9	10	11	12	13	14
Literature Review	■	■	■	■	■									
Methodology						■	■	■	■					
Hot Surface Deposition Test (HSDT)										■	■	■	■	■
FINAL YEAR PROJECT SEMESTER 2														
Data Collection	■	■	■	■	■	■	■							
Data Analysis								■	■	■				
Report Writing											■	■	■	■